Electron transfer and redox chemistry in hexa-coordinate hemoglobins

by

Navjot Singh

A dissertation submitted to the graduate faculty

in partial fulfillment of the requirements for the degree of

DOCTOR OF PHILOSPHY

Major: Biochemistry

Program of Study Committee:
Mark Hargrove, Major Professor
Amy Andreotti
Alan DiSpirito
Alan Myers
Laura Jarboe

Iowa State University

Ames, Iowa

2016

TABLE OF CONTENTS

CHAPTER I

INTRODUCTION: CHEMISTRY OF HEXACOORDINATE HEMOGLOBINS

A paper to be submitted to *Protein Science*

Navjot Singh Athwal, Xiaoguang Wang, and Mark S. Hargrove

Abstract:

The heme prosthetic group can be held into proteins in a variety of ways. Most often amino acid side chains coordinate one or both of the two available axial coordination sites of the heme iron. Coordination of both sites, such as in cytochrome b_5, produces a good electron transfer protein but excludes the binding of exogenous ligands. In hemoglobins, coordination can occur at a single site (as in the "pentacoordinate" hemoglobins associated with oxygen transport), or at both sites (as in the "hexacoordinate" hemoglobins found in a wider distribution of organisms and functions). Surprisingly, hexacoordination in hemoglobins is usually reversible and a variety of exogenous ligands can bind most hexacoordinate hemoglobins. Reversible coordination brings a variety of chemical features to hexacoordinate hemoglobins by affecting their affinity for ligands, redox equilibrium, and the kinetics and extent of electron transfer. These reactions are reviewed for hexa- and pentacoordinate hemoglobins with the goal of using these characteristics for understanding potential functions of hexacoordinate hemoglobins in different species.

Introduction:

The globins are a family of proteins sharing structural homology that are widely distributed across the domains of life. Globins often exist as "hemoglobins" (Hbs) in combination with a heme prosthetic group that bestows the ability to reversibly bind ligands without changing their structure, or to modify the ligand through oxidation or reduction along with the accompanying addition to, or removal of an electron from the heme iron. The most familiar Hbs are red blood cell hemoglobin (rbcHb) and muscle myoglobin (Mb), which facilitate the reversible transport of oxygen between the lungs and respiring tissues in vertebrate animals. But even these venerable proteins are capable of much more chemistry, including the reversible binding of many other ligands including nitric oxide and carbon monoxide, and redox reactions that are important alternatives to their principle transport function [1-4].

The porphyrin pyrrole nitrogens of heme provide four equatorial points of coordination to the iron, with the globin portions of rbcHb and Mb providing a single axial ligand, through a “proximal” histidine side chain. Because only five out of six possible iron coordination sites are occupied, these Hbs and their structural homologues are often referred to as "pentacoordinate" Hbs (pxHbs). The open coordination site in pxHbs is thus readily available for ligand binding. The arrangement of molecular orbitals in pxHbs is such that the heme irons of the ferric and ferrous oxidation states are often in the “high-spin” energy state in the absence of bound ligands. Another group of Hbs found mainly in

plants and animals are "hexacoordinate", with a second histidine side chain filling the sixth coordination site [5]. Coordination of the second histidine is energetically favorable, resulting in a transition to the “low-spin” molecular orbital energy state (particularly in the ferric oxidation state). Therefore it is somewhat surprising that hexacoordination is usually reversible, allowing exogenous ligand binding in most hxHbs. Although hexacoordination is reversible, rate and affinity constants for coordination of the second histidine are quite variable (Table 1). Coordination of the second histidine affects the general chemistry of hxHbs in four general ways compared to their pentacoordinate counterparts [5]. 1) Coordination causes the heme iron to reside in the low spin state in both the ferric and ferrous oxidation states. 2) The fact that coordination is disproportionately stronger in the ferric oxidation state lowers the midpoint redox potential of the ferrous/ferric transition by one to two hundred millivolts compared to pxHbs, favoring the ferric oxidation state. 3) Rate constants for reduction of hxHbs are faster than those of pxHbs. 4) Intermolecular histidine binding competes for the ligand-binding site, effectively lowing the affinity for exogenous ligands.

The major challenge to protein biochemists in the genomic age is identification of protein function starting from primary structure. Recombinant protein technology has allowed production and purification of many proteins in the laboratory to the extent that experiments can be conducted with wild type and mutant proteins, and high-resolution structures can be measured. Such is the case with hxHbs; to date, while structures of many have been solved, no hxHbs have been purified from a natural source. Thus, we are left to look at structures, and compare *in vitro* chemistries in an effort to rationalize the

results of relatively complex *in vivo* experiments. Eventually, these data must corroborate one another in support of physiological functions. The purpose of this review is to compare the chemistry of hxHbs to pxHbs with the goal of pinpointing some general features that might be indicative of potential physiological functions for hxHbs.

Structural features of hexacoordinate hemoglobins-

Crystal and NMR structures of many different hxHbs have been published [6-16] and reviewed previously [5]. The basic structural framework of each can be described with respect to that of Mb [17], with a few deviations. There are eight conserved alpha helices in eukaryotic hxHbs, designated A through H as they appear in the primary structure. They are arranged in antiparallel symmetric groups of three helices (A/E/F and B/G/H), also known as the “3-on-3” globin fold. In contrast, the hxHbs found in prokaryotes lack the A and D helices and exhibit "2-on-2" stacking of pairs of alpha-helices18. Regardless of the specific manifestation of the globin fold, hxHbs have the critical coordinating histidines on the E Helix (the “distal” histidine, often referred to as "HisE7" in reference to the homologous amino acid in Mb, which is the 7th in the E helix), and the F-helix (the “proximal” histidine, or "HisF8"). Although X-ray crystallography is the ultimate technique to measure heme coordination along with protein structure, UV-Visible absorbance (UV-Vis) and electron paramagnetic resonance (EPR) spectroscopy are often employed to quickly assess the coordination state of Hbs. UV-Vis spectroscopy is empirically indicative of all coordination and oxidations states across a wide range of temperatures. EPR is most often used with the ferric oxidation state at low temperatures

(< 10 ° K), but can be used for very sensitive a priori diagnoses of heme coordination in some electronic configurations and oxidation states. UV-Vis and EPR spectra characteristic of pxHbs and hxHbs are shown in Figure 1. EPR is also a powerful technique for studying changes in the oxidation state of the heme center, although this application is surprisingly underexploited [19,20].

The vertebrate hxHbs neuroglobin (Ngb) and Cytoglobin (Cgb) share 21-25% sequence identity with Mb and the α/β chains of rbcHb [1,21]. Coordination of the distal histidine is tighter in Ngb than Cgb, but both are > 99% hexacoordinated in both the ferrous and ferric oxidation states. There are multiple cysteines in these hxHbs; Ngb has three at CD5, D5 and G19, and Cgb has two at the B2 and E9 positions [7,22]. Experiments to address their impacts on protein structure and function have used disulfide-reactive reagents such as dithiothreitol (DTT) and Tris (2-carboxyethyl) phosphine hydrochloride (TCEP). Of course, these reagents are also potentially reactive with the heme iron, so one must pay heed to whether they also affect heme iron oxidation state. These cysteines are reported to have the potential to form intermolecular disulfide bonds (Ngb at D5 - G19, and Cgb at B2 - E9) as well as intramolecular disulfide linkages between chains (Ngb CD5 - D5 and Cgb B2 - E9) [7,22,23]. However, they have been shown to occur mostly in monomeric forms at the concentrations and conditions that are deemed physiological [7], though quaternary structure has been suggested to affect the chemistry of Cgb [24].

Internal disulfide bonds are proposed to have redox regulatory functions that can affect ligand affinity (both endogenous and exogenous). EPR spectroscopy has been used as a measure of structural alterations resulting from oxidation and reduction of the

cysteines involved in intramolecular disulfide bonds, especially as they affect the distances between the distal histidine and the heme iron atom [25-27]. These studies report that disulfide linkage decreases the strength of hexacoordination by a factor of ten in Ngb and by two in Cgb. In this mechanism, the formation of disulfide bonds stresses the E helix to destabilize distal histidine coordination, thus increasing oxygen affinity by removing competition form the histidine side chain.

Plants contain three phylogenetically and biochemically distinct classes of Hbs. Two of these (class 1 and class 2) are distantly related, but class 3 plant Hbs are more closely related to bacterial Hbs, and likely arrived in plants through horizontal gene transfer [28]. Class 1 and most class 2 plant Hbs are hexacoordinate, but the data for class 3 are equivocal, as only a few members have been investigated. Arabidopsis class 3 nsHb was originally reported to be transiently hexacoordinate when reduced from the ferric to the ferrous oxidation state [29], but in Lotus japonicas class 2 and 3 are both pentacoordinated [30]. All plants appear to have class 1 and class 3 Hbs, while dicotyledonous plants additionally contain class 2 proteins. In general plant Hbs are not oxygen transport proteins except for the "leghemoglobins" in the legume subset of dicots, which differentiated from class 2 Hbs into oxygen transport proteins in support of aerobic metabolism in the symbiotic nitrogen-fixing bacteria living in their roots [31]. Because the symbiotic leghemoglobin was discovered first [32], the other plant Hbs are referred to as "nonsymbiotic hemoglobins" (nsHbs) in comparison.

Crystal structures of class 1 nsHbs from rice, Arabidopsis, and barley have been reported [11,13,33-36]. Like the animal hxHbs, nsHbs have 3-on-3 myoglobin-like folds

with conserved proximal and distal histidine side chains coordinating the heme iron. Distal histidine coordination is weaker in nsHbs than in Ngb and Cgb, and weaker in class 1 than in class 2 nsHbs. In fact, hexacoordination is only ~ 50 % in ferrous class 1 nsHbs.

nsHbs can form dimers in solution. Ferric class 1 rice nsHb has a weak affinity for dimerization with an equilibrium dissociation constant of 80 μM, whereas the ferrous protein is even weaker (~ 600 μM) [34]. In contrast, the ferric hemoglobins from parasponia and trema species form tighter dimers (KD < 1μM) [37]. The dimer interface consists of parts of the CD helix region and the beginning of the G helix. In spite of the fact that kinetic constants for hexacoordination were measured at low protein concentrations that are largely monomeric, molecular dynamics simulations appear to implicate the dimer interactions in regulating coordination at the heme iron in rice nsHb [33]. Class 1 nsHbs have a conserved cysteine located in the E-helix that is potentially involved in alternative dimerization as well affecting autoxidation rates [38].

Bacteria and archaea contain a diverse group of Hbs that are 20-40 amino acids shorter in their primary structures than most other globins [39]. Crystal structures of these “truncated” Hbs have revealed that they lack an A helix, the CD/D helix region is shortened to just a few amino acids, and the F helix consists of only a single turn. Furthermore, they have "2-on-2" helix packing consisting of the B/E and G/H helices [40]. The proximal histidine is conserved, but the presence and nature of a coordinating side chain in the distal pocket is quite variable and has been shown to include tyrosine, glutamine, threonine, serine, and histidine in truncated Hbs from different organisms [1].

One well-characterized bacterial hxHb is that from the cyanobacterium Synechocystis. The structure of Synechocystis Hb (SynHb) has been measured by X-ray crystallography [10] and NMR spectroscopy [41] (along with its relative from Synechococcus [42]) in the hexacoordinate and ligand-bound states, and contains a novel covalent bond between another heme pocket histidine side chain and a heme vinyl which helps to hold the heme in place and affects the affinity constants for hexacoordination [43,44]. With respect to the strength of distal histidine coordination, SynHb is similar to Ngb and Cgb in that it is largely hexacoordinate in both the ferrous and ferric oxidation states.

Redox biochemistry of hexacoordinate hemoglobins-

HxHbs are generally found in lower concentrations, have higher oxygen affinities, slower oxygen dissociation rate constants, and more potential for electron transfer and disulfide-linked redox reactions than their oxygen transport counterparts. Research into the chemistry of hxHbs can be roughly grouped into reactions with oxygen, inorganic nitrogen compounds, peroxides, and electron transfer reactions. These groups of reactions are reviewed below and compared to those for other Hbs in an effort to gauge the specificity of each for hxHbs.

Reactions with oxygen- The key to the proper function of oxygen transport Hbs is reversible oxygen binding. Oxygen only binds to ferrous Hb, and it must do so with the appropriate affinity, and depart in a timely manner without taking an electron from the

heme iron. Failure to prevent the latter reaction produces superoxide and ferric Hb, and is termed "autoxidation" [45]. Oxidized (or "met") Hb leads to heme loss from rbcHb [46], heme degradation [47], and oxidative stress [48-51]. The role of the protein in affecting these properties is profound, and understanding these principles is a major challenge to the *de novo* design of stable heme proteins [52-55].

Comprehensive reviews on myoglobin auto-oxidation are available [56,57]. There are two starting points for the reaction: the deoxyferrous state (Reaction 1) (at sub-saturating oxygen concentrations), or the oxyferrous state (Reaction 2) (at saturating oxygen concentrations). In Reaction 1, oxygen binding can result in an outer-sphere electron transfer displaying bimolecular kinetics with oxygen, and producing superoxide anion [58].

$$Mb^{Fe(II)} + O_2 \longrightarrow Mb^{Fe(III)} + O_2^{*-} \qquad \text{(Reaction 1)}$$

$$Mb^{Fe(II)}O_2 + H^+ \longrightarrow {}^{+}HOO - Mb \longrightarrow Mb^{Fe(III)} + HO_2^{*} \qquad \text{(Reaction 2)}$$

The second mechanism (Reaction 2) starts with oxygen bound to the ferrous heme, which exists in resonance with superoxide and a ferric heme iron. Protonation of superoxide radical facilitates permanent extraction of an electron from the iron center followed by neutral superoxide radical dissociation. This inner-sphere mechanism is enhanced at lower pH, and exhibits kinetics independent of oxygen concentration. The superoxide radicals resulting from either mechanism can produce hydrogen peroxide directly, or be converted to hydrogen peroxide by superoxide dismutase [56]. Thus, Hb

autoxidation produces reactive oxygen species that are potentially damaging to cells and tissues.

The hxHbs have, on average, higher oxygen affinities, slower dissociation rate constants, and faster rate constants for autoxidation than their pentacoordinate counterparts [5]. Oxygen transport Hbs probably evolved pentacoordinate heme coordination because hexacoordination, being tighter in the ferric oxidation state, certainly favors autoxidation [59]. Kiger et al. [60], in a very insightful comparative examination of hxHbs, observed that autoxidation can be faster than oxygen binding or dissociation in tightly coordinated hxHbs, suggesting an outer-sphere reaction involving the bis-histidyl complex. Those hxHbs capable of oxygen binding also exhibit faster autoxidation starting from the oxy-complex, and are thus not suited for reversible oxygen transport. Such reactions, in combination with the observation of generally faster electron transport with hxHbs [61], support a role for hxHbs in redox chemistry rather than reversible oxygen binding. Thus, the presence or absence of hexacoordination in Hbs is generally predictive of whether the function is likely to involve oxygen transport or some form of redox biochemistry.

Reactions with inorganic nitrogen compounds- Reactions of heme proteins with inorganic nitrogen compounds are wide-spread in biology and have important roles in both dissimilatory and assimilatory nitrogen metabolism. In many of these cases the heme cofactors are only transferring elections, but in others they serve as the active site for binding and reacting with the nitrogen metabolite. Less is known about the reactions

of Hbs with nitrogenous compounds. Azide and cyanide bind tightly and reversibly to most ferric Hbs [17], and less tightly to the ferrous oxidation states. Exogenous imidazole will also bind to Hbs, and mimic hexacoordination [59,62]. Nitric oxide binds reversibly to both oxidation states, but tightest to ferrous heme [17]. The reactions described below outline not only the reversible reactions with Hbs, but also those that result in redox changes for the heme and substrate. These include chemical reactions with nitric oxide, nitrite, and hydroxylamine.

Nitrite: Hbs react with nitrite in both the deoxyferrous and oxyferrous oxidation states, with markedly different outcomes. The reaction between oxyhemoglobin (oxy-rbcHb) and nitrite was first reported by Arthur Gamgee in 1868 [63], who observed the oxidation of oxy-rbcHb upon addition of nitrite. Although the products of this reaction were firmly identified as ferric hemoglobin and nitrate [64], and the reaction is recognized as a nitrite-induced autooxidation [65], the actual mechanism is still unclear. Keszler *et al.* proposed a model with H_2O_2 and the ferryl hemoglobin (ferrylHb) radical in which nitrite is involved in the faster propagation-phase of the reaction [66]. Nevertheless, this reaction explains the toxicity of nitrite to humans due to hemoglobinemia resulting from heme oxidation and dissociation [67,68].

Surprisingly, all of the studies concerning nitrite reactions with oxyHb are with pxHbs (mostly human rbcHb and muscle myoglobin), but not hxHbs. The fact that many hxHbs are often unstable with oxygen is certainly to blame, but others, such as nsHb1 from plants, can form relatively stable oxy complexes [28,31]. Class 1 nsHbs are expressed

during hypoxia, which is also associated with elevated levels of nitrite [69,70] thus, if oxygen concentrations were high enough to bind the Hb, there would be a potential for the reaction.

The second reaction of Hbs with nitrite is much more relevant to hxHbs. At the beginning of twentieth century, John Haldane reported the reaction between deoxyhemoglobin (deoxy-rbcHb) and nitrite while researching the chemistry of meat curing [71]. He found that the red color of salted meat results from nitric oxide (NO) binding to deoxyferrous Hb, forming a ferrous-nitrosyl rbcHb complex (which to the eye resembles the color of fresh oxygenated meat more than the brown color associated with oxidation). NO is produced by the reaction of nitrite with deoxyHb in the absence of oxygen. The bimolecular reaction passes one electron from ferrous heme to nitrite, making NO and ferric heme (Reaction 5). Since binding of NO to ferrous Hb (reaction 4) is extremely rapid (k_{NO} ~ 100 μM^{-1} s^{-1}) [72], the NO formed in the reaction rapidly binds the remaining ferrous Hb making the stable ferrous-NO complex associated with red color.

$$Hb^{Fe(II)} + NO_2^- + H^+ \xrightarrow{k_{NO_2^-}} Hb^{Fe(III)} + NO + HO^- \qquad \text{(Reaction 3)}$$

$$Hb^{Fe(II)} + NO \xrightarrow{k_{NO}} Hb^{Fe(II)}NO \qquad \text{(Reaction 4)}$$

$$2Hb^{Fe(II)} + NO_2^- + H^+ \xrightarrow{k_{obs}} Hb^{Fe(III)} + Hb^{Fe(III)}NO + HO^- \qquad \text{(Reaction 5)}$$

Nitrite reductase activity only occurs with the deoxyferrous form of Hbs and is common in both pxHbs and hxHbs (Table 2). The speed of the reaction varies between

different Hbs, and does not correlate with coordination state or strength of coordination in hxHbs. Human rbcHb is not a good nitrite reductase in the deoxyferrous form (T state). But when it is saturated by 40-60% oxygen (about half T state, half R state), it shows its maximum nitrite reductase activity (6 M^{-1} s^{-1}) [73-75]. Deoxy Mb reduces nitrite with a bimolecular rate constant of 11 M^{-1} s^{-1}, reportedly protecting heart cells from myocardial ischemia-reperfusion injury [76,77].

Plant class 1 nsHbs and SynHb react relatively rapidly with nitrite (~ 160 M^{-1} s^{-1}) [78] compared to rbcHb, Mb, and animal hxHbs (Ngb and Cgb) [79,80]. In the case of Ngb, the wild type protein reduces nitrite very slowly, but when the distal histidine is mutated to leucine or glutamine, the rate increases dramatically to ~ 250 M^{-1} s^{-1}, on par with the plant nsHbs [79]. Thus, hexacoordination is not required for rapid rates of nitrite reduction, and in fact hexacoordination in wild type Ngb clearly inhibits the reaction.

The reduction of nitrite by both pxHbs and hxHbs is thought to play important roles in the diverse tissues where these different proteins are located. In plants and cyanobacteria, nitrate and nitrite concentration can increase to high (millimolar) levels, especially under hypoxic conditions [69,70]. In these conditions, plant nsHbs could effectively reduce nitrite to aid in nitrogen assimilation to produce ammonium, or dissimilation to aid the regeneration of NAD^+. In support of this mechanism is the fact that nsHb1 also reduces hydroxylamine to ammonia, another reaction on this pathway. Along these lines, the hxHb from the cyanobacteria synechococcus aids in growth on high concentrations of nitrate, possibly by detoxifying peroxynitrite that results from NO production by nitrate or nitrite reductase [42].

In animals, nitrite reductase activity of Ngb is proposed to be important in regulating NO metabolism for the protection of neurons during hypoxia [81-83]. Petersen *et al.* studied the reaction between murine deoxy Ngb and nitrite [84] reporting a second order rate constant of 5.1 M^{-1} s^{-1} for the reaction. They found that ferric Ngb was the main product, and ferrous nitrosyl Ngb was present in smaller amounts (less than 20% of total product). This high product ratio of ferric to ferrous nitrosyl Ngb was explained as being due to the lower affinity of Ngb for NO compared to Mb and Hb [72]. Another study of deoxyferrous human Ngb nitrite reduction by Tiso *et al.* [79] measured a rate constant of 0.12 M^{-1} s^{-1} resulting in a 1:1 ratio of ferric Ngb and ferrous nitrosyl Ngb. Tiso *et al*. also proposed that the nitrite reductase activity of Ngb is correlated with coordination state, based on the fact that the pentacoordinate Ngb mutant proteins H64L and H64Q speed up nitrite reduction ~2000 times compared to the wild type protein. Mutations that strengthen coordination (C55A and C46A) were shown to slow the reaction.

Cgb is a hxHb that is expressed in almost all tissues [85,86]. Despite its slow rate of nitrite reduction (0.14 M^{-1} s^{-1}), Li *et al.* have recently suggested that its function as a nitrite reductase might be significant [80]. Nitrite reduction by deoxyferrous Cgb produces a slightly smaller ratio of nitrosyl Cgb than ferric Cgb, and nM scale NO release from this reaction was measured by EPR and a gas phase chemiluminescence NO analyzer. Together with Cgb's up-regulation during hypoxia [87], these results support a hypothesis involving NO metabolism during hypoxia.

Nitric Oxide: Just as the reactions of Hbs with nitrite depends greatly on the starting oxidation and ligand state of the heme iron, so do those with NO. Deoxy Hbs generally reversibly bind NO with very high affinity constants, which are in the picomolar range for blood Hb and Mb [88]. Ferric Hbs also reversibly bind NO but typically with much lower affinity, and ferric Hbs can be slowly reduced by NO, suggesting NO is bound following reduction. In general, hexacoordination lowers NO affinity in both oxidations states [72,89], and has no clear effect on NO-induced reduction of the ferric proteins [90].

If NO contacts the oxyferrous form of Hb, a very rapid chemical reaction called "NO dioxygenation" (NOD) occurs, in which NO reacts with bound oxygen, eventually making nitrate and oxidizing the heme iron (Reaction 6). NOD is the function of bacterial and fungal "flavohemoglobins" (flavoHbs), who use it to detoxify NO in their surroundings or resulting from endogenous sources [91-94]. As implied by their name, flavoHbs have a heme domain and a flavin domain [95]. In the NOD reaction, the oxyferrous heme domain reacts with NO to make nitrate and ferric heme. The flavin domain then shuttles an electron from NADH to the heme to re-reduce it so that it can bind oxygen to start the cycle again.

$$Hb^{Fe(II)}O_2 + NO \longrightarrow Hb^{Fe(III)}\text{–}OONO \longrightarrow Hb^{Fe(III)} + NO_3^- \qquad \text{(Reaction 6)}$$

While NOD activity was first found in flavoHb [92], most Hbs (both hexa- and pentacoordinate) can carry out the oxidative NOD reaction very effectively [90]. However, flavoHb can rapidly finish the reductive half of the NOD reaction by using NADH to reduce

the ferric heme back to the ferrous form (Figure 2). For Hbs to scavenge NO using the NOD mechanism, there must be an effective mechanism for heme reduction. NOD activity has been ascribed to plant nsHbs, and three mechanisms of reduction have been proposed including specific enzymes, free flavins [96] and ascorbic acid [97]. In the ascorbic acid mechanism, it was proposed that monodehydroascorbate reductase (MDHAR)-mediated ascorbate reduction of metHb might facilitate NO scavenging. However, it has been shown that ascorbic acid reduction of ferric rice nsHb1 is very slow (0.01 $mM^{-1}min^{-1}$) compared to NADH reduction of flavoHb and that hemoglobin reduction by ascorbate is not affected by MDHAR *in vitro* [93,98].

Reactions with ROS and peroxides- Fenton chemistry (Reaction 7), described for the first time in 1894 [99], explains the role of ferrous iron in generating hydroxyl radical through a reaction with hydrogen peroxide. The resulting radicals are highly unstable and capable of oxidizing organic substances [100].

$$\mathrm{Fe(II)} + \mathrm{H_2O_2} \longrightarrow \mathrm{Fe(III)} + \mathrm{HO^*} + \mathrm{HO^-} \qquad \text{(Reaction 7)}$$

The fact that free iron is released by heme degradation, oxidative stress, and by heme oxygenase activity has led to speculation about the involvement Hbs in Fenton-related reactions. The reaction of hydrogen peroxide and respiratory Hbs (rbcHb and Mb) were shown to generate radicals by Gibson *et al.* in 1956 [101] and 1958 [102]. Since then, the reaction has been studied extensively [1,19,56,100]. Mb reacts with hydrogen

peroxide in the deoxy ferrous (II) and ferric (III) states, both becoming oxidized to the ferryl (IV) oxidation state [103]. Since the reduction of H_2O_2 is a two-electron process, ferrous heme is converted to the ferryl species directly (Reaction 8). The two-electron oxidation of ferric heme results in ferryl heme and the extraction of one electron from the protein matrix, generating a protein radical (Reaction 9) [1,56].

$$Mb^{Fe(II)} + H_2O_2 \longrightarrow [Mb^{Fe(IV)} = O] + H_2O \qquad \text{(Reaction 8)}$$

$$Mb^{Fe(III)} + H_2O_2 \longrightarrow [Mb^{*+\,Fe(IV)} = O] + H_2O \qquad \text{(Reaction 9)}$$

In Mb, the resulting ferryl species can combine with another ferrous deoxy (II) Mb resulting in two molecules of ferric Mb (III) (Reaction 10).

$$Mb^{Fe(II)} + \left[Mb^{Fe(IV)} = O\right] \longrightarrow 2\ Mb^{Fe(III)} + HO^- \qquad \text{(Reaction 10)}$$

In the case of the ferryl protein radical, the radical can migrate outwards from the heme center. The Tyr151 and Trp14 side chains of Mb have been shown to be involved in radical migration [1,104]. In dedicated peroxidases such as horseradish peroxidase and catalase, the radical is contained and employed in catalysis [1]. This radical is finally quenched by oxidation of external substrates such as lipids or lipid peroxides, a process that regenerates ferric heme. The newly formed ferric Mb can again undergo reaction with excess H_2O_2 leading to “pseudo-peroxidase” reactions consuming peroxide [56] as summarized in Figure 3 (derived from Richards [56]).

Highly reactive byproducts from H_2O_2 reactions with Hbs induce pathological conditions such as ischemic/reperfusion injuries, atherosclerosis, and complications with blood substitutes [1]. Lipid peroxides are formed by reaction of ROS (such as H_2O_2) and ferryl Hb in the presence of oxygen [105-107] (Figure 3). The process of lipid peroxidation, with its associated DNA alterations and posttranslational protein modifications, is central to these pathologies [1,108,109]. Red blood cells experience extensive lipid peroxidation that can weaken cell membranes causing hemolysis and associated disorders [110]. Lipid peroxidation has also been linked to genotoxicity and carcinogenicity [109], but recent research suggests cell signaling molecules generated in this way might be beneficial rather than deleterious, implying that the role of Cgb might be to regulate concentrations rather than in scavenging of ROS [1,111,112].

The reaction of ferric Mb with peroxide proceeds as a heterolytic reaction, meaning that both elections are lost from the heme-protein complex (Reaction 9). Ferric Mb can react with lipid peroxides (LOOH) (Reaction 11) in a similar fashion as hydrogen peroxide, but can also carry out a homolytic fission (reaction 12) of the lipid peroxide, generating a lipid alkoxyl radical (LO.). Figure 3 summarizes these reactions of Mb and the immediate branch reactions of physiological importance.

$$\mathrm{Mb}^{\mathrm{Fe(III)}} + \mathrm{LOOH} \longrightarrow [Mb^{*+\,\mathrm{Fe(IV)}} = O] + \mathrm{LOH} \qquad \text{(Reaction 11)}$$

$$\mathrm{Mb}^{\mathrm{Fe(III)}} + \mathrm{LOOH} \longrightarrow [Mb^{+\,\mathrm{Fe(IV)}} = O] + \mathrm{LO}^{*} + H^{+} \qquad \text{(Reaction 12)}$$

Instead of transferring an electron to an external substrate, Hb radicals can also cause covalent linkage between the heme porphyrin and the protein matrix [100]. Covalent linkages are formed by the reaction of a protonated ferryl heme with a protein radical (often a tyrosine) generated by H_2O_2 [113]. This covalent cross-link to the globin has different spectral characteristics that have been used to suggest the presence of unstable ferryl species, which are otherwise difficult to detect given their reactivity [114]. Nothnagel et al. tested whether the heme-protein cross link in SynHb and Synecococcus Hb might stabilize them against H_2O_2 bleaching, as is known to happen in dedicated peroxidases, but did not find a correlation between cross-linking and stability [115].

Pseudo-peroxidase and lipid peroxidase activities of respiratory Hbs are relevant physiologically and have thus been the focus of a number of studies [116]. HxHbs, being relatively recent discoveries, have not yet been subjected to the same degree of research, but appear to undergo similar reactions with peroxides. The hxHbs Ngb and Cgb have pseudo-peroxidase activities comparable with Mb, which are significantly lower than horse radish peroxidase [117] (Table 3). A similar conclusion was reached for rice nsHb1 and extended to other plant Hbs [118]. However, the chemistry of Cgb seems especially equipped for lipid oxidation compared to other hxHbs [119]. This is evinced by facile binding and oxidation of lipids by ferric Cgb, and the decrease in distal histidine coordination affinity upon lipid binding. The mechanism causing the unique interaction of Cgb with lipids is not well understood and, despite the structural similarity to other hxHbs, is not shared by Ngb or Mb.

Redox and ROS chemistry of the vertebrate hxHbs Ngb and Cgb have received a great deal of attention because of their presence in human tissues, and potential roles in medically relevant reactions [1,5,111,117,120-124]. It has been shown that expression of both is up-regulated 2 to 4 fold by hypoxia [125,126]. Additionally, Cgb expression is also induced by oxidative stress, as demonstrated by a similar increase in Cgb mRNA levels in mouse N2a neuroblastoma cells exposed to H_2O_2 [127].

The objective of research concerning these Hbs and their peroxidase/ROS activities has been to control and vary expression in tissues *in vivo*, and assay for the degree of damage resulting from different introduced or natural chemical challenges. For example, such work with Ngb has been actively pursued given its localization in brain tissue and potential for protection against ischemia/reperfusion injury [123,128-130]. Overexpression by a factor of 4-5 fold is generally achieved *in vivo* by the aforementioned groups, which results in lower infarct size following ischemia/reperfusion, and decreased peroxide-induced DNA mutations.

McRonald, et al. [120] investigated an oesophageal cell line known to decrease Cgb expression during the onset of cancer. If Cgb mitigates oxidative stress in normal cells, the lower levels in the Cgb-deficient cells were expected to show increased cancer progression due to increased sensitivity to redox damage. While the Cgb-deficient cells showed greater cancer progression compared to those overexpressing Cgb by 4-7 times, they were not significantly different from cells expressing normal levels of Cgb. Thus, the above experimental models often lead to results that are difficult to interpret, as the nonspecific

properties of over-expressed levels of Hb can potentially lead to new phenotypes that mask the natural function of the Hb in question at normal levels in the cell.

A relatively less explored role of hxHbs, particularly given their low cellular concentrations, is in cell signaling. Ferric Hbs can directly react with lipid peroxides leading to protein-based radicals, carbon-centered lipid radicals, and other biomolecular radicals (Figure 3). These highly unstable species are capable of reacting with and oxidizing a wide array of biomolecules such as ascorbate, or even phenol at higher pH [56]. Lipid peroxidation is an autocatalytic process that produces a spectrum of oxidized lipid-based byproducts called electrophilic lipids [1]. Isoprostanes are one example of electrophilic lipids that induce phosphorylation of p38 mitogen activated protein (MAP) kinase, which regulates cell contraction and hypertension [1,131]. Electrophilic lipids have also been implicated in both anti- and pro-apoptotic signaling pathways mediated through posttranslational protein modifications, depending on their concentrations [1,132]. Thus hxHbs share heme-based lipid chemistry with pxHbs and could have potential roles in cell signaling that need to be explored in more detail.

Electron transfer reactions between proteins- Heme is common cofactor in biological electron transfer reactions where it mediates the facile gain or loss of an electron to form the ferrous or ferric heme iron, respectively. Thus, a single heme is good for transferring one electron, but many hemes often work together toward multi-electron transfer reactions. The midpoint reduction potentials (E_m) of these cofactors obviously influence the direction of electron transfer [133], and the varied proteinaceous

environments surrounding heme can exert profound influences on E_m as evidenced by the 800 mv variation across different heme proteins [134]. Factors responsible for different E_m values for these hemes include the type of heme, the degree of solvent exposure [135], the nature of axial coordination [136], and the electrostatic environment near the heme propionates [137]. In general E_m is highest for His-Met coordination (282±102 mV), slightly lower for aquo-His or pentacoordinated proteins (-36 ±196 mV) and lowest for proteins with His-His coordination (-183±155mV) [134].

Experiments to directly measure electron transfer by heme proteins have been developed using a variety of techniques and reactions [138-145]. In some, net electron transfer from one protein to another is monitored, while in others the "self-exchange" of electrons within a population of molecules is monitored at equilibrium with no net exchange of electrons [138]. The former reactions (non equilibrium "net transfer") take advantage of spectrally distinct species to monitor the transfer of electrons from a reduced protein (most often with a lower E_m) to an oxidized partner (usually with a higher E_m). If the reaction were between two proteins with equivalent E_m values, it is driven forward by the differential concentration of electrons between the two starting populations. For pairs of proteins with distinct E_m values, the favorable flow of electrons from lower to higher E_m also contributes to the driving force for the reaction. "Self-exchange" refers to electron exchange between a population of oxidized and reduced molecules when there is no driving force for net electron transfer; rather, the experiment monitors the equilibrium exchange between the homogeneous populations of molecules. Both types of experiments yield bimolecular rate constants for electron transfer that are

deemed indicative of the general propensity for electron transfer, but there has been little comparison of rate constants between techniques and reactions in an effort to test this assumption.

Rate constants for electron transfer for Hbs and some heme proteins are listed in Table 4 in an effort to put electron transfer in hxHbs into perspective. The values vary between those of known electron transfer proteins to self-exchange between oxygen transport Hbs, and have a range of rate constants from 108 to 102 $M^{-1}s^{-1}$. The rate constants for oxygen transport Hbs are on the slower end of this spectrum, but even these values are probably over-estimated as the use of trimethylphosphine (PMe3) was necessary to get the reaction to occur on a time scale convenient for measurement. This is probably because PMe3 binds to pxHbs in both oxidation states and minimizes the change in spin state accompanying electron transfer that would otherwise slow the reaction [146]. In support of this theory is the fact that electron transfer by or between hxHbs requires no PMe3, as distal histidine coordination serves this role in hxHbs. As has been discussed earlier in this review, bis-histidyl heme coordination facilitates electron transfer kinetics and, in hxHbs, generally lowers E_m compared to pxHbs.

Two hxHbs that seem best suited for a dedicated role in electron transfer are GLB-6 ,16 and GLB-26 from *Caenorhabditis elegans* [147], which, like cytochrome b_5, do not bind oxygen or CO because of tight hexacoordination. Kiger *et al.* [60] conducted a comparative study of the ability of Mb (representing pxHbs) and several hxhbs (Ngb, Cgb and *C. elegans* GLB-26) to transfer electrons to cytochrome *c*. They found that transfer from ferrous hxHbs to cytochrome *c* is 10 to 1000 times faster than Mb. These results are

consistent with the generally faster rates of electron transfer in hxHbs when the reaction is initiated chemically [61]. Thus, if hxHbs such as GLB-6 and GLB-26 are incapable of binding ligands at their heme active sites but are efficient at transferring electrons, it is a safe assumption that their functions are related to the latter.

There are clear physiological implications from the reduction of cytochrome c by Ngb [148,149]. Cytochrome *c*, released from the mitochondria during cytotoxic stress, binds and induces oligomerization of Apaf-1 (apoptotic protease activating factor-1) to form a complex called the apoptosome. The apoptosome recruits and activates caspase 9, which further activates downstream "executioner" caspases that bring about cell damage [150]. Ngb is proposed to provide a protective mechanism by reducing ferric cytochrome *c* back to the ferrous state, and by binding to cytochrome *c* and disrupting its association with Apaf-1 [151,152]. This hypothesis is supported by 1) a ~ 40% decrease in triggering of apoptosis by ferrous cytochrome c compared to ferric cytochrome *c* [148], 2) a relatively tight association of ferrous Ngb with ferric cytochrome *c* (K_A= $2x10^4$ M^{-1}) measured by surface plasmon resonance [153], and 3) relatively rapid electron transfer from ferrous Ngb to ferric cytochrome *c in vitro* [60] (Table 4).

Electron transfer between proteins must also be involved in hydroxylamine reduction by plant nsHb and SynHb [154]. The reduction of hydroxylamine to ammonium (Reaction 13), requires the input of two electrons, and converts two Hb molecules from the ferrous to the ferric oxidation state with no evidence for partially reduced intermediates. One Hb monomer must bind hydroxylamine and deliver one electron, followed by intermolecular transfer of the second electron from another Hb molecule. A

hexacoordinate heme site alone is not sufficient for rapid hydroxylamine reduction, as Ngb and Cgb are no faster than Mb, suggesting that the specific structures of nsHb and SynHb are tailored for rapid electron exchange. The structural and chemical mechanisms of this reaction, including whether or not electron transfer is rate-limiting, is not yet understood. Electron self-exchange has been directly measured in SynHb and Synechococcus hxHb, yielding values around 10^3 $M^{-1}s^{-1}$ (Table 4), which is on-par with cytochrome b_5 (10^3 $M^{-1}s^{-1}$), and rates estimated for PMe3-Mb [155], but slightly slower than self-exchange in cytochrome *c* (105 $M^{-1}s^{-1}$) [156]. However, the value of 103 $M^{-1}s^{-1}$ is at least 100-fold too slow to support the observed rates of hydroxylamine reduction by SynHb [154]. Thus, this reaction mechanism requires further study.

$$2\mathrm{Hb}^{\mathrm{Fe(II)}} + \mathrm{NH_2OH} \xrightarrow{\mathrm{Aq}} 2\mathrm{Hb}^{\mathrm{Fe(III)}} + \mathrm{NH_4^+} \qquad \text{(Reaction 13)}$$

A role for electron transfer and hexacoordination has also been reported in rbcHb alpha chains [157,158]. RbcHb assembly requires a chaperone for alpha chains to prevent aggregation, unfolding, and heme loss. This chaperone, “Alpha Hemoglobin Stabilizing Protein” (AHSP), binds ferric alpha chains and prevents denaturation. Binding triggers a change in the alpha globin coordination state, causing bis-histidyl hexacoordination [159], which stabilizes them against hemin loss, ROS production, and precipitation. Hexacoordination also facilitates hemin reduction, which is a necessary step in rbcHb assembly, and could the trigger for alpha chain release from AHSP [160].

Conclusion:

Attempts to understand the biochemical functions of hxHbs are caged in the context of more than a half-century of biophysical studies of oxygen transport pxHbs such as rbcHb and Mb. The heme prosthetic group found in both groups of Hbs clearly conveys a propensity for reversible ligand binding, electron transfer, pseudo peroxidase activity with a variety of substrates, and direct redox biochemistry with a variety of substrates. These activities are found in both pxHbs and hxHbs, and arguments have been made that they are significant to innate physiology, bioengineering, agriculture and medicine for both classes of Hbs. The clearest general differences between pxHbs and hxHbs that might be used in consideration of potential functions for hxHbs are: 1) hxHbs are less stable for reversible oxygen binding, and are more likely to autoxidize, thus producing ROS. 2) HxHbs are better suited for gaining or losing electrons at the heme iron, facilitating electron transfer, multi-electron reactions, and catalytic redox chemistry requiring cyclic reduction or oxidation of the heme iron. 3) Cgb stands out for its ability to rapidly oxidize lipids, and 4) plant and cyanobacterial Hbs reduce nitrite much more rapidly than other Hbs.

References:

1. Reeder BJ. The redox activity of hemoglobins: from physiologic functions to pathologic mechanisms. Antioxidants & redox signaling 2010;13(7):1087-1123.

2. Cossins A, Berenbrink M. Physiology: Myoglobin's new clothes. Nature 2008;454(7203):416-417.

3. Brunori M. Nitric oxide moves myoglobin centre stage. Trends in biochemical sciences 2001;26(4):209-210.

4. Straub AC, Lohman AW, Billaud M, Johnstone SR, Dwyer ST, Lee MY, Bortz PS, Best AK, Columbus L, Gaston B, Isakson BE. Endothelial cell expression of haemoglobin alpha regulates nitric oxide signalling. Nature 2012;491(7424):473-477.

5. Kakar S, Hoffman FG, Storz JF, Fabian M, Hargrove MS. Structure and reactivity of hexacoordinate hemoglobins. Biophysical chemistry 2010;152(1-3):1-14.

6. de Sanctis D, Dewilde S, Vonrhein C, Pesce A, Moens L, Ascenzi P, Hankeln T, Burmester T, Ponassi M, Nardini M, Bolognesi M. Bishistidyl heme hexacoordination, a key structural property in Drosophila melanogaster hemoglobin. The Journal of biological chemistry 2005;280(29):27222-27229.

7. Sugimoto H, Makino M, Sawai H, Kawada N, Yoshizato K, Shiro Y. Structural basis of human cytoglobin for ligand binding. Journal of molecular biology 2004;339(4):873-885.

8. Vallone B, Nienhaus K, Matthes A, Brunori M, Nienhaus GU. The structure of carbonmonoxy neuroglobin reveals a heme-sliding mechanism for control of ligand affinity. Proceedings of the National Academy of Sciences of the United States of America 2004;101(50):17351-17356.

9. Vallone B, Nienhaus K, Brunori M, Nienhaus GU. The structure of murine neuroglobin: Novel pathways for ligand migration and binding. Proteins 2004;56(1):85-92.

10. Trent JT, 3rd, Kundu S, Hoy JA, Hargrove MS. Crystallographic analysis of synechocystis cyanoglobin reveals the structural changes accompanying ligand binding in a hexacoordinate hemoglobin. Journal of molecular biology 2004;341(4):1097-1108.

11. Hoy JA, Robinson H, Trent JT, 3rd, Kakar S, Smagghe BJ, Hargrove MS. Plant hemoglobins: a molecular fossil record for the evolution of oxygen transport. Journal of molecular biology 2007;371(1):168-179.

12. Hoy JA, Kundu S, Trent JT, 3rd, Ramaswamy S, Hargrove MS. The crystal structure of Synechocystis hemoglobin with a covalent heme linkage. The Journal of biological chemistry 2004;279(16):16535-16542.

13. Hargrove MS, Brucker EA, Stec B, Sarath G, Arredondo-Peter R, Klucas RV, Olson JS, Phillips GN, Jr. Crystal structure of a nonsymbiotic plant hemoglobin. Structure 2000;8(9):1005-1014.

14. de Sanctis D, Dewilde S, Pesce A, Moens L, Ascenzi P, Hankeln T, Burmester T, Bolognesi M. Crystal structure of cytoglobin: the fourth globin type discovered in man displays heme hexa-coordination. Journal of molecular biology 2004;336(4):917-927.

15. de Sanctis D, Ascenzi P, Bocedi A, Dewilde S, Burmester T, Hankeln T, Moens L, Bolognesi M. Cyanide binding and heme cavity conformational transitions in Drosophila melanogaster hexacoordinate hemoglobin. Biochemistry 2006;45(33):10054-10061.

16. Yoon J, Herzik MA, Jr., Winter MB, Tran R, Olea C, Jr., Marletta MA. Structure and properties of a bis-histidyl ligated globin from Caenorhabditis elegans. Biochemistry 2010;49(27):5662-5670.

17. Antonini EaB, M. Hemoglobin and Myoglobin in their interaction with ligands North-Holland, Amsterdam; 1971. 436 p.

18. Pesce A, Couture M, Dewilde S, Guertin M, Yamauchi K, Ascenzi P, Moens L, Bolognesi M. A novel two-over-two alpha-helical sandwich fold is characteristic of the truncated hemoglobin family. The EMBO journal 2000;19(11):2424-2434.

19. Rifkind JM, Ramasamy S, Manoharan PT, Nagababu E, Mohanty JG. Redox reactions of hemoglobin. Antioxidants & redox signaling 2004;6(3):657-666.

20. More C, Belle V, Asso M, Fournel A, Roger G, Guigliarelli B, Bertrand P. EPR spectroscopy: a powerful technique for the structural and functional investigation of metalloproteins. Biospectroscopy 1999;5(5 Suppl):S3-18.

21. Pesce A, Bolognesi M, Bocedi A, Ascenzi P, Dewilde S, Moens L, Hankeln T, Burmester T. Neuroglobin and cytoglobin. Fresh blood for the vertebrate globin family. EMBO reports 2002;3(12):1146-1151.

22. Hamdane D, Kiger L, Dewilde S, Green BN, Pesce A, Uzan J, Burmester T, Hankeln T, Bolognesi M, Moens L, Marden MC. The redox state of the cell regulates the ligand binding affinity of human neuroglobin and cytoglobin. The Journal of biological chemistry 2003;278(51):51713-51721.

23. Burmester T, Weich B, Reinhardt S, Hankeln T. A vertebrate globin expressed in the brain. Nature 2000;407(6803):520-523.

24. Lechauve C, Chauvierre C, Dewilde S, Moens L, Green BN, Marden MC, Celier C, Kiger L. Cytoglobin conformations and disulfide bond formation. The FEBS journal 2010;277(12):2696-2704.

25. Ezhevskaya M, Trandafir F, Moens L, Dewilde S, Van Doorslaer S. EPR investigation of the role of B10 phenylalanine in neuroglobin - evidence that B10Phe mediates structural changes in the heme region upon disulfide-bridge formation. Journal of inorganic biochemistry 2011;105(9):1131-1137.

26. Van Doorslaer S, Vinck E, Trandafir F, Ioanitescu I, Dewilde S, Moens L. Tracing the structure-function relationship of neuroglobin and cytoglobin using resonance Raman and electron paramagnetic resonance spectroscopy. IUBMB life 2004;56(11-12):665-670.

27. Vinck E, Van Doorslaer S, Dewilde S, Moens L. Structural change of the heme pocket due to disulfide bridge formation is significantly larger for neuroglobin than for cytoglobin. Journal of the American Chemical Society 2004;126(14):4516-4517.

28. Smagghe BJ, Hoy JA, Percifield R, Kundu S, Hargrove MS, Sarath G, Hilbert JL, Watts RA, Dennis ES, Peacock WJ, Dewilde S, Moens L, Blouin GC, Olson JS, Appleby CA. Review: correlations between oxygen affinity and sequence classifications of plant hemoglobins. Biopolymers 2009;91(12):1083-1096.

29. Watts RA, Hunt PW, Hvitved AN, Hargrove MS, Peacock WJ, Dennis ES. A hemoglobin from plants homologous to truncated hemoglobins of microorganisms. Proceedings of the National Academy of Sciences of the United States of America 2001;98(18):10119-10124.

30. Sainz M, Perez-Rontome C, Ramos J, Mulet JM, James EK, Bhattacharjee U, Petrich JW, Becana M. Plant hemoglobins may be maintained in functional form by

reduced flavins in the nuclei, and confer differential tolerance to nitro-oxidative stress. The Plant journal : for cell and molecular biology 2013;76(5):875-887.

31. Kundu S, Trent JT, 3rd, Hargrove MS. Plants, humans and hemoglobins. Trends in plant science 2003;8(8):387-393.

32. Duff SMG, Guy PA, Nie XZ, Durnin DC, Hill RD. Haemoglobin expression in germinating barley. Seed Sci Res 1998;8(4):431-436.

33. Morzan UN, Capece L, Marti MA, Estrin DA. Quaternary structure effects on the hexacoordination equilibrium in rice hemoglobin rHb1: insights from molecular dynamics simulations. Proteins 2013;81(5):863-873.

34. Goodman MD, Hargrove MS. Quaternary structure of rice nonsymbiotic hemoglobin. The Journal of biological chemistry 2001;276(9):6834-6839.

35. Mukhi N, Dhindwal S, Uppal S, Kumar P, Kaur J, Kundu S. X-ray crystallographic structural characteristics of Arabidopsis hemoglobin I and their functional implications. Biochimica et biophysica acta 2013;1834(9):1944-1956.

36. Kakar S, Sturms R, Tiffany A, Nix JC, DiSpirito AA, Hargrove MS. Crystal structures of Parasponia and Trema hemoglobins: differential heme coordination is linked to quaternary structure. Biochemistry 2011;50(20):4273-4280.

37. Sturms R, Kakar S, Trent J, 3rd, Hargrove MS. Trema and parasponia hemoglobins reveal convergent evolution of oxygen transport in plants. Biochemistry 2010;49(19):4085-4093.

38. Bykova NV, Igamberdiev AU, Ens W, Hill RD. Identification of an intermolecular disulfide bond in barley hemoglobin. Biochemical and biophysical research communications 2006;347(1):301-309.

39. Vinogradov SN, Tinajero-Trejo M, Poole RK, Hoogewijs D. Bacterial and archaeal globins - a revised perspective. Biochimica et biophysica acta 2013;1834(9):1789-1800.

40. Wittenberg JB, Bolognesi M, Wittenberg BA, Guertin M. Truncated hemoglobins: a new family of hemoglobins widely distributed in bacteria, unicellular eukaryotes, and plants. The Journal of biological chemistry 2002;277(2):871-874.

41. Falzone CJ, Christie Vu B, Scott NL, Lecomte JT. The solution structure of the recombinant hemoglobin from the cyanobacterium Synechocystis sp. PCC 6803 in its hemichrome state. Journal of molecular biology 2002;324(5):1015-1029.

42. Scott NL, Xu Y, Shen G, Vuletich DA, Falzone CJ, Li Z, Ludwig M, Pond MP, Preimesberger MR, Bryant DA, Lecomte JT. Functional and structural characterization of the 2/2 hemoglobin from Synechococcus sp. PCC 7002. Biochemistry 2010;49(33):7000-7011.

43. Hoy JA, Smagghe BJ, Halder P, Hargrove MS. Covalent heme attachment in Synechocystis hemoglobin is required to prevent ferrous heme dissociation. Protein science : a publication of the Protein Society 2007;16(2):250-260.

44. Scott NL, Falzone CJ, Vuletich DA, Zhao J, Bryant DA, Lecomte JT. Truncated hemoglobin from the cyanobacterium Synechococcus sp. PCC 7002: evidence for

hexacoordination and covalent adduct formation in the ferric recombinant protein. Biochemistry 2002;41(22):6902-6910.

45. Linberg R, Conover CD, Shum KL, Shorr RG. Hemoglobin based oxygen carriers: how much methemoglobin is too much? Artificial cells, blood substitutes, and immobilization biotechnology 1998;26(2):133-148.

46. Whitaker TL, Berry MB, Ho EL, Hargrove MS, Phillips GN, Jr., Komiyama NH, Nagai K, Olson JS. The D-helix in myoglobin and in the beta subunit of hemoglobin is required for the retention of heme. Biochemistry 1995;34(26):8221-8226.

47. Nagababu E, Rifkind JM. Heme degradation during autoxidation of oxyhemoglobin. Biochemical and biophysical research communications 2000;273(3):839-845.

48. Boretti FS, Buehler PW, D'Agnillo F, Kluge K, Glaus T, Butt OI, Jia Y, Goede J, Pereira CP, Maggiorini M, Schoedon G, Alayash AI, Schaer DJ. Sequestration of extracellular hemoglobin within a haptoglobin complex decreases its hypertensive and oxidative effects in dogs and guinea pigs. The Journal of clinical investigation 2009;119(8):2271-2280.

49. Goldman DW, Breyer RJ, 3rd, Yeh D, Brockner-Ryan BA, Alayash AI. Acellular hemoglobin-mediated oxidative stress toward endothelium: a role for ferryl iron. The American journal of physiology 1998;275(3 Pt 2):H1046-1053.

50. Balaji SN, Trivedi V. Extracellular Methemoglobin Mediated Early ROS Spike Triggers Osmotic Fragility and RBC Destruction: An Insight into the Enhanced Hemolysis During Malaria. Indian journal of clinical biochemistry : IJCB 2012;27(2):178-185.

51. Plotnikov EY, Chupyrkina AA, Pevzner IB, Isaev NK, Zorov DB. Myoglobin causes oxidative stress, increase of NO production and dysfunction of kidney's mitochondria. Biochimica et biophysica acta 2009;1792(8):796-803.

52. Huang SS, Koder RL, Lewis M, Wand AJ, Dutton PL. The HP-1 maquette: from an apoprotein structure to a structured hemoprotein designed to promote redox-coupled proton exchange. Proceedings of the National Academy of Sciences of the United States of America 2004;101(15):5536-5541.

53. Koder RL, Anderson JL, Solomon LA, Reddy KS, Moser CC, Dutton PL. Design and engineering of an O(2) transport protein. Nature 2009;458(7236):305-309.

54. Koder RL, Dutton PL. Intelligent design: the de novo engineering of proteins with specified functions. Dalton transactions 2006(25):3045-3051.

55. Haehnel W. Chemical synthesis of TASP arrays and their application in protein design. Molecular diversity 2004;8(3):219-229.

56. Richards MP. Redox reactions of myoglobin. Antioxidants & redox signaling 2013;18(17):2342-2351.

57. Kamga C, Krishnamurthy S, Shiva S. Myoglobin and mitochondria: a relationship bound by oxygen and nitric oxide. Nitric oxide : biology and chemistry / official journal of the Nitric Oxide Society 2012;26(4):251-258.

58. Shikama K. The Molecular Mechanism of Autoxidation for Myoglobin and Hemoglobin: A Venerable Puzzle. Chemical reviews 1998;98(4):1357-1374.

59. Halder P, Trent JT, 3rd, Hargrove MS. Influence of the protein matrix on intramolecular histidine ligation in ferric and ferrous hexacoordinate hemoglobins. Proteins 2007;66(1):172-182.

60. Kiger L, Tilleman L, Geuens E, Hoogewijs D, Lechauve C, Moens L, Dewilde S, Marden MC. Electron transfer function versus oxygen delivery: a comparative study for several hexacoordinated globins across the animal kingdom. PloS one 2011;6(6):e20478.

61. Weiland TR, Kundu S, Trent JT, 3rd, Hoy JA, Hargrove MS. Bis-histidyl hexacoordination in hemoglobins facilitates heme reduction kinetics. Journal of the American Chemical Society 2004;126(38):11930-11935.

62. Barrick D. Replacement of the proximal ligand of sperm whale myoglobin with free imidazole in the mutant His-93-->Gly. Biochemistry 1994;33(21):6546-6554.

63. Gamgee A. Researches on the Blood. On the Action of Nitrites on Blood. Philos Trans R Soc London 1868;158:589-625.

64. Kim-Shapiro DB, Gladwin MT, Patel RP, Hogg N. The reaction between nitrite and hemoglobin: the role of nitrite in hemoglobin-mediated hypoxic vasodilation. Journal of inorganic biochemistry 2005;99(1):237-246.

65. Kosaka H, Imaizumi K, Tyuma I. Mechanism of autocatalytic oxidation of oxyhemoglobin by nitrite. An intermediate detected by electron spin resonance. Biochimica et biophysica acta 1982;702(2):237-241.

66. Keszler A, Piknova B, Schechter AN, Hogg N. The Reaction between Nitrite and Oxyhemoglobin: A MECHANISTIC STUDY. Journal of Biological Chemistry 2008;283(15):9615-9622.

67. Smith RP. The nitrite methemoglobin complex--its significance in methemoglobin analyses and its possible role in methemoglobinemia. Biochemical pharmacology 1967;16(9):1655-1664.

68. Swann PF. The toxicology of nitrate, nitrite and n-nitroso compounds. Journal of the Science of Food and Agriculture 1975;26(11):1761-1770.

69. Ferrari TE, Varner JE. Intact tissue assay for nitrite reductase in barley aleurone layers. Plant physiology 1971;47(6):790-794.

70. Gupta KJ, Fernie AR, Kaiser WM, van Dongen JT. On the origins of nitric oxide. Trends in plant science 2011;16(3):160-168.

71. Haldane J. The Red Colour of Salted Meat. The Journal of hygiene 1901;1(1):115-122.

72. Van Doorslaer S, Dewilde S, Kiger L, Nistor SV, Goovaerts E, Marden MC, Moens L. Nitric oxide binding properties of neuroglobin. A characterization by EPR and flash photolysis. The Journal of biological chemistry 2003;278(7):4919-4925.

73. Huang Z, Shiva S, Kim-Shapiro DB, Patel RP, Ringwood LA, Irby CE, Huang KT, Ho C, Hogg N, Schechter AN, Gladwin MT. Enzymatic function of hemoglobin as a nitrite reductase that produces NO under allosteric control. The Journal of clinical investigation 2005;115(8):2099-2107.

74. Kozlov AV, Costantino G, Sobhian B, Szalay L, Umar F, Nohl H, Bahrami S, Redl H. Mechanisms of vasodilatation induced by nitrite instillation in intestinal lumen: possible role of hemoglobin. Antioxidants & redox signaling 2005;7(3-4):515-521.

75. Rong Z, Cooper CE. Modeling hemoglobin nitrite reductase activity as a mechanism of hypoxic vasodilation? Advances in experimental medicine and biology 2013;789:361-368.

76. Hendgen-Cotta UB, Merx MW, Shiva S, Schmitz J, Becher S, Klare JP, Steinhoff HJ, Goedecke A, Schrader J, Gladwin MT, Kelm M, Rassaf T. Nitrite reductase activity of myoglobin regulates respiration and cellular viability in myocardial ischemia-reperfusion injury. Proceedings of the National Academy of Sciences of the United States of America 2008;105(29):10256-10261.

77. Hendgen-Cotta UB, Kelm M, Rassaf T. A highlight of myoglobin diversity: the nitrite reductase activity during myocardial ischemia-reperfusion. Nitric oxide : biology and chemistry / official journal of the Nitric Oxide Society 2010;22(2):75-82.

78. Sturms R, DiSpirito AA, Hargrove MS. Plant and cyanobacterial hemoglobins reduce nitrite to nitric oxide under anoxic conditions. Biochemistry 2011;50(19):3873-3878.

79. Tiso M, Tejero J, Basu S, Azarov I, Wang X, Simplaceanu V, Frizzell S, Jayaraman T, Geary L, Shapiro C, Ho C, Shiva S, Kim-Shapiro DB, Gladwin MT. Human neuroglobin functions as a redox-regulated nitrite reductase. The Journal of biological chemistry 2011;286(20):18277-18289.

80. Li H, Hemann C, Abdelghany TM, El-Mahdy MA, Zweier JL. Characterization of the mechanism and magnitude of cytoglobin-mediated nitrite reduction and nitric oxide generation under anaerobic conditions. The Journal of biological chemistry 2012;287(43):36623-36633.

81. Brown GC. Nitric oxide and mitochondrial respiration. Biochimica et biophysica acta 1999;1411(2-3):351-369.

82. Loke KE, Laycock SK, Mital S, Wolin MS, Bernstein R, Oz M, Addonizio L, Kaley G, Hintze TH. Nitric oxide modulates mitochondrial respiration in failing human heart. Circulation 1999;100(12):1291-1297.

83. Allen JD, Gow AJ. Nitrite, NO and hypoxic vasodilation. British journal of pharmacology 2009;158(7):1653-1654.

84. Petersen MG, Dewilde S, Fago A. Reactions of ferrous neuroglobin and cytoglobin with nitrite under anaerobic conditions. Journal of inorganic biochemistry 2008;102(9):1777-1782.

85. Trent JT, 3rd, Hargrove MS. A ubiquitously expressed human hexacoordinate hemoglobin. The Journal of biological chemistry 2002;277(22):19538-19545.

86. Burmester T, Ebner B, Weich B, Hankeln T. Cytoglobin: A Novel Globin Type Ubiquitously Expressed inVertebrate Tissues. Molecular Biology and Evolution 2002;19(4):416-421.

87. Schmidt M, Gerlach F, Avivi A, Laufs T, Wystub S, Simpson JC, Nevo E, Saaler-Reinhardt S, Reuss S, Hankeln T, Burmester T. Cytoglobin is a respiratory protein in connective tissue and neurons, which is up-regulated by hypoxia. The Journal of biological chemistry 2004;279(9):8063-8069.

88. Eich RF, Li T, Lemon DD, Doherty DH, Curry SR, Aitken JF, Mathews AJ, Johnson KA, Smith RD, Phillips GN, Jr., Olson JS. Mechanism of NO-induced oxidation of myoglobin and hemoglobin. Biochemistry 1996;35(22):6976-6983.

89. Herold S, Fago A, Weber RE, Dewilde S, Moens L. Reactivity studies of the Fe(III) and Fe(II)NO forms of human neuroglobin reveal a potential role against oxidative stress. The Journal of biological chemistry 2004;279(22):22841-22847.

90. Smagghe BJ, Trent JT, III, Hargrove MS. NO Dioxygenase Activity in Hemoglobins Is Ubiquitous In Vitro, but Limited by Reduction In Vivo. PloS one 2008;3(4):e2039.

91. Poole RK, Anjum MF, Membrillo-Hernandez J, Kim SO, Hughes MN, Stewart V. Nitric oxide, nitrite, and Fnr regulation of hmp (flavohemoglobin) gene expression in Escherichia coli K-12. Journal of bacteriology 1996;178(18):5487-5492.

92. Gardner PR, Gardner AM, Martin LA, Salzman AL. Nitric oxide dioxygenase: an enzymic function for flavohemoglobin. Proceedings of the National Academy of Sciences of the United States of America 1998;95(18):10378-10383.

93. Gardner AM, Martin LA, Gardner PR, Dou Y, Olson JS. Steady-state and transient kinetics of Escherichia coli nitric-oxide dioxygenase (flavohemoglobin). The B10 tyrosine hydroxyl is essential for dioxygen binding and catalysis. The Journal of biological chemistry 2000;275(17):12581-12589.

94. Gardner PR. Nitric oxide dioxygenase function and mechanism of flavohemoglobin, hemoglobin, myoglobin and their associated reductases. Journal of inorganic biochemistry 2005;99(1):247-266.

95. Bonamore A, Boffi A. Flavohemoglobin: structure and reactivity. IUBMB life 2008;60(1):19-28.

96. Sainz M, Pérez-Rontomé C, Ramos J, Mulet JM, James EK, Bhattacharjee U, Petrich JW, Becana M. Plant hemoglobins may be maintained in functional form by reduced flavins in the nuclei, and confer differential tolerance to nitro-oxidative stress. The Plant Journal 2013:n/a-n/a.

97. Igamberdiev AU, Bykova NV, Hill RD. Nitric oxide scavenging by barley hemoglobin is facilitated by a monodehydroascorbate reductase-mediated ascorbate reduction of methemoglobin. Planta 2006;223(5):1033-1040.

98. Wang X, Hargrove MS. Nitric oxide in plants: the roles of ascorbate and hemoglobin. PloS one 2013;8(12):e82611.

99. Fenton HJH. OXIDATION OF TARTARIC ACID IN PRESEXCE OF IRON. Journal of the Chemical Society, Transactions 1894;65(65):899-911.

100. Reeder BJ, Svistunenko DA, Cooper CE, Wilson MT. The radical and redox chemistry of myoglobin and hemoglobin: from in vitro studies to human pathology. Antioxidants & redox signaling 2004;6(6):954-966.

101. Gibson JF, Ingram DJE. Location of Free Electrons in Porphin Ring Complexes. Nature 1956;178(4538):871-872.

102. Gibson JF, Ingram DJE, Nicholls P. Free Radical Produced in the Reaction of Metmyoglobin with Hydrogen Peroxide. Nature 1958;181(4620):1398-1399.

103. Alayash AI, Ryan BA, Eich RF, Olson JS, Cashon RE. Reactions of sperm whale myoglobin with hydrogen peroxide. Effects of distal pocket mutations on the formation and stability of the ferryl intermediate. The Journal of biological chemistry 1999;274(4):2029-2037.

104. Lardinois OM, Ortiz de Montellano PR. Intra- and intermolecular transfers of protein radicals in the reactions of sperm whale myoglobin with hydrogen peroxide. The Journal of biological chemistry 2003;278(38):36214-36226.

105. Kellogg EW, 3rd, Fridovich I. Superoxide, hydrogen peroxide, and singlet oxygen in lipid peroxidation by a xanthine oxidase system. The Journal of biological chemistry 1975;250(22):8812-8817.

106. Siddique YH, Ara G, Afzal M. Estimation of lipid peroxidation induced by hydrogen peroxide in cultured human lymphocytes. Dose-response : a publication of International Hormesis Society 2012;10(1):1-10.

107. Girotti AW. Lipid hydroperoxide generation, turnover, and effector action in biological systems. Journal of lipid research 1998;39(8):1529-1542.

108. Vaca CE, Wilhelm J, Harms-Ringdahl M. Interaction of lipid peroxidation products with DNA. A review. Mutation research 1988;195(2):137-149.

109. Marnett LJ. Lipid peroxidation-DNA damage by malondialdehyde. Mutation research 1999;424(1-2):83-95.

110. Ostrea EM, Jr., Cepeda EE, Fleury CA, Balun JE. Red cell membrane lipid peroxidation and hemolysis secondary to phototherapy. Acta paediatrica Scandinavica 1985;74(3):378-381.

111. Poli G, Leonarduzzi G, Biasi F, Chiarpotto E. Oxidative stress and cell signalling. Current medicinal chemistry 2004;11(9):1163-1182.

112. Farmer EE, Mueller MJ. ROS-mediated lipid peroxidation and RES-activated signaling. Annual review of plant biology 2013;64:429-450.

113. Reeder BJ, Svistunenko DA, Sharpe MA, Wilson MT. Characteristics and mechanism of formation of peroxide-induced heme to protein cross-linking in myoglobin. Biochemistry 2002;41(1):367-375.

114. Catalano CE, Choe YS, Ortiz de Montellano PR. Reactions of the protein radical in peroxide-treated myoglobin. Formation of a heme-protein cross-link. The Journal of biological chemistry 1989;264(18):10534-10541.

115. Nothnagel HJ, Preimesberger MR, Pond MP, Winer BY, Adney EM, Lecomte JT. Chemical reactivity of Synechococcus sp. PCC 7002 and Synechocystis sp. PCC 6803 hemoglobins: covalent heme attachment and bishistidine coordination. Journal of biological inorganic chemistry : JBIC : a publication of the Society of Biological Inorganic Chemistry 2011;16(4):539-552.

116. Arduini A, Eddy L, Hochstein P. Detection of ferryl myoglobin in the isolated ischemic rat heart. Free radical biology & medicine 1990;9(6):511-513.

117. Trandafir F, Hoogewijs D, Altieri F, Rivetti di Val Cervo P, Ramser K, Van Doorslaer S, Vanfleteren JR, Moens L, Dewilde S. Neuroglobin and cytoglobin as potential enzyme or substrate. Gene 2007;398(1-2):103-113.

118. Violante-Mota F, Tellechea E, Moran JF, Sarath G, Arredondo-Peter R. Analysis of peroxidase activity of rice (Oryza sativa) recombinant hemoglobin 1: implications for in vivo function of hexacoordinate non-symbiotic hemoglobins in plants. Phytochemistry 2010;71(1):21-26.

119. Reeder BJ, Svistunenko DA, Wilson MT. Lipid binding to cytoglobin leads to a change in haem co-ordination: a role for cytoglobin in lipid signalling of oxidative stress. The Biochemical journal 2011;434(3):483-492.

120. McRonald FE, Risk JM, Hodges NJ. Protection from intracellular oxidative stress by cytoglobin in normal and cancerous oesophageal cells. PloS one 2012;7(2):e30587.

121. Kawada N, Kristensen DB, Asahina K, Nakatani K, Minamiyama Y, Seki S, Yoshizato K. Characterization of a stellate cell activation-associated protein (STAP) with peroxidase activity found in rat hepatic stellate cells. The Journal of biological chemistry 2001;276(27):25318-25323.

122. Fordel E, Thijs L, Moens L, Dewilde S. Neuroglobin and cytoglobin expression in mice. Evidence for a correlation with reactive oxygen species scavenging. The FEBS journal 2007;274(5):1312-1317.

123. Li RC, Guo SZ, Lee SK, Gozal D. Neuroglobin protects neurons against oxidative stress in global ischemia. Journal of cerebral blood flow and metabolism : official journal of the International Society of Cerebral Blood Flow and Metabolism 2010;30(11):1874-1882.

124. Greenberg DA, Jin K, Khan AA. Neuroglobin: an endogenous neuroprotectant. Current opinion in pharmacology 2008;8(1):20-24.

125. Fordel E, Geuens E, Dewilde S, Rottiers P, Carmeliet P, Grooten J, Moens L. Cytoglobin expression is upregulated in all tissues upon hypoxia: an in vitro and in vivo

study by quantitative real-time PCR. Biochemical and biophysical research communications 2004;319(2):342-348.

126. Fordel E, Geuens E, Dewilde S, De Coen W, Moens L. Hypoxia/ischemia and the regulation of neuroglobin and cytoglobin expression. IUBMB life 2004;56(11-12):681-687.

127. Li D, Chen XQ, Li WJ, Yang YH, Wang JZ, Yu AC. Cytoglobin up-regulated by hydrogen peroxide plays a protective role in oxidative stress. Neurochemical research 2007;32(8):1375-1380.

128. Jin K, Mao Y, Mao X, Xie L, Greenberg DA. Neuroglobin expression in ischemic stroke. Stroke; a journal of cerebral circulation 2010;41(3):557-559.

129. Raida Z, Hundahl CA, Nyengaard JR, Hay-Schmidt A. Neuroglobin over expressing mice: expression pattern and effect on brain ischemic infarct size. PloS one 2013;8(10):e76565.

130. Sun Y, Jin K, Mao XO, Zhu Y, Greenberg DA. Neuroglobin is up-regulated by and protects neurons from hypoxic-ischemic injury. Proceedings of the National Academy of Sciences of the United States of America 2001;98(26):15306-15311.

131. Huber J, Bochkov VN, Binder BR, Leitinger N. The isoprostane 8-iso-PGE2 stimulates endothelial cells to bind monocytes via cyclic AMP- and p38 MAP kinase-dependent signaling pathways. Antioxidants & redox signaling 2003;5(2):163-169.

132. Levonen AL, Dickinson DA, Moellering DR, Mulcahy RT, Forman HJ, Darley-Usmar VM. Biphasic effects of 15-deoxy-delta(12,14)-prostaglandin J(2) on glutathione

induction and apoptosis in human endothelial cells. Arteriosclerosis, thrombosis, and vascular biology 2001;21(11):1846-1851.

133. Dutton PL. Redox potentiometry: determination of midpoint potentials of oxidation-reduction components of biological electron-transfer systems. Methods in enzymology 1978;54:411-435.

134. Zheng Z, Gunner MR. Analysis of the electrochemistry of hemes with E(m)s spanning 800 mV. Proteins 2009;75(3):719-734.

135. Sutin N, Yandell JK. Mechanisms of the reactions of cytochrome c. Rate and equilibrium constants for ligand binding to horse heart ferricytochrome c. The Journal of biological chemistry 1972;247(21):6932-6936.

136. Walker FA. Models of the bis-histidine-ligated electron-transferring cytochromes. Comparative geometric and electronic structure of low-spin ferro- and ferrihemes. Chemical reviews 2004;104(2):589-615.

137. Moore GR. Control of redox properties of cytochrome c by special electrostatic interactions. FEBS letters 1983;161(2):171-175.

138. Simonneaux G, Bondon A. Mechanism of electron transfer in heme proteins and models: the NMR approach. Chemical reviews 2005;105(6):2627-2646.

139. Nocek JM, Zhou JS, De Forest S, Priyadarshy S, Beratan DN, Onuchic JN, Hoffman BM. Theory and Practice of Electron Transfer within Proteinminus signProtein Complexes: Application to the Multidomain Binding of Cytochrome c by Cytochrome c Peroxidase. Chemical reviews 1996;96(7):2459-2490.

140. Firer-Sherwood MA, Bewley KD, Mock JY, Elliott SJ. Tools for resolving complexity in the electron transfer networks of multiheme cytochromes c. Metallomics : integrated biometal science 2011;3(4):344-348.

141. Winkler JR, Gray HB. Electron-Transfer in Ruthenium-Modified Proteins. Chemical reviews 1992;92(3):369-379.

142. Zarzycki P, Kerisit S, Rosso K. Computational methods for intramolecular electron transfer in a ferrous-ferric iron complex. Journal of colloid and interface science 2011;361(1):293-306.

143. Wallrapp FH, Voityuk AA, Guallar V. In-silico assessment of protein-protein electron transfer. a case study: cytochrome c peroxidase--cytochrome c. PLoS computational biology 2013;9(3):e1002990.

144. Amini A, Harriman A. Computational methods for electron-transfer systems. J Photoch Photobio C 2003;4(2):155-177.

145. Justinek M, Grampp G, Landgraf S, Hore PJ, Lukzen NN. Electron self-exchange kinetics determined by MARY spectroscopy: Theory and experiment. Journal of the American Chemical Society 2004;126(17):5635-5646.

146. Brunel CB, A.; Simonneaux, G. Mechanism of Electron Transfer in Hemoglobin: Evidence of Both Homosubunit and Heterosubunit Intermolecular Electron Transfers. Journal of the American Chmical Society 1994;116(26):11827–11832.

147. Geuens E, Hoogewijs D, Nardini M, Vinck E, Pesce A, Kiger L, Fago A, Tilleman L, De Henau S, Marden MC, Weber RE, Van Doorslaer S, Vanfleteren J, Moens L, Bolognesi

M, Dewilde S. Globin-like proteins in Caenorhabditis elegans: in vivo localization, ligand binding and structural properties. BMC biochemistry 2010;11:17.

148. Raychaudhuri S, Skommer J, Henty K, Birch N, Brittain T. Neuroglobin protects nerve cells from apoptosis by inhibiting the intrinsic pathway of cell death. Apoptosis : an international journal on programmed cell death 2010;15(4):401-411.

149. Fago A, Mathews AJ, Moens L, Dewilde S, Brittain T. The reaction of neuroglobin with potential redox protein partners cytochrome b5 and cytochrome c. FEBS letters 2006;580(20):4884-4888.

150. Li P, Nijhawan D, Budihardjo I, Srinivasula SM, Ahmad M, Alnemri ES, Wang X. Cytochrome c and dATP-dependent formation of Apaf-1/caspase-9 complex initiates an apoptotic protease cascade. Cell 1997;91(4):479-489.

151. Wei Y, McLendon GL, Hamilton AD, Case MA, Purring CB, Lin Q, Park HS, Lee CS, Yu T. Disruption of protein-protein interactions: design of a synthetic receptor that blocks the binding of cytochrome c to cytochrome c peroxidase. Chemical communications 2001(17):1580-1581.

152. Yu T, Wang X, Purring-Koch C, Wei Y, McLendon GL. A mutational epitope for cytochrome C binding to the apoptosis protease activation factor-1. The Journal of biological chemistry 2001;276(16):13034-13038.

153. Bonding SH, Henty K, Dingley AJ, Brittain T. The binding of cytochrome c to neuroglobin: a docking and surface plasmon resonance study. International journal of biological macromolecules 2008;43(3):295-299.

154. Sturms R, DiSpirito AA, Fulton DB, Hargrove MS. Hydroxylamine reduction to ammonium by plant and cyanobacterial hemoglobins. Biochemistry 2011;50(50):10829-10835.

155. Preimesberger MR, Pond MP, Majumdar A, Lecomte JT. Electron self-exchange and self-amplified posttranslational modification in the hemoglobins from Synechocystis sp. PCC 6803 and Synechococcus sp. PCC 7002. Journal of biological inorganic chemistry : JBIC : a publication of the Society of Biological Inorganic Chemistry 2012;17(4):599-609.

156. Dixon DW, Hong X, Woehler SE. Electrostatic and steric control of electron self-exchange in cytochromes c, c551, and b5. Biophysical journal 1989;56(2):339-351.

157. Mollan TL, Yu X, Weiss MJ, Olson JS. The role of alpha-hemoglobin stabilizing protein in redox chemistry, denaturation, and hemoglobin assembly. Antioxidants & redox signaling 2010;12(2):219-231.

158. Feng L, Gell DA, Zhou S, Gu L, Kong Y, Li J, Hu M, Yan N, Lee C, Rich AM, Armstrong RS, Lay PA, Gow AJ, Weiss MJ, Mackay JP, Shi Y. Molecular mechanism of AHSP-mediated stabilization of alpha-hemoglobin. Cell 2004;119(5):629-640.

159. Feng L, Zhou S, Gu L, Gell DA, Mackay JP, Weiss MJ, Gow AJ, Shi Y. Structure of oxidized alpha-haemoglobin bound to AHSP reveals a protective mechanism for haem. Nature 2005;435(7042):697-701.

160. Kiger L, Vasseur C, Domingues-Hamdi E, Truan G, Marden MC, Baudin-Creuza V. Dynamics of alpha-Hb chain binding to its chaperone AHSP depends on heme coordination and redox state. Biochimica et biophysica acta 2014;1840(1):277-287.

161. Smagghe BJ, Sarath G, Ross E, Hilbert JL, Hargrove MS. Slow ligand binding kinetics dominate ferrous hexacoordinate hemoglobin reactivities and reveal differences between plants and other species. Biochemistry 2006;45(2):561-570.

162. Bruno S, Faggiano S, Spyrakis F, Mozzarelli A, Abbruzzetti S, Grandi E, Viappiani C, Feis A, Mackowiak S, Smulevich G, Cacciatori E, Dominici P. The reactivity with CO of AHb1 and AHb2 from Arabidopsis thaliana is controlled by the distal HisE7 and internal hydrophobic cavities. Journal of the American Chemical Society 2007;129(10):2880-2889.

163. Ioanitescu AI, Dewilde S, Kiger L, Marden MC, Moens L, Van Doorslaer S. Characterization of nonsymbiotic tomato hemoglobin. Biophysical journal 2005;89(4):2628-2639.

164. Watts R. Characterisation of Non-symbiotic Haemoglobins from Dicotyledonous Plants. PhD Thesis, Division of Biochemistry and Molecular Biology Australian National University 1999.

165. Dou Y, Admiraal SJ, Ikeda-Saito M, Krzywda S, Wilkinson AJ, Li T, Olson JS, Prince RC, Pickering IJ, George GN. Alteration of axial coordination by protein engineering in myoglobin. Bisimidazole ligation in the His64-->Val/Val68-->His double mutant. The Journal of biological chemistry 1995;270(27):15993-16001.

166. Hankeln T, Jaenicke V, Kiger L, Dewilde S, Ungerechts G, Schmidt M, Urban J, Marden MC, Moens L, Burmester T. Characterization of Drosophila hemoglobin. Evidence for hemoglobin-mediated respiration in insects. The Journal of biological chemistry 2002;277(32):29012-29017.

167. Dewilde S, Ebner B, Vinck E, Gilany K, Hankeln T, Burmester T, Kreiling J, Reinisch C, Vanfleteren JR, Kiger L, Marden MC, Hundahl C, Fago A, Van Doorslaer S, Moens L. The nerve hemoglobin of the bivalve mollusc Spisula solidissima: molecular cloning, ligand binding studies, and phylogenetic analysis. The Journal of biological chemistry 2006;281(9):5364-5372.

168. Tiso M, Tejero J, Kenney C, Frizzell S, Gladwin MT. Nitrite reductase activity of nonsymbiotic hemoglobins from Arabidopsis thaliana. Biochemistry 2012;51(26):5285-5292.

169. SHIRAZI AB, M,; GHOSH, S.; DIXON, D.W. Electron Self-Exchange in Bis(imidazole)iron Porphyrins. Inorganic chemistry 1985;24(16):2495–2502.

170. Brunel CB, A.; Simonneaux, G. Electron-transfer self-exchange kinetics of trimethylphosphinc horse-heart myoglobin. Biochim Biophys Acta 1992;1101:73-78.

171. Ubbink M, Canters GW. Mutagenesis of the conserved lysine 14 of cytochrome c-550 from Thiobacillus versutus affects the protein structure and the electron self-exchange rate. Biochemistry 1993;32(50):13893-13901.

172. Timkovich R, Cork MS. Proton NMR spectroscopy of cytochrome c-554 from Alcaligenes faecalis. Biochemistry 1984;23(5):851-860.

173. Brunt CE, Cox MC, Thurgood AG, Moore GR, Reid GA, Chapman SK. Isolation and characterization of the cytochrome domain of flavocytochrome b2 expressed independently in Escherichia coli. The Biochemical journal 1992;283 (Pt 1):87-90.

Figures and Legends:

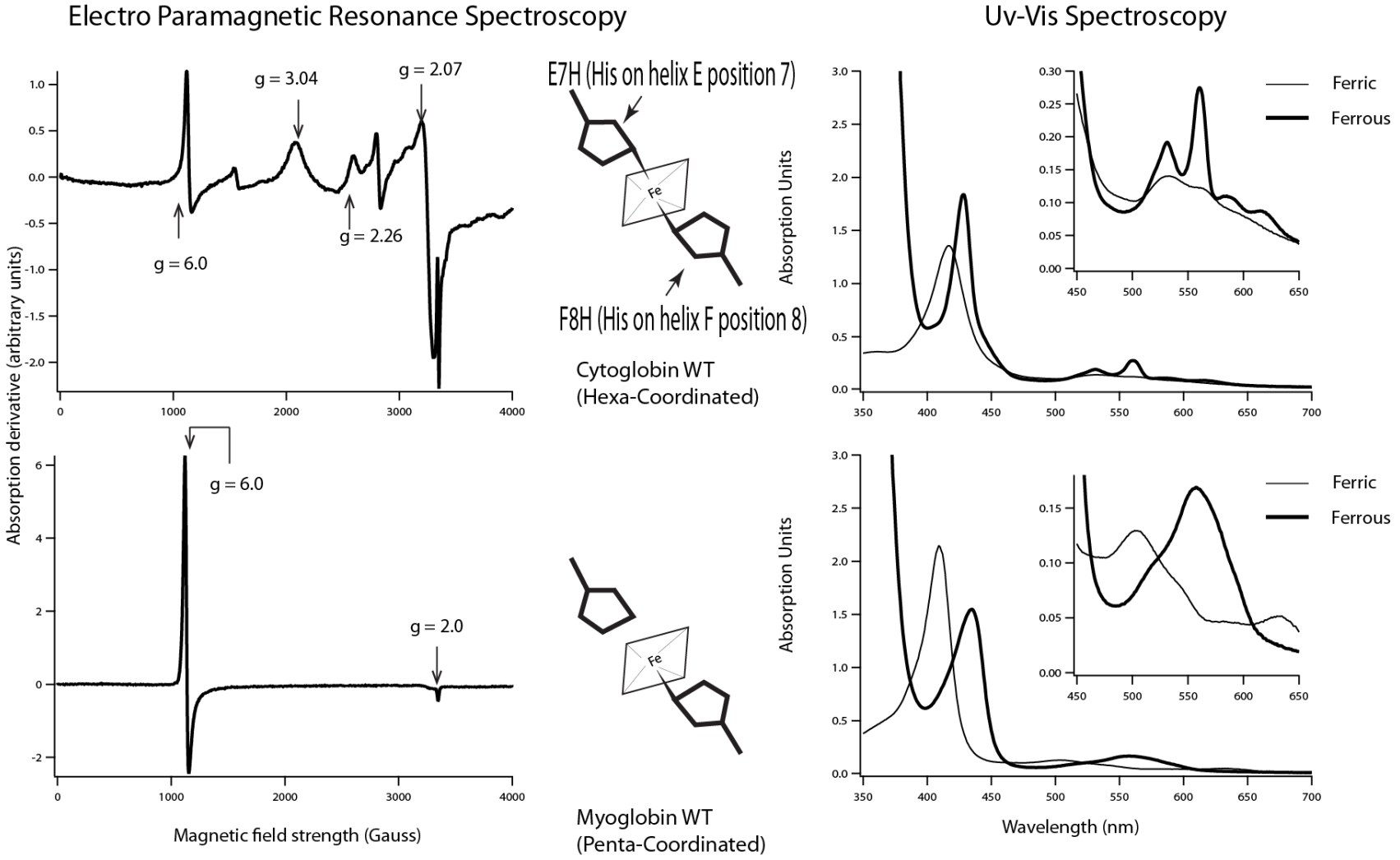

Figure 1: UV-Vis and EPR spectroscopy distinguishing pxHbs and hxHbs. The EPR spectra (left) and UV-Vis spectra (right) are aligned to schematics (center) of heme coordination for cytoglobin (a hxHb), and myoglobin (a pxHb). In the EPR spectra, high spin peaks (at g= 6.0) correlate with pentacoordination, whereas peaks in the region of ~2000 – 3000 Gauss signify hexacoordination. Uv-Vis spectra for reduced (ferrous) hxHbs have a split peaks in visible region (~450-650 nm) in contrast to pxHbs such as Mb, which have a single prominent visible-region peak near 555 nm.

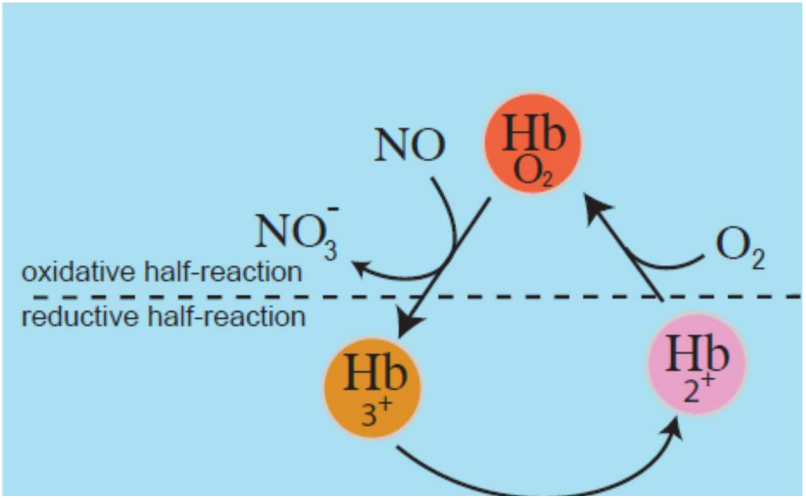

Figure 2: The nitric oxide dioxygenase (NOD) reaction. Oxy hemoglobins (Hb) will react with NO to make nitrate and ferric Hb. After the ferric Hb is reduced back to ferrous state (in the case of flavohemoglobin, using NADH), it will bind oxygen (if present) to start the reaction again. Thus the complete NOD reaction has both a reductive and oxidative half-reactions.

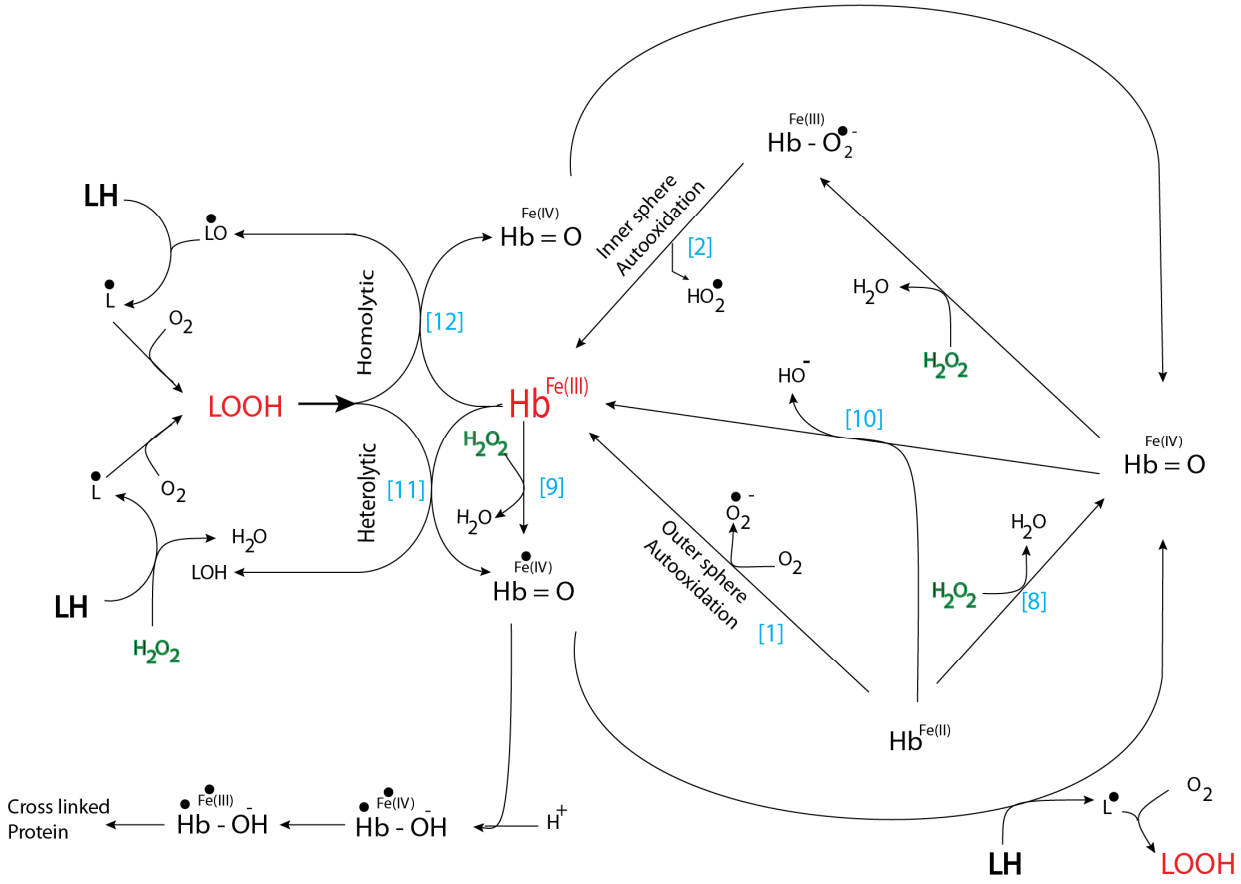

Figure 3: Peroxidase chemistry of hemoglobins. Both ferrous and ferric Hbs will react with H_2O_2. Reactions with oxygen and hydrogen peroxide are the right, and reactions with lipids (LH) peroxides (LOOH) are on the left. The central point to all reactions is ferric Hb, which can be formed from ferrous Hb through two distinct pathways. Ferric Hb can also react with lipid peroxides, become oxidized to the ferryl state, and is eventually reduced back to the ferric state through the cyclic pathway on the right, which endows Hbs with pseudo peroxidase activity. Blue numbering references reactions to their discussion in the text.

Tables:

Table 1: Hexacoordination rate and affinity constants

	k_H (s^{-1})	k_{-H} (s^{-1})	K_H	References
Rice nsHb1	75	40	1.9	[161]
Rice nsHb1b	6.7	15	0.45	[161]
Maize nsHb1a	22	25	0.9	[161]
Maize nsHb1b	43	19	2.3	[161]
Arabidopsis nsHb1	230	110	2.1	[28]
Arabidopsis nsHb2	330	12	30	[162]
Barley nsHb1	170	62	2.8	[11]
Tomato nsHb1	200	200	1.0	[163]
Tomato nsHb2	1400	30	60	[28]
Soyabean 1	160	80	2	[164]
Chicory nsHb2a	2900	11	260	[28]
Chicory nsHb2b	920	27	35	[28]
Neuroglobin (Ngb)	≥2000	2.3 (70%) 0.2 (30%)	~1000	[161]
Cytoglobin (Cgb)	430	0.5 (70%) 0.09 (30%)	860	[161]
Mb H64V/V68H	>20000	>200	~100	[5,165]
Drosophilla Hb	550	30	18	[166]
Mollusk nHb	14000	1000	14	[167]
SynHb	4200	14	300	[161]

Table 2. Observed rate constant of deoxyferrous Hb-nitrite reaction

Heme coordination state	Hemeprotein	Source	k_{obs} (M^{-1} s^{-1})	Reference
Pentacoordinate	Erythrocyte Hb	Human	0.12 (T state)	[73]
Pentacoordinate	Mb	Horse heart	11	[78]
Hexacoordinate	Ngb	Murine	5.1	[84]
		Human	0.12	[79]
Hexacoordinate	Cgb	Human	0.14	[80]
Hexacoordinate	Plant nsHb	Rice class 1	166	[78]
		Arabidopsis class 1	19.8	[168]
		Arabidopsis class 2	4.9	[168]
Hexacoordinate	Cyanobacterium Hb	*Synechocystis*	130	[78]

Table 3: Peroxidase activity of hemoglobins.

	% activity relative to horse radish peroxidase [117]	Pseudo peroxidase relative to Mb	Rate of lipid peroxidation [119]	Rate of lipid peroxidation relative to Mb
Neuroglobin (Ngb)	0.004	0.8	0	0
Cytoglobin (Cgb)	0.005-0.006	1-1.2	134	5
Mb	0.005	1	27	1
Hb-RBC	0.011	2.2	-	-
Rice ns Hb1	0.0035 [118]	0.7	-	-

Table 4 Electron transfer in hemoglobins and some heme proteins

	Electron transfer rate $M^{-1}s^{-1}$	Type of electron transfer	Reference
bis(1-methylimidazole)-ligated tetraphenylporphyrin (TPP)	$8.1x10^7$	Self-exchange	[169]
Myoglobin PMe_3 horse heart	$3.1x10^3$	Self-exchange	[170]
Hemoglobin PMe_3 human α/α	$3.2x10^3$	Self-exchange	[146]
Hemoglobin PMe_3 human β/β	$2.09x10^3$	Self-exchange	[146]
Hemoglobin α(II)PMe_3/β(III) PMe_3	$1.02x10^3$	Self-exchange	[146]
Hemoglobin α(III)PMe_3/β(II) PMe_3	$4.3x10^2$	Self-exchange	[146]
Synechococcus GlbN-A	$4.5 (\pm 0.4) \times 10^2$	Self-exchange	[155]
Synechocystis GlbN-A	$1.4 (\pm 0.4) \times 10^3$	Self-exchange	[155]
C. elegans GLB-26 (II)/ Cyt *c* (III)	$10x10^6$	Net transfer	[60]
Human Ngb (II)/ Cyt *c* (III)	$15x10^6$	Net transfer	[60]
Human Cgb (II)/ Cyt *c* (III)	$2x10^4$	Net transfer	[60]
Horse Heart Mb (II)/ Cyt c (III)	$3x10^3$	Net transfer	[60]
Cytochrome C_{550} (*Thiobacillus versutus* WT)	$2x10^5$	Self-exchange	[171]
Cytochrome C_{554} (*Alcaligenes faecalis*)	$3x10^8$	Self-exchange	[172]
Cytochrome b_5	$2.6x10^3$	Self-exchange	[156]
Cytochrome b_2	$2.6x10^3$	Self-exchange	[173]

CHAPTER 2

ELECTRON SELF-EXCHANGE IN HEMOGLOBINS REVEALED BY DEUTERO-HEMIN SUBSTITUTION

Modified from a paper published in Journal of Inorganic Biochemistry

Navjot Singh Athwal, Jagannathan Alagurajan, Ryan Sturms, D. Bruce Fulton, Amy H. Andreotti, and Mark S. Hargrove

Abstract

Hemoglobins (phytoglobins) from rice plants (nsHb1) and from the cyanobacterium *Synechocystis* (PCC 6803) (SynHb) can reduce hydroxylamine with two electrons to form ammonium. The reaction requires intermolecular electron transfer between protein molecules, and rapid electron self-exchange might play a role in distinguishing these hemoglobins from others with slower reaction rates, such as myoglobin. A relatively rapid electron self-exchange rate constant has been measured for SynHb by NMR, but the rate constant for myoglobin is equivocal and a value for nsHb1 has not yet been measured.

Here we report electron self-exchange rate constants for nsHb1 and Mb as a test of their role in hydroxylamine reduction. These proteins are not suitable for analysis by NMR ZZ exchange, so a method was developed that uses cross-reactions between hemoglobin and its deutero-hemin substituted counterpart. The resulting electron transfer is between identical proteins with low driving forces and thus closely approximates true electron self-exchange. The reactions can be monitored spectrally due to the distinct spectra of the prosthetic groups, and from this electron self-exchange rate constants of 880 (SynHb), 2,900

(nsHb1), and 0.05 $M^{-1}s^{-1}$ (Mb) have been measured for each hemoglobin. Calculations of cross-reactions using these values accurately predict hydroxylamine reduction rates for each protein, suggesting that electron self-exchange plays an important role in the reaction.

1 Introduction

Nonsymbiotic plant hemoglobins (Hbs, a.k.a. phytoglobins) have proposed functions in survival during hypoxia [1-5], nitrogen metabolism [6-8], and signal transduction [9, 10]. Their *in vitro* biochemistry includes reversible binding of oxygen, carbon monoxide, and nitric oxide, and the ability of the oxy-Hb to react with nitric oxide converting it to nitrate (known as the "nitric oxide dioxygenase", or "NOD" reaction). These reactions are common to most Hbs and, while they could be important components of physiological functions, they do not generally distinguish between Hbs from plants, animals, or bacteria. Hbs can also react with inorganic nitrogen compounds, for which there has been a recurrence of interest in light of the signaling and vasodilation affects of nitrites and nitric oxide, and the relationship between nitrate and hypoxia in plants [6, 11-15].

Under anaerobic conditions, the nonsymbiotic Hb from rice (nsHb1) and the Hb from the cyanobacterium *Synechocystis* (SynHb) reduce nitrite and catalyze the reduction of hydroxylamine (HA) to ammonia with rate constants several orders of magnitude larger than mammalian Hbs [7, 8, 11]. These reactions could reflect physiological roles in each system, as both share associations between Hb gene expression and inorganic nitrogen-related growth phenotypes in studies of the respective wild-type and Hb-mutant variants [6, 10, 16, 17]. Redox reactions such as NOD and nitrite and HA reduction require electron transfer to

the heme prosthetic group. Single-domain Hbs such as nsHb1, SynHb, neuroglobin, red blood cell Hbs, and (Mb) most likely receive electrons from other protein molecules in support of these reactions [18-22].

HA reduction by nsHb1 and SynHb requires the input of two electrons to form ammonium, with both electrons originating from ferrous heme [8]. This reaction (Scheme 1) involves an intermolecular electron transfer between the ferrous Hb^{2+} and the Hb-HA complex {Hb^{2+}:HA}. {Hb^{2+}:HA} is not detected in the reaction [8], suggesting that the rate limiting step is HA binding, and that both k_{HA} and the electron transfer cross-reaction between Hb^{2+} and {Hb^{2+}:HA} are rapid. Thus, it is possible that rapid electron self-exchange (ESE) rates in nsHb1 and SynHb might support their exceptional abilities to carry out the two-electron reduction of HA (Scheme 1).

$$Hb^{2+} + HA \underset{k_2}{\overset{k_1}{\rightleftharpoons}} \{Hb^{2+}:HA\}$$

$$Hb^{2+} + \{Hb^{2+}:HA\} \xrightarrow{k_{HA}} 2Hb^{3+} + NH_4^+$$

Scheme 1.

Marcus theory [23] provides a quantitative relationship for rates of electron transfer between two different reactants (the "cross-reaction", $k_{cross1,2}$) based on the abilities of each participant to share electrons within their individual populations ("self exchange" (ESE), k_{ESE1}, and k_{ESE2}), and the energetic driving force for the reaction. Under simple experimental conditions, this relationship is:

$$k_{cross1,2} = \left(k_{ESE1} k_{ESE2} K_{eq}\right)^{1/2}$$

Equation 1.

where K_{eq}, the equilibrium constant for the cross-reaction, represents the driving force for the reaction [24]. Measurement of redox cross-reactions in Hbs is often straightforward, but direct measurement of ESE rate constants can be difficult (see below). Thus, most of the ESE rate constants reported for Hbs are calculated from cross-reactions along with knowledge of the ESE rate for the redox partner and the driving force for the reaction [25, 26]. ESE rate constants for Mb and mammalian blood cell Hb have been calculated in this way yielding values ranging from 0.04 to 1 $M^{-1}s^{-1}$, which are several orders of magnitude slower than ESE in heme proteins with functions dedicated to electron transfer [27, 28], and are therefore consistent with slow HA reduction by Mb and blood cell Hb.

The difficulty in directly measuring ESE in Hbs stems from the challenge of monitoring a population of molecules that are exchanging electrons but whose overall redox state is not changing. Chemical exchange and line-shape NMR spectroscopy are ideally suited for this challenge, but are limited to samples that exhibit clear and distinct resonances in each oxidation state, and to timescales with rate constants > 10 s^{-1} and < ~ 10,000 s^{-1} [29]. An ESE rate constant within this range (3,100 $M^{-1}s^{-1}$) was measured for the trimethlyphosphine (TMP) derivative of horse heart Mb [30]. TMP binds uniformly to ferrous and ferric Mb [31], and was used to maintain equivalent low-spin coordination during electron exchange while providing NMR signals for each oxidation state [30, 31]. This ESE rate constant differs from that estimated by cross-reactions by more than four orders of magnitude, suggesting either a problem with the indirect calculation of ESE, or a large effect of TMP on the reaction.

SynHb is monomeric and hexacoordinate with low-spin heme iron in both the ferric and ferrous oxidation states, making it well-suited for analysis by NMR [32]. An ESE rate

constant of 1,400 $M^{-1}s^{-1}$ has been directly measured for SynHb by chemical exchange NMR [28], which is consistent with the enhanced ability of SynHb to reduce HA. In our interest to explore the relationship between ESE and HA reduction, we have measured ESE in nsHb1 and Mb for comparison to SynHb. The rate constant for SynHb ESE was first measured by chemical exchange NMR spectroscopy at a range of concentrations and under the same pH used for HA reduction measurements. Neither nsHb1 nor Mb were amenable to NMR analysis, so a novel alternative method was developed to measure ESE in these proteins that takes advantage of the auspicious properties of deutero- hemin (d-hemin) substituted Hbs.

The substitution of d-hemin for natural proto-hemin results in Hbs with ~ 10 nm blue-shifted absorbance spectra, a general decrease in the absorption extinction coefficient, but little change in midpoint redox potential or other chemical properties [26, 33, 34]. Using SynHb as a control, we demonstrate that the cross-reaction between SynHb and d-SynHb provides an accurate measurement of ESE. Cross-reactions between normal and d-hemin substituted nsHb1 and Mb, and cross-reactions between SynHb, nsHb1, and Mb were used to measure ESE rate constants for these proteins. Results are discussed in terms of their contribution to electron transfer reactions in Hbs and the cross-reaction associated with HA reduction.

2 Material and Methods

2.1 Preparation of proteins

SynHb and nsHb1 were expressed in *E. coli* and purified as described earlier [7, 35, 36]. ^{15}N-labeled Hbs were produced in BL21DE3 (Agilent Cat#200131) cells transformed with

pET28 plasmids containing respective cDNAs inserted using restriction sites *NdeI* and *HindIII*. The cells were grown in M9 minimal media supplemented with BME vitamin solution form Sigma cat# B6891 and with ^{15}N-ammonium, producing pure insoluble inclusion bodies of the recombinant apo-proteins. The culture conditions were 37°C incubation with shaking at 200 rpm and 1mM IPTG (Sigma cat#I6758) induction when cell density reached an absorbance at 600nm of 0.6-0.8, followed by overnight growth. Upon harvesting, concentrated cell suspensions were lysed by sonication, and insoluble proteins and cell debris were collected by centrifugation. This fraction was solubilized in 6 M guanidine hydrochloride (GdmCl, Fisher Scientfic cat#BP178) in the presence of 0.1 mM hemin (Sigma Cat#H-5533) dissolved in 0.1 N NaOH, and dialysed against 0.1 M phosphate buffer. Centrifugation of this dialyzed solution provided pure holo-protein, which was concentrated and exchanged with 0.1 M phosphate pH 7, over a G25 column prior to storage at -80°C for later use.

Production of deutero-hemin ($Fe^{(III)}$ deuteroporphyrin IX chloride, Frontier scientific Cat#D40654) (d-hemin) containing Hbs (d-Hbs) followed the same method above for the production of apo-Hb (with the exception of using unlabeled ammonium). 0.1 mM d-hemin (in 0.1 N NaOH) was then added to the apo-Hb followed by dialysis, centrifugation, gel filtration, and concentration as described above.

Horse heart Mb was purchased from Sigma (cat# 100684-32-0) and d-Mb was prepared by first generating apo-Mb using the acid acetone method [37], followed by dialysis into 0.1 M potassium phosphate buffer, pH 7. Two-times excess of d-hemin (dissolved in 0.1 N sodium hydroxide) was added to the apo-Mb followed by dialysis in 0.1 M phosphate buffer, pH 7. The dialyzed solution was centrifuged to remove any insoluble material, then

passed over a Sephadex G25 (Sigma cat#G25150) column equilibrated in 0.1 M phosphate, pH 7, concentrated to ≥ 1 mM, and stored at -80°C.

Extinction coefficients for d-Hbs were measured by dissolving a known mass of d-hemin in 0.1 M phosphate buffer, pH 7, containing excess sodium cyanide (Sigma Cat#380970) and 6 M GdmCl. An absorbance spectrum was measured to provide the reference extinction coefficient for cyano-d-hemin in GdmCl (Σ = 64 $M^{-1}cm^{-1}$ at 415 nm). Absorbance spectra of d-Hbs were then collected in both 0.1 M phosphate buffer and 6 M GdmCl/CN^-. The spectra in GdmCl/CN^-, which produces free cyano-d-hemin, were compared to the reference spectrum to assign extinction coefficients for each d-Hb. The procedure was also used with proto-Hbs to ensure that the expected values were obtained (the extinction coefficient for proto-cyanohemin was measured to be 81 $M^{-1}cm^{-1}$ at 425 nm).

2.2 Redox potential measurements

Spectroelectrochemical titrations were used to measure midpoint reduction potentials as previously described [35, 38]. In brief, ~ 20 µM of ferric Hb (or d-Hb) was titrated with a stock solution of ~ 40 mM sodium dithionite (Sigma Cat#157953) in an anaerobic chamber (Coy Laboratories, 95% argon and 5% hydrogen). A platinum-based glass electrode (SG500CD-ORP from Sensorex) was used to measure the working potential of the reactions. The data were adjusted to reflect a Standard Hydrogen Electrode and fitted to the following equation to obtain the mid-point potential. All the reactions were set up in 0.1M phosphate buffer, pH 7 at room temperature.

$$F_{reduced} = \frac{e^{-\left(\frac{nF(E_{obs}-E_{mid})}{RT}\right)}}{1+e^{-\left(\frac{nF(E_{obs}-E_{mid})}{RT}\right)}}$$ Equation 2.

2.3 NMR measurements of ESE

ESE measurements by NMR were conducted as described by Preimesberger *et al* [28], with a few exceptions discussed below. All samples were prepared in the anaerobic glove box described above. Deoxygenated ferric proteins were concentrated to the desired levels using a centrifugal concentrator, and then reduced to ~ 50% by titration with sodium dithionite while actively monitoring the visible region absorbance spectrum using an Ocean Optics USB 2000 spectrophotometer housed in the glove box. Samples were then transferred into Shigemi NMR tubes and sealed with parafilm. Samples were prepared in either 0.1 M potassium phosphate, pH 7, or sodium borate, pH 9, containing 1mM EDTA, and glucose oxidase (0.05mg/ml), D-glucose (0.36mg/ml) and catalase (0.13mg/ml) to actively combat oxygen contamination and oxidation outside the anaerobic chamber.

The ^{15}N ZZ exchange experiment [39] was executed using the following order of mixing time delays at pH 9 (in ms): 497, 294, 136, 1288, 633, 1582, 1084, 384, 836, 68, 10, 25, 88, 497. For pH 7 the times were: 497, 10, 250, 40, 750, 120, 1100, 90, 1500, 497. HSQC spectra were obtained intermittently to check sample integrity and stability throughout the course of the experiment. Likewise, the two flanking 497 ms time points were used to check for sample variation within the course of the experiment [28]. The FIDs were processed using NMRPipe for each time point [40]. The volumes of the well-resolved peaks for Gly^{113} were

used for analysis of auto and cross-peak time courses at pH 7, and those for Ile^{31} were used at pH 9 [41]. These peak volumes were measured using NMRViewJ (Nmr View Java, One Moon Scientific).

The peak volumes of quartets of auto peaks and cross peaks were analyzed using the following variables and equations (adapted from [28, 39]):

Variables: $a_{11} = k_{R,2} + k_{ESE,obs}$; $a_{22} = k_{R,3} + k_{ESE,obs}$; $\lambda_{1,2} = 0.5\{(a_{11}+a_{22}) \pm [(a_{11}+a_{22})^2+4k_{ESE,obs}^2]^{1/2}\}$

Equations:

$$I_{2x,t} = I_{2,0}\left(\frac{a_{21}e^{(-\lambda_1 t)} - a_{21}e^{(-\lambda_2 t)}}{\lambda_1 - \lambda_2}\right) \quad (3) \qquad I_{3x,t} = I_{3,0}\left(\frac{a_{12}e^{(-\lambda_1 t)} - a_{12}e^{(-\lambda_2 t)}}{\lambda_1 - \lambda_2}\right) \quad (4)$$

These four equations relate the auto and cross peak intensities to five parameters: $k_{R,2}$ and

$$I_{2a,t} = I_{2,0}\left(\frac{-(\lambda_2 - a_{11})e^{(-\lambda_1 t)} + (\lambda_1 - a_{11})e^{(-\lambda_2 t)}}{\lambda_1 - \lambda_2}\right) \quad (5) \qquad I_{3a,t} = I_{3,0}\left(\frac{-(\lambda_2 - a_{22})e^{(-\lambda_1 t)} + (\lambda_1 - a_{22})e^{(-\lambda_2 t)}}{\lambda_1 - \lambda_2}\right) \quad (6)$$

$k_{R,3}$ are the longitudinal NMR relaxation rate constants for the ferrous and ferric oxidation states, respectively; $k_{ESE,obs}$ is the observed rate constant for ESE at the particular Hb concentration for the experiment in question; $I_{2,0}$ and $I_{3,0}$ are the initial intensities of the ferrous and ferric auto peaks, respectively. Each set of data consists of four curves relating intensity and mixing time, and are described by Equations 3-6. $I_{2x,t}$ and $I_{2a,t}$ are the intensities for the respective ferrous cross and auto peaks, and $I_{3x,t}$ and $I_{3a,t}$ are those for the ferric Hb. These equations were fit in Igor Pro to global parameters for $k_{R,2}$, $k_{R,3}$, and $k_{ESE,obs}$. $I_{2,0}$ and $I_{3,0}$ were constrained within the respective pairs of ferrous and ferric peaks. The k_{ESE} values

reported in the Results section are calculated by dividing $k_{ESE,obs}$ by the total protein concentration. $k_{R,2}$ and $k_{R,3}$ for each set of data in Figure 1 were 2.0 and 1.0 s^{-1} for Figure 1B, 1.8 and 0.7 for Figure 1C, and 1.3 and 1.7 for Figure 1D.

2.4 Kinetic measurements of electron transfer using d-hemin derivatives

All samples were prepared in the anaerobic chamber to avoid oxygen contamination. All buffers used in the chamber were boiled and purged with nitrogen. Ferric proteins were purged with argon before being brought into the chamber, and ferrous Hbs were generated in the chamber by reducing ferric samples with excess dithionite, followed by passage over a G25 column (to remove dithionite after reduction has occurred). Dry chemicals were weighed and reconstituted in anaerobic buffers inside the anaerobic chamber. All of the reactions were carried out at room temperature in 0.1M phosphate buffer, pH 7.

Reactions were initiated by mixing equal concentrations of proto-Hb and d-Hb of different oxidation states. A 1 cm sealed split-cell anaerobic cuvette (Divided Rectangular, Starna Cells, model 58-Q-10 with custom made anaerobic screw top) was used to obtain absorbance spectra prior to mixing, then inverted to initiate the reaction. This method was used for the spectra shown in Figures 2A,C, and 3A,C, and all of the reactions with Mb (Figure 4), where time courses were slow. These scans were recorded with an Agilent Cary-60 UV-Vis Spectrophotometer. Time courses for the faster reactions with SynHb and nsHb1 (Figures 2B,D, and 3B,D) were monitored with a stopped-flow reactor (Bio-Logic SFM-400) installed inside the anaerobic chamber.

In all cases, spectra of the unmixed Hbs and a final spectrum at equilibrium were collected, along with kinetic curves at appropriate wavelengths (listed in each figure legend). Spectra were fit in Igor Pro to the component spectra (Figures S1, S2, and S3 for each protein) to measure starting and equilibrium concentrations to ensure equal starting concentrations, to measure equilibrium constants, and to normalize the ordinate axes of Figures 2B,D and 3B,D. Kinetic traces for reactions between Hbs and d-Hbs were fit to Equation 9 (described in the Results section). The ordinate axis of each trace was converted to "μM product formed" by dividing the change in absorbance by the change in extinction coefficient for the reaction (calculated from the components of the reaction) and the path of the cuvette. A 1 cm path was used for all reactions except the higher concentrations of SynHb and nsHb1 (Figures 2B,D and 3B,D), for which a 0.15 cm cuvette was installed in the stopped flow reactor. Equation 9 was derived for starting conditions with $[d\text{-}Hb^{2+}] = [Hb^{3+}]$. If initial spectra indicated that our samples deviated by more than 10% from this condition, or if excess ferric Hb was detected in the final spectrum, the reactions were not used for kinetic analysis. The average values for ESE rate constants results from at least four independent measurements. The fitted values included in each figure are those for the specific set of data used in that figure, and the average values for each rate constant with their associated errors are listed in Table 1.

2.5 Electron-transfer cross-reactions with Mb

Cross-reactions between Mb and other Hbs were set up as described above for reactions between proto- and d-Hbs using 0.1m phosphate buffer, pH7 and room temperature. Reactions with Mb were all much slower, and could be initiated and

monitored in the split-cell cuvette without loss of signal. The low reduction potentials of SynHb (-200 mv) and nsHb1 (-125 mv) compared to Mb (46 mv) means that only the reduction of ferric Mb by ferrous SynHb or nsHb1 could be measured, resulting from driving force K_{eq} values of 29,700 for Mb^{3+}-$SynHb^{2+}$ and 1,600 for Mb^{3+}-$nsHb1^{2+}$ (calculated from Equation 10). The large driving force caused each reaction to proceed to completion, and the kinetic traces thus fit to single observed rate constants in Igor Pro, which were divided by the total protein concentrations to estimate bimolecular rate constants for electron transfer.

3 Results

3.1 Chemical exchange NMR measurements of ESE

^{15}N-^{1}H Heteronuclear NMR spectra of Hb have resonance peaks that are specific to the ferric or ferrous oxidation states. ^{15}N-^{1}H ZZ Exchange NMR Spectroscopy [39] (ZZ) can be used to measure chemical exchange between these distinct "auto" peaks, which is manifested in "cross" peaks associated with them. During the experiment, the redox state of the mixture is at equilibrium, with electrons free to exchange among the ferrous (Hb^{2+}) and ferric (Hb^{3+}) oxidation states. ESE measurement is initiated by transfer of ^{15}N magnetization to the Z axis, effectively labeling an instantaneous population of ferric and ferrous Hb molecules. The ZZ experiment involves waiting for various "mixing" times before transferring the magnetization to the transverse plane for detection, during which ferric and ferrous species are free to interconvert. As mixing time is increased, cross peak volumes first increase due to ESE, and then decrease due to loss of NMR signal by longitudinal

relaxation; auto peaks decrease due to both processes. Together, the variation of auto and cross peak volumes with mixing time can usually be unambiguously fit for ESE and longitudinal relaxation rate constants.

With the goal of measuring an ESE rate constant for SynHb at pH 7.0 and testing the feasibility of using chemical exchange NMR to measure ESE in nsHb1, ZZ was first performed at pH 9.0 with SynHb to reproduce the results of Preimesberger *et al* [28]. Figure 1A shows a representative ZZ spectrum for a mixture of $SynHb^{2+}$ and $SynHb^{3+}$, including two sets of auto and cross peaks used for analysis. Figure 1B is a plot of the variation of the auto and cross peaks with mixing time, along with curves fitted to Equations 3-6, yielding a value for k_{ESE} of 600 $M^{-1}s^{-1}$ for SynHb at a concentration of 1.63 mM. The concentration dependence of the bimolecular ESE rate constant was tested directly by conducting the ZZ experiment at a much higher (7.9 mM) SynHb concentration (Figure 1C). As expected, the time courses for these data have notably larger observed rate constants, but yield nearly the same bimolecular ESE rate constant (780 $M^{-1}s^{-1}$). These rate constants are consistent with the value of 1,400 $M^{-1}s^{-1}$ reported previously at a single concentration [28]. Figure 1D presents ZZ data at pH 7.0, which provide a slightly lower value for k_{ESE} equal to 320 $M^{-1}s^{-1}$. Ideally, one could use the ZZ experiment to measure k_{ESE} for nsHb1 as well. A ZZ spectrum for a mixture of $nsHb1^{2+}$ and $nsHb1^{3+}$ is shown in Figure 1E. In this case, ZZ spectra do not contain clear and distinct peaks for each oxidation state, and are not useful for analysis due to a number of factors (discussed below).

3.2 Calculation of ESE using cross-reactions with d-hemin substituted Hbs

Since measurement of ESE by NMR is not tractable in all Hb systems, it was necessary to apply other methods for examination of nsHb1 and Mb. Cross-reactions (Equation 1) can be used to estimate ESE rate constants if K_{eq} and the k_{ESE} values for one of the participants are known with confidence, and if there is a good signal associated with the transfer of electrons from one reactant to the other [23-26]. d-hemin differs from regular hemin by lacking two vinyl groups on the pyrrole rings opposite of the propionates. The absence of these vinyl groups does not greatly affect the chemistry of d-hemin compared to hemin when they are incorporated into Hbs, but causes a blue-shift and decrease in absorbance [26, 33, 34]. Thus, electron exchange cross-reactions between a Hb and its d-Hb derivative would be ideal for calculating k_{ESE} because the K_{eq} values are near unity, reaction time courses can be measured by clear changes in absorbance, and the proteins exchanging electrons are the same so that Equation 1 can be simplified to Equation 7, where k_{pd} and K_{pd} are the rate and equilibrium constants, respectively, for the cross reaction between the "proto" and "deutero" derivatives.

$$k_{pd} = \left(k_{ESE}^2 K_{pd}\right)^{1/2} \qquad \text{Equation 7.}$$

To interpret time courses for such reactions we must derive a rate equation from the following chemical reaction:

$$\text{d-Hb}^{2+} + \text{Hb}^{3+} \underset{k_{pd}}{\overset{k_{pd}}{\rightleftharpoons}} \text{d-Hb}^{3+} + \text{Hb}^{2+} \qquad \text{Reaction 2}$$

If the reaction is initiated with equal concentrations of d-Hb^{2+} and Hb^{3+} (or *vice versa*), there is a convenient integrated solution for k_{pd} [42, 43]:

$$k_{pd} = \frac{1}{t}\left(\frac{P_e}{2R_i(R_i - P_e)}\right)\ln\left(\frac{R_i P_e + P_t(R_i - 2P_e)}{R_i(P_e - P_t)}\right) \qquad \text{Equation 8}$$

In Equation 8, R_i is the initial concentration of each reactant (R_i = d-Hb^{2+} = Hb^{3+} as written in Reaction 2), P_e is the concentration of each new product formed at equilibrium (right hand side of Reaction 2), and P_t is the concentration of products at time t. Equation 8 can be rearranged to solve for P_t with the following solution:

$$P_t = \frac{R_i P_e\left(e^{\left(\frac{2R_i(R_i - P_e)k_{pd}t}{P_e}\right)} - 1\right)}{R_i - 2P_e + R_i e^{\left(\frac{2R_i(R_i - P_e)k_{pd}t}{P_e}\right)}} \qquad \text{Equation 9}$$

Thus, time courses for product formation can be fit for k_{pd}.

3.3 Cross-reactions with d-SynHb-

To test this method, SynHb was used as a control. The absorbance spectra for d-SynHb are shown in Figure S1, and have the characteristic effects expected for d-hemin substitution. In both the ferrous (Figure S1A) and ferric (Figure S1B) oxidation states, the spectra have similar shapes, but are decreased in intensity and blue-shifted by ~ 10 nm for d-SynHb. The midpoint redox potential of d-SynHb is shifted by only -30 mv compared to SynHb, similar in magnitude to that observed for other d-hemin substituted Hbs (Figure S1C) [26].

The electron transfer cross-reaction between SynHb and d-SynHb was measured in the experiments presented in Figure 2. Figure 2A shows the spectral transition that occurs when d-SynHb^{2+} is mixed with SynHb^{3+}. The spectrum of the two proteins prior to mixing can be fit to the component spectra of Figure S1 to measure the concentrations of each species in the reaction. The combination of component spectra reflecting the unmixed and final reaction components are referred to as the "fitted" spectra in Figure 2A, and provide the concentrations of each reactant in Figure 2B. Figure 2B shows reaction time courses at two different concentrations of SynHb and d-SynHb that have been fit to Equation 9 with k_{pd} as a global parameter, yielding a value of 2,700 $M^{-1}s^{-1}$.

To calculate k_{ESE} from k_{pd} using Equation 7, we must have a value of K_{pd} for the reaction. K_{pd} can be determined either from the equilibrium product concentrations evident

$$\ln K_{pd} = \frac{nF(E_{cell} + E_{mix})}{RT} \qquad \text{Equation 10.}$$

from the spectral component fit to the final equilibrium spectrum (Figure 2A, final spectrum), or calculated from the difference in midpoint reduction potentials between SynHb and d-SynHb using the following equation where E_{cell} is the difference in midpoint reduction potentials between the reactants, and E_{mix} driving force resulting from the entropy of mixing. E_{mix} is calculated as follows to be 18 mV for a two-fold dilution such as in the present mixing experiments.

$$E_{mix} = \frac{\Delta S}{nF} = \frac{-RT\ln(2)}{nF} = 18mV \qquad \text{Equation 11.}$$

Using either the observed product profiles or E_m values (Equation 10), K_{pd} is ~ 8. The fitted value of k_{pd} can be used along with K_{pd} to calculate k_{ESE} from Equation 7. For the data in Figure 2A, k_{ESE} is equal to 950 $M^{-1}s^{-1}$.

A rigorous test of this method is shown in Figure 2C and 2D, in which the reaction is run in reverse compared to Figure 2A and 2B, starting with $SynHb^{2+}$ and d-$SynHb^{3+}$. In this case the equilibrium constant is 1/8, the reaction proceeds with less net electron transfer, and the observed value of k_{pd} is lower (300 $M^{-1}s^{-1}$). However, these values combine in Equation 7 to calculate a k_{ESE} value of 830 $M^{-1}s^{-1}$. The k_{ESE} values above (the average over five independent experiments being 880 $M^{-1}s^{-1}$ (Table 1)) are consistent with those measured by ZZ NMR methods for SynHb, and support the confident use of cross-reactions between deutero- and proto- derivatives for measuring k_{ESE} in other Hbs.

3.4 Measurement of nsHb1 ESE using cross-reactions with d-nsHb1

The spectral and electrochemical analysis of d-nsHb1 compared to nsHb1 are shown in Figure S2. As is the case for d-SynHb, spectra are shifted ~ 10 nm and decrease in intensity, but their shapes are unperturbed. The midpoint reduction potential for d-nsHb1 is likewise decreased by 45 mV compared to nsHb1. Spectra and time courses for cross-reactions between nsHb1 and d-nsHb1 are presented in Figure 3.

Figure 3A shows the spectra associated with transfer of electrons from d-$nsHb1^{2+}$ to $nsHb1^{3+}$ alongside the fitted initial and final spectra. Time courses for this reaction at two different starting concentrations are shown in Figure 3B, which are fitted to a global k_{pd} with a value of 2,500 $M^{-1}s^{-1}$. The reverse reaction is shown in Figures 3C and 3D. The fitted value

of k_{pd} for these data is 4,000 $M^{-1}s^{-1}$. E_m (Equation 10) predicts K_{pd} values of 12 and 0.3 for the reactions of d-nsHb^{2+}/nsHb^{3+} and d-nsHb^{3+}/nsHb^{2+}, respectively, whereas the empirical product profiles following mixing report K_{pd} equal to 1 in both cases. The reason for this difference is not known, and the empirical measurement was used for the calculation of k_{ESE} from Equation 7, providing values of 2,500 $M^{-1}s^{-1}$ and 4,000 $M^{-1}s^{-1}$. The average of these k_{ESE} values with four independent measurements is 2,900 $M^{-1}s^{-1}$ (Table 1).

3.5 Measurement of ESE for Mb-

Literature values for Mb ESE range from 0.04 to 3,100 $M^{-1}s^{-1}$ [25, 26, 30]. If k_{ESE} were ≤ 1 $M^{-1}s^{-1}$, the ESE time course at 4 µM Mb and d-Mb would have a half-time of ≥ 3,000 minutes. If k_{ESE} were 3,100 $M^{-1}s^{-1}$, the half-time of the same reaction would be about a minute. Thus, a measurement of electron exchange between Mb and d-Mb would provide a good test of previous estimates. Figure S3 and Figure 4 present data associated with Mb ESE measured by electron exchange between Mb and d-Mb. d-Mb was produced by addition of d-hemin to apoMb, resulting in the spectra and electrochemical analysis for d-Mb shown in Figure S3. Figure 4 shows the spectra resulting from a mixture of Mb^{2+} and d-Mb^{3+}. The initial spectrum of Figure 4A (following mixing) does not change up to time points ≥ 1,200 seconds. After this, slow oxidation of both Mb^{2+} and d-Mb^{2+} begins, precluding quantitative analysis of time courses. Nonetheless, these results set a conservative upper limit of ~ 100 $M^{-1}s^{-1}$ for Mb ESE.

A better estimate of k_{ESE} for Mb was obtained using cross-reactions between Mb, SynHb, and nsHb1. The midpoint reduction potential of Mb is 246 mv higher than SynHb.

Thus, reactions initiated with equal concentrations of $SynHb^{2+}$ and Mb^{3+} will proceed completely to Mb^{2+}. The spectra associated with this reaction are shown in Figure 4B along with the fitted curve for the initial and final products. The fitted observed rate constant for this reaction (Figure 4D) is 0.007 s^{-1}. Given a total heme protein concentration of 7 µM, k_{pd} can be estimated at 1,000 $M^{-1}s^{-1}$. Equation 1 can be used to calculate k_{ESE} with $k_{ESE,synHb}$ = 880 $M^{-1}s^{-1}$, and K_{eq} = 29,700 (from Equation 7). Using these values with Equation 2 provides a k_{ESE} estimate for Mb equal to 0.05 $M^{-1}s^{-1}$.

The cross reaction between Mb and nsHb1 may also be used to estimate k_{ESE} for Mb. Again, the difference in midpoint reduction potentials for nsHb1 and Mb ensures that $nsHb^{2+}$ will transfer electrons to Mb^{3+} (with K_{eq} = 1,600). Spectra for this reaction are shown in Figure 4C, along with a time course in Figure 4D. The fitted k_{obs} for the reaction is 0.0034 s^{-1}. Using the calculation described above (with $k_{ESE,nsHb1}$ = 2,900 $M^{-1}s^{-1}$) and Equation 1, $k_{ESE,Mb}$ is estimated from the cross-reaction with nsHb1 to be 0.05 $M^{-1}s^{-1}$. Thus, two different electron donors with distinct k_{ESE} and K_{eq} values provide a common value for $k_{ESE,Mb,}$ which is consistent with the slow Mb/d-Mb exchange observed in Figure 4A.

4 Discussion

The goal of these experiments was to measure ESE rate constants for nsHb1 and Mb in order to know if they play a limiting role in the 100-fold slower rate constant for HA reduction by Mb compared to SynHb and nsHb1 [8]. Although the ideal NMR technique for this measurement works well for SynHb, we were challenged by the failure of its application to nsHb1 and Mb. Instead, we used electron transfer cross-reactions between natural and d-

hemin substituted versions of each Hb to enable spectral monitoring of electron transfer within mixtures of each. The ESE rate constant measured for SynHb using this method (880 $M^{-1}s^{-1}$) was similar to that measured by NMR, and the method provided a value of 2,900 $M^{-1}s^{-1}$ for nsHb1. The Mb/d-Mb reaction was extremely slow, precluding accurate measurement. Therefore, cross-reactions between $nsHb1^{2+}$ and Mb^{3+}, and $SynHb^{2+}$ and Mb^{3+}, where used to independently measure ESE rate constants for Mb: both report a value of 0.05 $M^{-1}s^{-1}$.

4.1 Strengths and weaknesses of different methods for measuring ESE-

NMR ZZ exchange is ideal for direct measurements of ESE but limited in application to Hbs by several technical hurdles. ^{15}N labeling is a requirement for the ZZ experiment. Labeling is not required for the related ^{1}H-^{1}H EXSY experiment but it is very difficult to deconvolute the contribution of ESE from other contributions to exchange in the case of EXSY. For this reason, and due to the higher (> 100 μM) concentrations of protein needed for NMR, recombinant expression systems capable of heteronulcear labeling are required for sample preparation. ZZ spectra must also have well-resolved auto and cross peaks. Spectral resolution can be reduced by line broadening due to high molecular mass or paramagnetism. High spin ferrous Hbs (such as Mb) contain four unpaired electrons, and ferric Hbs are paramagnetic in both spin states. nsHb1 has a larger contribution of high spin ferrous heme than SynHb, and ferric nsHb1 dimerizes with a K_D of 83 μM [44] resulting in higher average mass; these are the most likely causes of poor NMR spectral quality for this protein (Figure 1E).

ZZ exchange (with a minimum delay time of 10 ms) is capable of measuring observed rate constants of ~ 100 s^{-1}. With a minimum sample concentration of 100 μM, one can estimate a generous upper limit for k_{ESE} measurement of $1x10^6$ $M^{-1}s^{-1}$ for Hbs and other bimolecular reactions. On the slow end however, NMR relaxation rates on the order of 1 s^{-1} preclude measurement of observed ESE rate constants much slower than this, and if the maximum sample concentration is 10 mM, the lower limit to measurement would be 100 $M^{-1}s^{-1}$. Thus, for proteins such as Mb, ZZ exchange cannot be used for measurement of ESE.

With the exception of NMR, all techniques for measuring ESE are indirect methods. Cross-reactions (Equation 1) involve measuring the transfer of electrons from one reactant to another, and require knowledge of k_{ESE} for one reactant and K_{eq} for the reaction. Perturbations from true ESE (between identical partners) can result from interactions between dissimilar pairs of reactants [27], or from large K_{eq} standard errors that can dwarf smaller k_{ESE} values. The use of Hb/d-Hb pairs for cross-reactions minimizes these problems by having the same protein fold in both reactants, and K_{eq} values near unity. Such K_{eq} values also allow reactions to be monitored in both directions giving independent observations of the ESE rate constant, a condition that is not often accessible in cross-reactions that are strongly favored thermodynamically [27]. Finally, because K_{eq} is near unity, it can be measured accurately from the product profiles at equilibrium in addition to its calculation from redox potentials (Equation 10).

The drawback to the low driving force for Hb/d-Hb cross-reactions is that proteins with very small ESE rate constants, like Mb, cannot be measured accurately due to the slow rate of the reaction. In this case, cross-reactions such as those using nsHb1^{2+} and SynHb^{2+},

where K_{eq} is large, will speed up the reaction (although it cannot be run in the reverse direction). Nonetheless, cross-reactions between Mb^{3+} and $SynHb^{2+}$ (k_{ESE} = 880 $M^{-1}s^{-1}$, K_{eq} = 29,700), and $nsHb1^{2+}$ (k_{ESE} = 2,900 $M^{-1}s^{-1}$, K_{eq} = 1,600) result in identical values of 0.05 $M^{-1}s^{-1}$ for $k_{ESE,Mb}$ in spite of the different k_{ESE} and K_{eq} values involved. In the future, knowledge of these k_{ESE} values will allow the confident use of cross-reactions with Mb, SynHb, and nsHb1 for the calculation of ESE for other Hbs.

The value of 0.05 $M^{-1}s^{-1}$ is on the low end of those previously reported for Mb using cross-reactions with small inorganic molecules [25]. It is much smaller than the value of 3,100 $M^{-1}s^{-1}$ reported for TMP-bound Mb [30]. Electron transfer is known to be faster in low spin heme systems, as the reorganization energy is lower for hexacoordinate compared to the pentacoordinate heme, which often coordinates a water molecule in the ferric (but not the ferrous) oxidation state [26]. TMP binds Mb in both oxidation states, presumably in a low-spin manner. Thus, the more rapid ESE observed for TMP-Mb probably reflects the low-spin system with lower reorganization energy.

4.2 The role of ESE in Hbs-

ESE is an integral component of electron transfer mechanisms that gives insight into the reorganizational energy and thus the energy of activation and kinetics of a system [27]. Variations in ESE among similar Hbs reflect the variation in their geometric, electrostatic and reorganizational characteristics and can likely distinguish between their functions. Electron transfer is important in nearly every aspect of Hb function; even red blood cell Hb with the primary function of inert oxygen transfer must be reduced upon assembly, and be maintained

in the ferrous state through reactions with methemoglobin reductase. Many single domain hexacoordinate Hbs have been associated with electron transfer rather than ligand transport [45]. Neuroglobin has links to cytochrome mediated apoptosis [46], NOD reactions [47-50], and nitrite reduction [22]. Cytoglobin uses lipid peroxidation [51] and auto-oxidation [45] as components of its function. *C. elegans* contains globin genes that appear to carry out a diverse set of functions [52] many of which involve electron transfer or even nitrite reduction [45, 53]. SynHb uses ESE directly to achieve a novel post-translational modification [28] within a protein that appears to be involved in anaerobic inorganic nitrogen metabolism [17].

Electron transfer is a key component of *in vitro* HA reduction by SynHb and nsHb1. HA is an unreleased intermediate in the conversion of nitrite to ammonium by nitrite reductase in plants and bacteria [54-56], and is produced by ammonia monoxygenase in nitrifying bacteria [57]. But it is difficult to detect *in vivo* and *in vitro* so its importance in biological systems is still unclear. Hydroxylamine is undoubtedly a toxic substance that could not be tolerated in high concentrations *in vivo* [58]. Our focus on HA reduction in this study is directed at its participation in a two-electron reaction that requires electron transfer between Hb molecules, with the thought that such behavior might reflect the innate abilities of Hbs to exchange electrons in support of catalysis.

Reaction Scheme 1 proposes the mechanism for reduction of HA by a ferrous Hb^{2+}. The mechanism involves electron exchange between Hb^{2+} and a HA-bound Hb^{2+} complex {Hb^{2+}-HA}. It has been hypothesized that the electron transfer cross-reaction between Hb^{2+} and {Hb^{2+}-HA} might dictate the observed rates of HA reduction by Hb^{2+}, and that it might be reflected in the ESE rate constant for the Hb. If so, k_{ESE} for SynHb and nsHb1 are expected to

be much larger than that of Mb, and the rate constant for HA reduction (k_{HA}) should be approximated by the cross-reaction rate constant calculated from Equation 1. This argument is supported by the k_{ESE} values reported here for each Hb, and previously for SynHb [28]. Calculation of $k_{cross,HA}$ requires knowledge of K_{eq} for the reaction and k_{ESE} for {Hb^{2+}-HA}, neither of which can be easily measured. Thus, some approximations for these values are necessary in order to test the correlation between observed values of k_{HA} and calculations of $k_{cross,HA}$ using Equation 1.

It is known that K_{eq} for HA reduction to ammonium by each Hb^{2+} is large, as the reaction goes to completion even at stoichiometric (2:1) concentrations of Hb^{2+} and HA [8]. K_{eq} must be larger than 100, representing 99% oxidation of Hb^{2+}, because this would be easily detectable experimentally as 1% remaining ferrous Hb. Therefore, because there is no justification for much larger values, we will use the value of 500 to represent K_{eq} for Equation 1. Values of k_{ESE} for each Hb^{2+} are now known (Table 1). If we assume that k_{ESE} for the {Hb^{2+}-HA} complex is the same as for each respective Hb^{2+}, then values of $k_{cross,HA}$ for each are calculated to be 20,000 $M^{-1}s^{-1}$ (SynHb), 65,000 $M^{-1}s^{-1}$ (nsHb1), and 1 $M^{-1}s^{-1}$ (Mb). The values for SynHb and nsHb1 are similar to their respective observed values of k_{HA} (Table 1), but the value for Mb is much smaller than its observed k_{HA}. However, if we assume that HA binding to Mb converts the heme iron to the low spin state in {Mb^{2+}-HA}, then we could estimate $k_{ESE2,Mb}$ to be 3,100 $M^{-1}s^{-1}$ (the value measure by NMR for TMP-Mb). In this case a value of 280 $M^{-1}s^{-1}$ is calculated for $k_{cross,HA}$ from Equation 1, which is very close to the observed value of k_{HA}. These results suggest that ESE plays a role in HA reduction by ferrous Hbs and that HA binding at the heme iron might be general to most Hbs. The difference between those that

reduce HA rapidly and those that don't might lie in the ESE rate constants for each and their respective HA-bound intermediates.

5 Abbreviations

d-Hb	deutero-hemoglobin
d-hemin	deutero-hemin
d-Mb	deutero-myoglobin
d-nsHb1	deutero-rice nonsymbiotic hemoglobin (class 1)
d-SynHb	deutero-*synechocystis* hemoglobin
GdmCl	guanidine hydrochloride
HA	hydroxylamine
Hb	hemoglobin
Mb	Myoglobin
NOD	Nitric oxide dioxygenase
nsHb1	rice nonsymbiotic hemoglobin (class 1)
SynHb	*synechocystis* hemoglobin
TMP	trimethylphosphine

6 Acknowledgments

We would like to thank Grant Mauk for his advice on this project, John Olson and Alejandro Andreotti for discussions concerning the interpretation of kinetics reactions, and Matt Preimesberger, Juliette Lecomte, and Chris Falzone along with Adam Barb for their help

getting our ZZ experiments running and interpreted correctly. This work was supported by the Iowa State University College of Liberal Arts and Sciences Signature Research Initiative.

7 References

[1] E.R. Taylor, X.Z. Nie, A.W. MacGregor, R.D. Hill, Plant Mol. Biol. 24 (1994) 853-862.

[2] A.W. Sowa, S.M. Duff, P.A. Guy, R.D. Hill, Proc. Natl. Acad. Sci. 95 (1998) 10317-10321.

[3] P. Hunt, E. Klok, B. Trevaskis, R. Watts, M. Ellis, W. Peacock, E. Dennis, Proc. Natl. Acad. Sci. 99 (2002) 17197-17202.

[4] C. Dordas, B.B. Hasinoff, A.U. Igamberdiev, N. Manac'h, J. Rivoal, R.D. Hill, Plant J. 35 (2003) 763-770.

[5] L. Zhao, R. Gu, P. Gao, G. Wang, Plant Cell Tiss. Org. 95 (2008) 227-237.

[6] Y. Ohwaki, M. Kawagishi-Kobayashi, K. Wakasa, S. Fujihara, T. Yoneyama, Plant Cell Physiol. 46 (2005) 324-331.

[7] R. Sturms, A.A. DiSpirito, M.S. Hargrove, Biochemistry 50 (2011) 3873-3878.

[8] R. Sturms, A.A. DiSpirito, D.B. Fulton, M.S. Hargrove, Biochemistry 50 (2011) 10829-10835.

[9] S. Huang, R.D. Hill, C. Stasolla, Plant Signaling Behav. 9 (2014).

[10] R.D. Hill, AoB Plants 2012 (2012).

[11] M. Tiso, J. Tejero, S. Basu, I. Azarov, X. Wang, V. Simplaceanu, S. Frizzell, T. Jayaraman, L. Geary, C. Shapiro, C. Ho, S. Shiva, D.B. Kim-Shapiro, M.T. Gladwin, J. Biol. Chem. 286 (2011) 18277-18289.

[12] D.A. Bazylinski, R.A. Arkowitz, T.C. Hollocher, Arch. Biochem. Biophys. 259 (1987) 520-526.

[13] U.B. Hendgen-Cotta, M. Kelm, T. Rassaf, Trends Cardiovasc. Med. 24 (2014) 69-74.

[14] J. Tejero, M.T. Gladwin, Biol. Chem. 395 (2014) 631-639.

[15] M. Tiso, J. Tejero, C. Kenney, S. Frizzell, M.T. Gladwin, Biochemistry 51 (2012) 5285-5292.

[16] R. Arredondo-Peter, J.F. Moran, G. Sarath, F1000Res. 3 (2014) 253.

[17] N.L. Scott, Y. Xu, G. Shen, D.A. Vuletich, C.J. Falzone, Z. Li, M. Ludwig, M.P. Pond, M.R. Preimesberger, D.A. Bryant, J.T. Lecomte, Biochemistry 49 (2010) 7000-7011.

[18] B.J. Smagghe, J.T. Trent, III, M.S. Hargrove, PloS one 3 (2008).

[19] A.U. Igamberdiev, N.V. Bykova, R.D. Hill, Planta 223 (2006) 1033-1040.

[20] M. Sainz, C. Perez-Rontome, J. Ramos, J.M. Mulet, E.K. James, U. Bhattacharjee, J.W. Petrich, M. Becana, Plant J. 76 (2013) 875-887.

[21] A.M. Gardner, M.R. Cook, P.R. Gardner, J. Biol. Chem. 285 (2010) 23850-23857.

[22] D.B. Kim-Shapiro, M.T. Gladwin, Nitric Oxide. 38 (2014) 58-68.

[23] R.A. Marcus, N. Sutin, Biochim. Biophys. Acta, Rev. Bioenerg. 811 (1985) 265-322.

[24] M. Chou, C. Creutz, N. Sutin, J. Am. Chem. Soc. 99 (1977) 5615-5623.

[25] A.G. Mauk, H.B. Gray, Biochem. Biophys. Res. Commun. 86 (1979) 206-210.

[26] K. Tsukahara, J. Am. Chem. Soc.111 (1989) 4.

[27] G. Simonneaux, A. Bondon, Chem. Rev. 105 (2005) 2627-2646.

[28] M.R. Preimesberger, M.P. Pond, A. Majumdar, J.T. Lecomte, J. Biol. Inorg. Chem. 17 (2012) 599-609.

[29] A.G. Palmer, 3rd, Chem. Rev.104 (2004) 3623-3640.

[30] C. Brunel, A. Bondon, G. Simonneaux, Biochim. Biophys. Acta. 1101 (1992) 73-78.

[31] C.B. Brunel, A.; Simonneaux, G., J. Am. Chem. Soc. 116 (1994) 11827–11832.

[32] N.L. Scott, J.T. Lecomte, Protein Sci. 9 (2000) 587-597.

[33] K.O. Tsukahara, T.; Takahashi, H.; Yamamoto, Y., Inorg. Chem. 25 (1986) 4756-4760.

[34] E.S. Ryabova, P. Rydberg, M. Kolberg, E. Harbitz, A.-L. Barra, U. Ryde, K.K. Andersson, E. Nordlander, J. Inorg. Biochem. 99 (2005) 852-863.

[35] M.B. Steup, B.B. Muhoberac, J. Inorg. Biochem. 37 (1989) 233-257.

[36] P. Halder, J.T. Trent, 3rd, M.S. Hargrove, Proteins 66 (2007) 172-182.

[37] M.P. Doyle, D.M. LePoire, R.A. Pickering, J. Biol. Chem. 256 (1981) 12399-12404.

[38] S. Kakar, R. Sturms, A. Tiffany, J.C. Nix, A.A. DiSpirito, M.S. Hargrove, Biochemistry 50 (2011) 4273-4280.

[39] N.A. Farrow, O.W. Zhang, J.D. Formankay, L.E. Kay, J. Biomol. Nmr 4 (1994) 727-734.

[40] F. Delaglio, S. Grzesiek, G.W. Vuister, G. Zhu, J. Pfeifer, A. Bax, J. Biomol. Nmr 6 (1995) 277-293.

[41] C.J. Falzone, J.T. Lecomte, J. Biomol. Nmr. 23 (2002) 71-72.

[42] S.W. Benson, The Foundation of Chemical Kinetics, McGraw-Hill, New York, 1960.

[43] C. Capellos, B.H. Bielski, Kinetic systems mathematical description of chemical kinetics in solution, Wiley-InterScience, 1972.

[44] M.D. Goodman, M.S. Hargrove, J. Biol. Chem. 276 (2001) 6834-6839.

[45] L. Kiger, L. Tilleman, E. Geuens, D. Hoogewijs, C. Lechauve, L. Moens, S. Dewilde, M.C. Marden, PloS One 6 (2011).

[46] S. Raychaudhuri, J. Skommer, K. Henty, N. Birch, T. Brittain, Apoptosis 15 (2010) 401-411.

[47] D.A. Greenberg, K. Jin, A.A. Khan, Curr. Opin. Pharmacol. 8 (2008) 20-24.

[48] M. Brunori, A. Giuffre, K. Nienhaus, G.U. Nienhaus, F.M. Scandurra, B. Vallone, Proc. Natl. Acad. Sci. U.S.A. 102 (2005) 8483-8488.

[49] M.M. Rahaman, A.C. Straub, Redox Biol. 1 (2013) 405-410.

[50] P.R. Gardner, Scientifica (Cairo). 2012 (2012).

[51] B.J. Reeder, Antioxid. Redox Signaling 13 (2010) 1087-1123.

[52] D. Hoogewijs, E. Geuens, S. Dewilde, A. Vierstraete, L. Moens, S. Vinogradov, J.R. Vanfleteren, BMC Genomics. 8 (2007).

[53] J. Yoon, M.A. Herzik, Jr., M.B. Winter, R. Tran, C. Olea, Jr., M.A. Marletta, Biochemistry 49 (2010) 5662-5670.

[54] S. Kuznetsova, D.B. Knaff, M. Hirasawa, B. Lagoutte, P. Setif, Biochemistry 43 (2004) 510-517.

[55] S. Kuznetsova, D.B. Knaff, M. Hirasawa, P. Setif, T.A. Mattioli, Biochemistry 43 (2004) 10765-10774.

[56] M. Hirasawa, J.N. Tripathy, F. Sommer, R. Somasundaram, J.S. Chung, M. Nestander, M. Kruthiventi, M. Zabet-Moghaddam, M.K. Johnson, S.S. Merchant, J.P. Allen, D.B. Knaff, Photosynth. Res. 103 (2010) 67-77.

[57] N. Vajrala, W. Martens-Habbena, L.A. Sayavedra-Soto, A. Schauer, P.J. Bottomley, D.A. Stahl, D.J. Arp, Proc. Natl. Acad. Sci. U.S.A. 110 (2013) 1006-1011.

[58] C.T. Evelo, A.A. Spooren, R.A. Bisschops, L.G. Baars, J.M. Neis, Blood Cells Mol. Dis. 24 (1998) 280-295.

8 Tables

Table 1. A comparison of ESE and HA reduction rate constants for SynHb, nsHb1, and Mb.

Hb	k_{ESE} *(NMR)* $M^{-1}s^{-1}$	k_{ESE} *(cross)* $M^{-1}s^{-1}$	$k_{cross,HA}$ $M^{-1}s^{-1}$ *(calculated)*	k_{HA} $M^{-1}s^{-1}$
SynHb	690 (±70) pH 9 320 (±20) pH 7	880 (±70)	20,000	28,000
nsHb1		2,900 (±700)	65,000	25,000
Mb		0.05 (±0.01)	280*	250

k_{ESE} are the values measured by NMR or cross reaction. $k_{cross,HA}$ (the cross reaction that would support HA reduction) is calculated using Equation 1 and a value of 500 for $K_{eq.}$ The values of $k_{cross,HA}$ for SynHb and nsHb1 are calculated with $k_{ESE} = k_{ESE1} = k_{ESE2}$. *The calculation for Mb used 3,100 $M^{-1}S^{-1}$ (the ESE rate constant for TMP-Mb [30]) as an estimate for k_{ESE2}. k_{HA} values are taken from [8].

9 Figure Legends

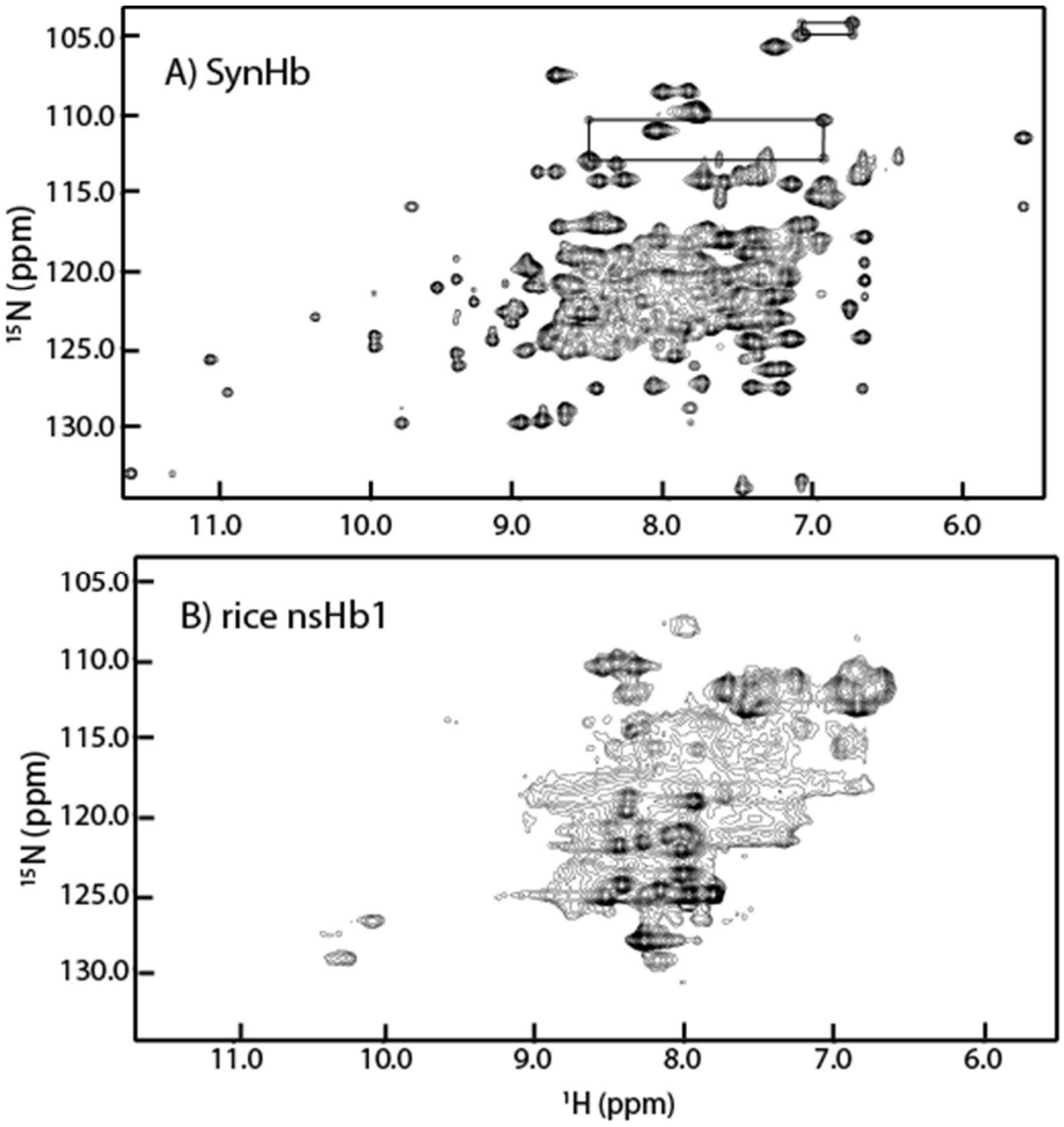

Figure 1. Chemical exchange NMR spectra of SynHb and nsHb1. A) A representative ZZ spectrum for SynHb showing two sets of resonances (connected by rectangles) associated with exchange between the ferric and ferrous oxidations states. B) A representative ZZ spectrum for nsHb1 demonstrates the poor quality of these data, which precludes ESE measurement using NMR.

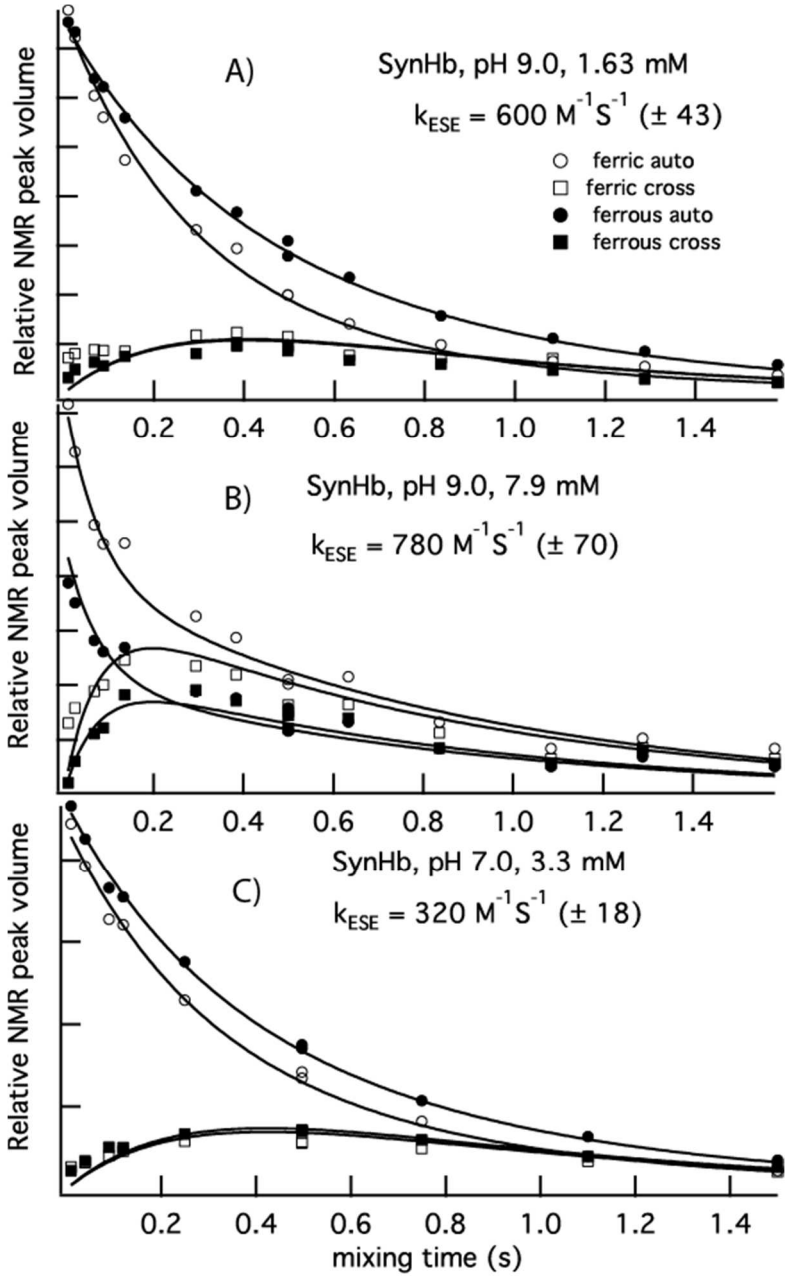

Figure 2. ESE kinetics for SynHb measured by chemical exchange NMR. A) Intensities of ferric and ferrous auto and cross peaks plotted versus ZZ mixing time for 1.63 mM SynHb at pH 9.0 along with fitted curves for Eqs. (4) – (7). B) ZZ data for 7.9 mM SynHb at pH 9.0, and C) 3.3 mM SynHb at pH 7.0. The peaks associated with Ile31 and Gly113 were used for the pH 9.0 and pH 7.0 analyses, respectively.

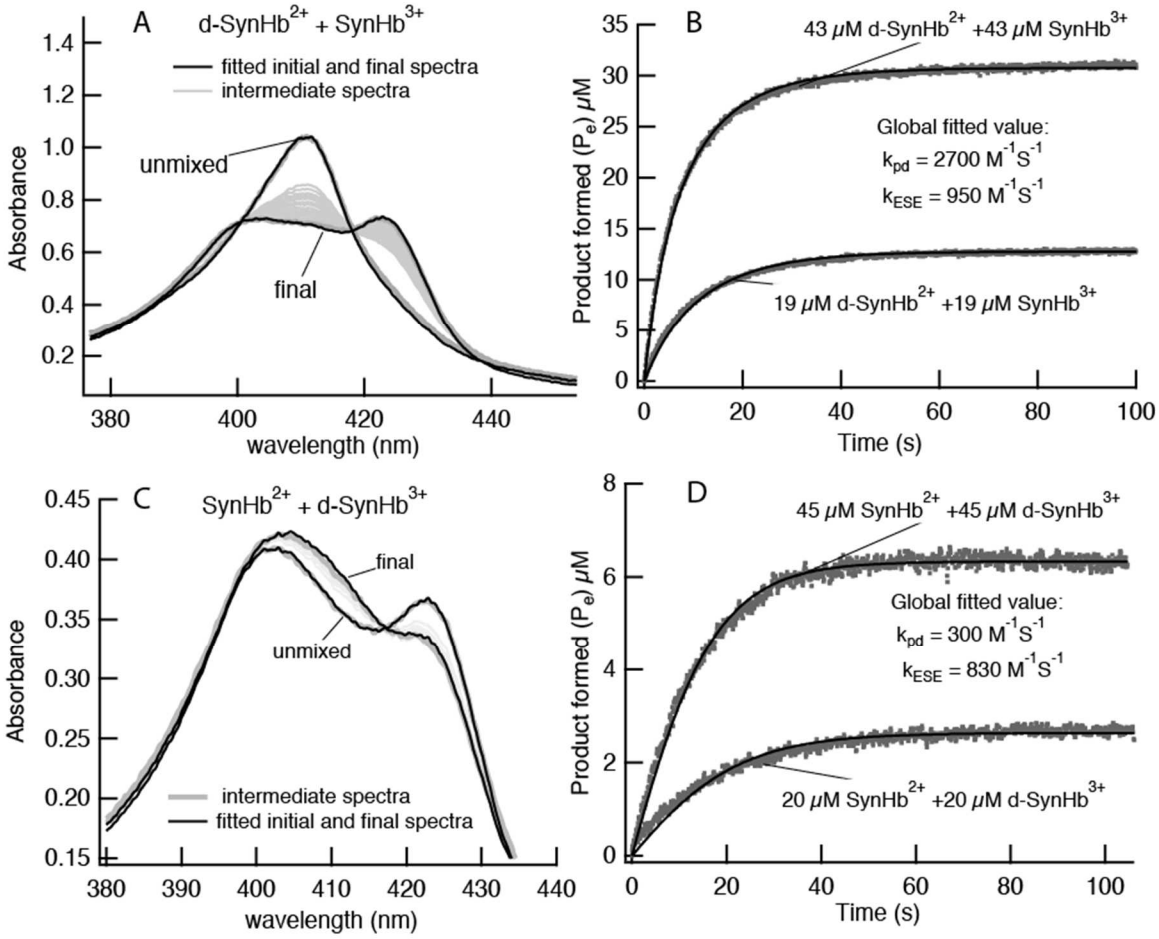

Figure 3. Electron transfer cross-reactions between SynHb and d-SynHb. A) Spectra for a mixture of d-SynHbII and SynHbIII are shown before mixing and after mixing at equilibrium, along with the respective spectral component fits. The lighter curves are intermediate spectra observed on this mixing time scale. B) Time courses at 411 nm for the reaction shown in A) at two concentrations are monitored in a stopped flow reactor. A global fit of both time courses to Eq. (11) produced kpd, the rate constant for the cross-reaction described by Eq. (8). The kESE value is calculated from kpd using Eqs. (8) and (12) (for Kpd). The reaction of SynHbII and d-SynHbIII is shown in C) and D).

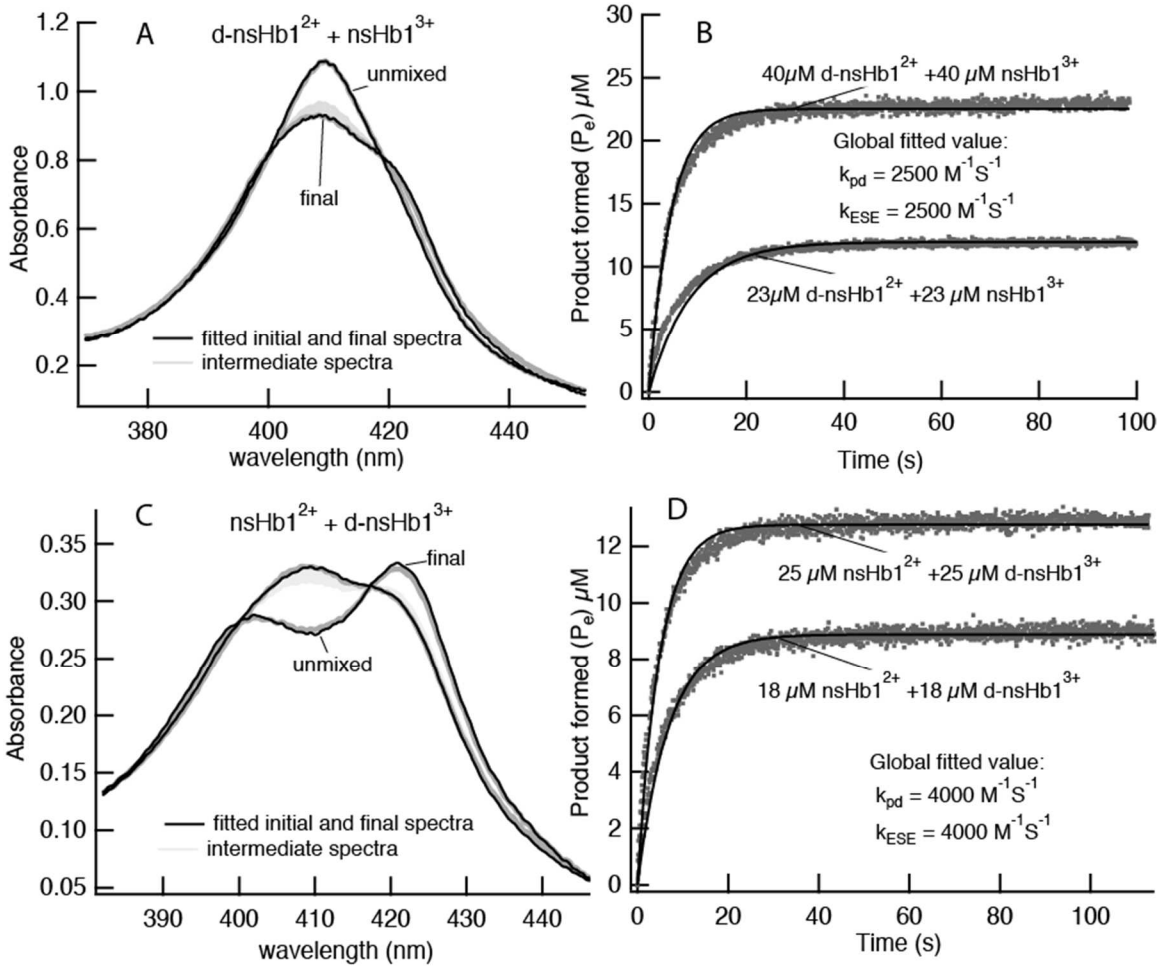

Figure 4. Electron transfer cross-reactions between nsHb1 and d-nsHb1. A) Spectra for a mixture of nsHbIII and d-nsHb1II are shown before mixing and after mixing at equilibrium, along with the respective spectral component fits. The lighter curves are intermediate spectra observed on this mixing time scale (there are fewer than Fig. 3 because more are lost in the mixing time of this faster reaction). B) Time courses for reactions monitored at 409 nm in a stopped flow reactor. Calculations of the fitted rate constants are described in Fig. 3 legend. The reaction of nsHbIII and d-nsHb1II is shown in C) and D).

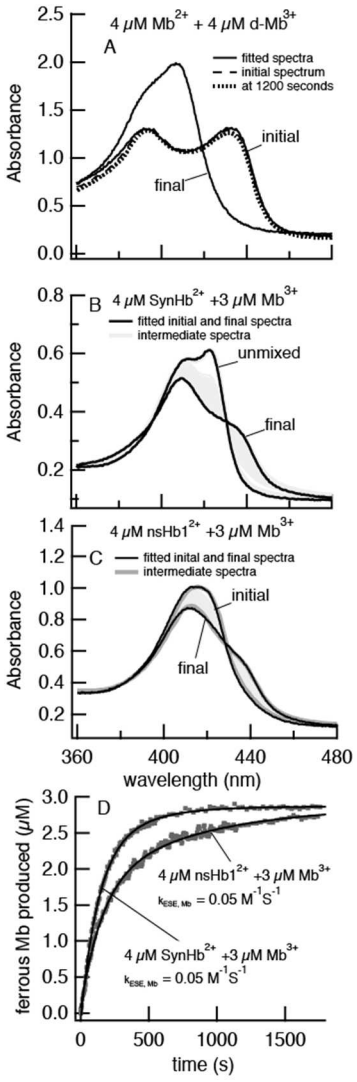

Figure 5. Measurement of electron exchange in Mb. A) Spectra for a mixture of MbII and d-MbIII are shown before mixing and at 1200 s after mixing along with spectral component fits showing that there is no reaction over this time period. The "final" spectrum is a simulation of the end point to provide some perspective on the reaction. B) The cross-reaction between SynHbII and MbIII and C) nsHb1II and MbIII along with spectral component fits to the initial and final states, indicating that the reactions proceed with complete reduction of Mb. D) Time courses for the reactions in B) and C) provide bimolecular ESE rate constants for Mb reduction of 0.05 M^{-1} s^{-1}.

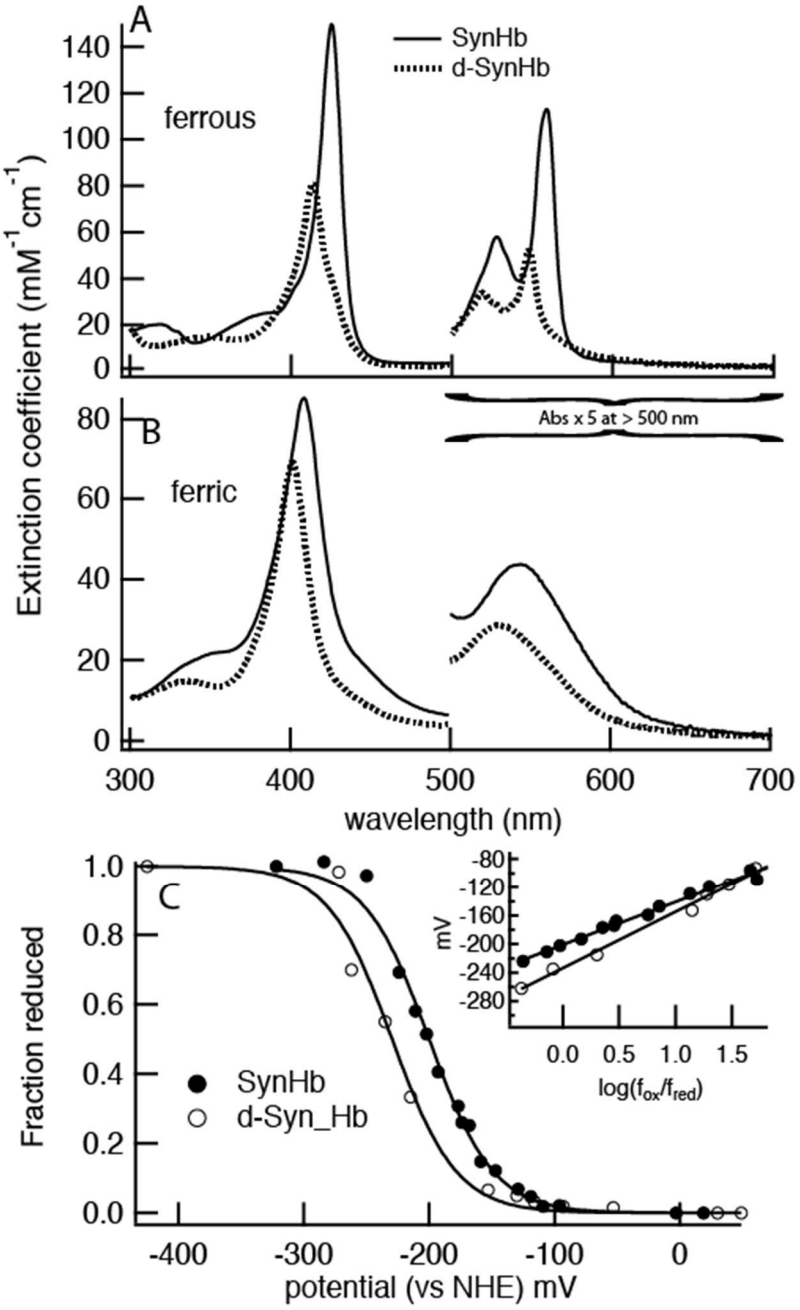

Figure S1. Spectral and electrochemical characterization of d-SynHb. Absorbance spectra of ferrous A) and ferric B) d-SynHb are compared to SynHb. C) Potentiometric titrations were used to measure redox potentials for each. The inset is a Nernst plot with fitted slopes of 59 mv for SynHb, and 69 mv for d-SynHb. The midpoint reduction potentials are -200 ±1.3 mV for SynHb, and -230 ±3.3 mV for d-SynHb.

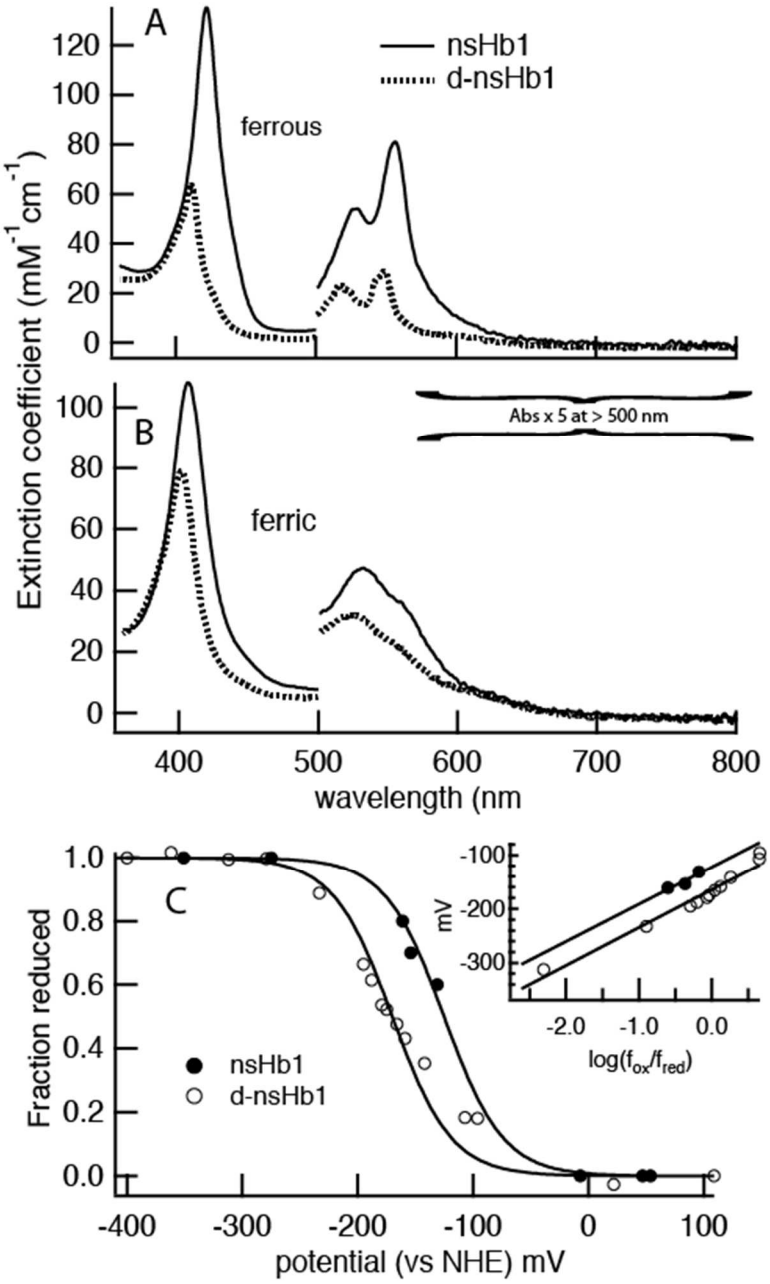

Figure S2. Spectral and electrochemical characterization of d-nsHb1. Absorbance spectra of ferrous A) and ferric B) d-nsHb1 are compared to nsHb1. C) Potentiometric titrations were used to measure redox potentials for each. The inset is a Nernst plot with fitted slopes of 69 mv for each protein. The midpoint reduction potentials are -125 ±2.0 mV for nsHb1, and -170 ±2.5 mV for d-nsHb1.

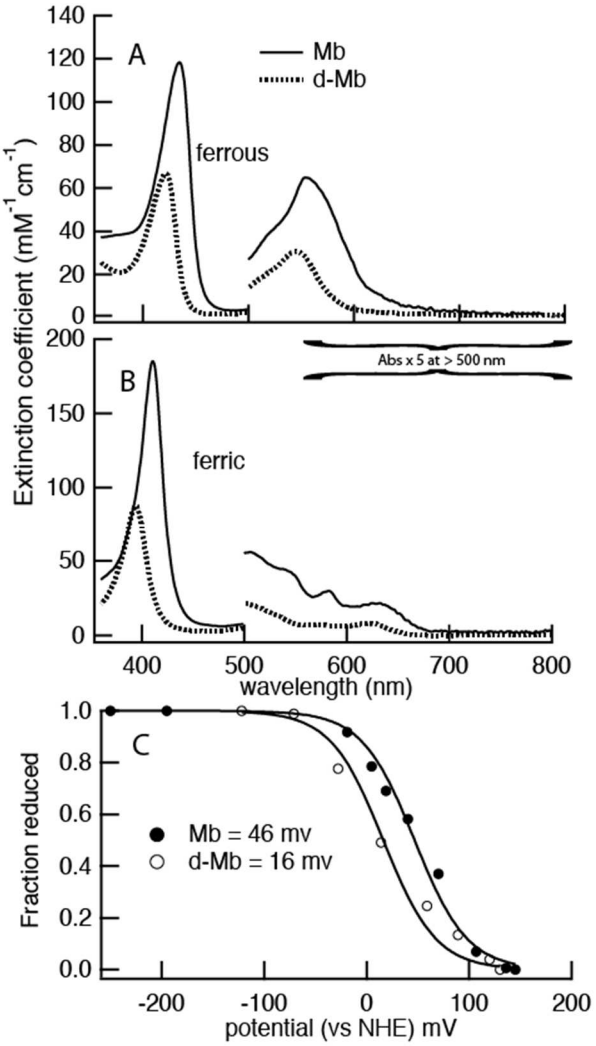

Figure S3. Spectral and electrochemical characterization of d-Mb. Absorbance spectra of ferrous A) and ferric B) d-Mb are compared to Mb. C) Potentiometric titrations were used to measure redox potentials for each. The inset is a Nernst plot with fitted slopes of 49 mv for Mb, and 59 mv for d-Mb. The midpoint reduction potentials are 46 ±2.5 mV for Mb, and 16 ±4.4 mV for d-Mb.

CHAPTER 3

THE ROLE OF REVERSIBLE HISTIDINE COORDINATION IN HYDROXYLAMINE REDUCTION BY PLANT HEMOGLOBINS (PHYTOGLOBINS)

A manuscript to be submitted to *Biochemistry*

Navjot Singh Athwal, Jagannathan Alagurajan, Amy H. Andreotti, and Mark S. Hargrove

INTRODUCTION

Hexacoordinate hemoglobins (hxHbs) are found in all plants and animals, and some bacteria. They are defined by a globin fold that surrounds the binding sites for heme *b* with two sources of coordination. Many hxHbs are coordinated by two histidine side chains. One remains coordinated to the heme iron akin to the "proximal" histidine of blood cell hemoglobin, and the other binds reversibly allowing for the competitive binding of other molecules such as oxygen, carbon monoxide (CO), nitric oxide (NO), nitrite, hydroxylamine (HA), oxide, cyanide, water, or hydroxide to name a few. Proposed functions for hexacoordinate hemoglobins in plants and animals have included NO production,[1,3] NO scavenging,[4-6] oxygen transport,[7] and signaling.[8-10] Recent interest has focused on hypoxic nitrite and HA reduction by hxHbs including the plant nonsymbiotic hemoglobins (phytoglobins) and neuroglobin in animals. It is thought that the NO produced from nitrite reduction might have a role in signaling in animals,[11] and that nitrite and HA reduction might be related to hypoxic metabolism in plants.[3] Regardless of function, the rates of nitrite and HA reduction by phytoglobins are generally much faster than neuroglobin,

cytoglobin, and the pentacoordinate oxygen transport hemoglobins found in animals.[3,12-14]

The reduction of HA by phytoglobins is interesting because it requires the delivery of two electrons to HA to make the stable end-product ammonium, yet each ferrous heme only delivers one electron.[12]

$$(1) \quad 2Hb^{2+} + NH_2OH + 2H^+ \rightarrow 2Hb^{3+} + NH_4^+ + OH^-$$

We have hypothesized that one Hb^{2+} molecule binds HA and then accepts an electron from another Hb^{2+} molecule to form ammonium and two molecules of Hb^{3+}. Electron transfer between hxHbs is rapid enough to support the previously observed rates of HA reduction,[15] but do not explain why phytoglobins carry out the reaction so much faster than other hxHbs such as neuroglobin and cytoglobin.

An important distinction between phytoglobins and other hxHbs is the fraction of hexacoordinate and pentacoordinate states found at rapid equilibrium in their populations (Figure 1).[16,17] The class 1 phytoglobins exist in solution with ~ 50 % of the molecules coordinated by the distal histidine, and 50% pentacoordinate. Figure 1 shows the case for the class 1 phytoglobin from rice (RHb). In RHb, the equilibrium constant for distal histidine coordination is 1.9, which indicates a 65/45 ratio of hexacoordinate (Hb_{Hx}) to pentacoordinate (Hb_p) species. These molecules interconvert with rates constants of 40 s^{-1} and 75 s^{-1} for histidine dissociation and rebinding, respectively. It is this mixture of states

that reacts with ligands, and CO and oxygen binding show distinct phases for reactions with the hexacoordinate and pentacoordinate species.[18]

It is not yet known whether physical properties such as histidine coordination are responsible for the stark differences in HA reduction rates between plant and animal hemoglobins. In the present experiments we have used kinetic methods to study HA reduction by RHb, RHb mutant proteins, and natural phytoglobin variants that have different rate and equilibrium constants for hexacoordination. Our results demonstrate that K_H values near unity (such as those of class 1 phytoglobins) are required for efficient HA reduction, with the Hb_p species able to rapidly bind HA, and Hb_{Hx} quickly donating the second electron. In proteins with $K_H >> 1$ (such as neuroglobin), HA binding is blocked, and when $K_H << 1$ (such as in oxygen transport hemoglobins), HA saturation inhibits the electron transfer reaction needed to finish the reaction. Thus, the details of reversible histidine coordination are critical in the mechanism for HA reduction by hxHbs.

MATERIAL AND METHODS

Preparation of proteins. All proteins, including mutants, were expressed in E. Coli BL21 (DE3) cells (Agilent Cat#200131) and purified as reported earlier.[12, 19, 20] Briefly, the host cells were transformed with pET28 plasmid containing cDNA coding for respective protein. The transformed E.coli cells were grown overnight at 37°C with shaking at 200rpm in 2L flasks containing 1L of terrific broth media. The harvested cells were concentrated, lysed by sonication and protein was pulled out of lysate using their His-tag.

Hydroxylamine reduction kinetics. All reactions were set up inside anaerobic chamber maintained at 8% hydrogen in Argon (Coy laboratories). Anaerobic 100mM K_2HPO_4 buffer at pH 7.0 was prepared by boiling and subsequently flushing with nitrogen for 30 min. Deoxy-ferrous Hbs were prepared using sodium dithionite followed by desalting over sephadex G-25 column to get rid of excess dithionite.

Rapid mixing kinetics measurements. The reactions were setup as described earlier,[12] in brief Bio-Logic stopped flow SFM-400 reactor coupled with MOS-200 scanning spectrometer was used to collect kinetic traces at give wavelengths. Biokine software was used for collection and processing of kinetic data thus obtained. Hydroxylamine (HA) was prepared by dissolving pre-weighed amount of hydroxylamine-HCL salt in 100mM K_2HPO_4, pH 7.0 anaerobic buffer. Equal volume of deoxy-ferrous Hb and HA were mixed by the reactor and reaction time course measured at 555nm.

Rice E7L hydroxylamine binding. Deoxy-ferrous Rice E7L upon mixing with HA gave a split visible spectra characteristic of heme coordination by a distal ligand. This spectra was transient and its magnitude varied with HA concentration mixed. The initial spectra upon mixing using SFM-400 reactor were saved and their amplitude at 553nm was used to calculate fraction of Hb bound to HA and that was plotted against HA concentration. The dissociation equilibrium constant was obtained by fitting the following equation:

$$F_{B-HA} = \frac{[HA]}{K_{D-HA} + [HA]}$$

Equation 1

RESULTS

Kinetic analysis of the reaction mechanism. The hypothesized mechanism for HA reduction by hxHbs is shown in Figure 1, along with rate and equilibrium constants for hexacoordination that are specific to RHb. In this mechanism, HA reacts with the equilibrium mixture of RHb_{Hx} and Hb_P to form the RHb:HA complex, which then reacts with another ferrous RHb_{Hx} for electron transfer and product formation. Earlier work has demonstrated electron exchange between RHb molecules that is fast enough so as to not serve as a kinetic limit,[15] but this possibility was not tested directly. The experiments leading to the results in Figure 2 were designed to test the kinetic limit to the reaction.

Figure 2A shows rate constants for HA reduction as a function of $[RHb^{2+}]$ at fixed (50 μM) HA concentration. These observed rate constants show no dependence on RHb concentration. Also shown in Figure 2A are the calculated rate constants for bimolecular electron transfer at these RHb^{2+} concentrations. Clearly some protein concentration dependence for the HA reduction rate constant is expected if the electron transfer reaction were rate limiting. The fact that this is not observed supports our previous conclusion that electron transfer is not a limit to the reaction.

In Figure 2B, RHb concentration is fixed, and [HA] is increased in an effort to determine if some other kinetic limit is reached, or if the concentration dependence of the rate constant is linear to the limit of our rapid mixing device (~ 300 s^{-1}). The observed rate

constants reach a limit of 83 s^{-1} with a saturation midpoint at 1.6 mM HA. Because we have never observed spectral intermediates in this reaction with RHb, we propose that the binding of HA must be the rate limiting step, and that once bound, the reaction proceeds to completion very rapidly.

This conclusion is supported by analysis of the reaction time courses at each HA concentration (Figure 2C,D). The complete expected change in absorbance for RHb oxidation is observed at lower [HA], but as the concentration is increased, an increasing fraction of the time course is lost in the reaction dead time (3 ms). The same phenomenon is observed for CO binding to RHb, and the fraction lost is a direct measure of K_H.[18,20] The lost amplitude at high [HA] is ~ 50% so we propose that HA binding to RHb_P is followed by rapid electron transfer and product formation, such that half of the reaction is complete within the dead time of the apparatus.

The results from Figures 1 and 2 suggest that HA binding to RHb is the rate limiting step of the reaction, and that RHbP binds first and then rapidly consumes a molecule of RHbHx for the electron transfer step. This series of reactions is as follows.

$$(2)\quad Hb_{Hx} \underset{k_H}{\overset{k_{-H}}{\rightleftharpoons}} Hb_P$$

$$(3)\quad Hb_P + HA \underset{k_{-HA}}{\overset{k_{HA}}{\rightleftharpoons}} Hb_P{:}HA$$

$$(4)\quad Hb_P{:}HA + Hb_{Hx} \xrightarrow{k_3} 2Hb^{3+} + NH_4^+$$

$$(5)\quad Hb_P{:}HA + Hb_P{:}HA \xrightarrow{k_4} 2Hb^{3+} + NH_4^+\ HA$$

The first two reactions are the series associated with ligand binding to any hxHb [18]. As shown in Figure 2D, we know that HA binds Hb_P rapidly. Subsequent binding of HA to Hb_{Hx} (associated with the rate constants observed in Figure 2B) will thus obey the following equation where k_H and k_{-H} are the rate constants for binding and dissociation of the distal histidine, and k_{HA} is the association rate constant for HA once the coordinating histidine is out of the way[18]:

$$k_{obs,HA} = \frac{k_{-H}k'_{HA}[HA]}{k_H + k_{-H} + k'_{HA}[HA]} \qquad \text{Equation 2.}$$

Reactions 4 and 5 consider that the electron transfer and product formation steps could proceed either via RHb_P:HA reacting with Hb_{Hx} (reactions 2, 3, and 4; “model 1”) or with another molecule of RHbp:HA (reactions 2, 3, and 5; “model 2”). Fortunately the concentration dependence of the reaction we have measured can be used to distinguish between these possibilities. Figure 1 and Equation 2 predict a rate limit for HA binding to RHb_{Hx} of 40 s^{-1} (equal to k_{-H}). However, we are monitoring the reaction as the production of Hb^{3+}. If reaction 4 is very fast, then two molecules of Hb^{3+} are produced for every HA binding event, and the rate limit should be 2*k_{-H} (80 s-1), which is observed.

Figure 2B shows fitted curves for the [HA] dependence of the observed rate constants resulting from numerical simulation of the reactions above in an effort to distinguish between models 1 (solid lines) and 2 (dashed lines). It is evident that the former

series of reactions culminating in electron transfer between RHb_{Hx} and RHbp:HA fit our data well, and predict a rate limit of 2*k-H. Model 2 predicts a rate limit of k-H because completion requires saturation of RHb with HA, which must wait for k_{-H}, whereas in the former set of reactions RHb_{Hx} can be consumed even without histidine dissociation.

The results from Figure 2 predict that the kinetic limit of hxHb reacting with HA should equal 2*k-H. Figure 3 tests the generality of this conclusion by examining rate constants for HA reduction by a series of hxHbs as a function of [HA]. It has previously been reported that the RHb mutant protein F40G (RHb:F40G) has a slower value for k_{-H} (8 s^{-1})[20]. Additionally, class 1 phytoglobins from soybean and tomato have k_{-H} values larger than RHb, equal to 80 and 185 s^{-1}, respectively [16]. As shown in Figure 3, the asymptotes reached for HA reduction for each of these proteins are equal to twice their respective k_{-H} values.

The role of the distal histidine in HA reduction. The results above support the hypothesis that HA reduction is limited by binding to the Hb and not by electron transfer and ammonia formation. The distal histidine has at least two important roles in this reaction. 1) It lowers the affinity for HA by competing for the binding site, and 2) it contributes to the electron transfer reaction through formation of Hb_{Hx}. The next set of experiments tests the effect of removal of the distal histidine on HA reduction by examination of the RHb:H73L mutant protein, in which the distal histidine has been replaced by Leucine.

Figure 4A shows the high-spin spectrum of ferrous RHb:H73L prior to mixing with HA along with spectra following mixing at increasing HA concentrations. The formation of a

low-spin reaction intermediate (presumably RHb:H73L-HA) is readily evident upon mixing with HA, which then slowly decays to the spectrum of ferric RHb:H73L. The fractional saturation associated with formation of the intermediate is measurable from the magnitude of the low-spin spectrum, and this is plotted in Figure 4B to fit for a dissociation equilibrium constant ($K_{D\text{-}HA}$) of 470 μM.

The results from Figure 4B demonstrate that the distal histidine is directly competing with HA for access to the heme iron. If hexacoordination were the only factor determining the difference in KHA between RHb and RHb:H73L, the relationship between the two would be:

$$K_{D-HA,Obs} = K_{D-HA,pent}\,(1 + K_H)$$

Equation 3.

In Equation 3, $K_{D,HA,pent}$ is the dissociation equilibrium constant for HA binding to the Hb without any competing hexacoordination (RHb:H73L), $K_{D,HA,obs}$ is that taking into account hexacoordination, and K_H is the equilibrium constant for association of the distal histidine.[21] For RHb:H73L, $K_{D,HA,pent}$ is 470 μM, and for RHb K_H is 1.9. Thus Equation 3 predicts a value of 1,360 μM for $K_{D\text{-}HA}$ for RHb, which not too dissimilar from the value of 1,600 μM that is observed. This suggests that, with respect to HA binding, the major role of the distal histidine is simply providing competition for binding at the heme iron.

The data in Figure 4 suggest a rapid-equilibrium formation of RHb: H73L-HA followed by Hb oxidation and product formation obeying the following reaction scheme:

$$(6)\ \mathrm{RHb{:}H73L + HA} \underset{k_{-HA}}{\overset{k_{HA}}{\rightleftharpoons}} \mathrm{RHb{:}H73L\text{-}HA} \xrightarrow{k_{product}} \mathrm{RHb{:}H73L^{3+} + NH_4^+}$$

The concentration dependence of the observed rate constant would then be:

$$k_{Obs} = \frac{k_{oxidation}\,[HA]}{K_{HA}+[HA]}$$

Equation 4.

Figure 5A shows the rate constants for the decay of the intermediate species as a function of [HA]. Fitting these data to Equation 4 provides an independent observation of K_{HA} (also equal to 470 μM) and the rate constant for $k_{oxidation}$ = 0.2 s^{-1}.

There are clearly much larger affects of distal histidine removal on aspects of the reaction unrelated to HA binding, as the maximum k_{obs} value for RHb:H73L is ~400 times smaller than that for RHb. To test whether or not the concentration of RHb:H73L is a rate limiting factor, [RHb:H73L] was varied between 10 and 75 μM with [HA] fixed at 5 mM, but no dependence of k_{obs} on [RHb:H73L] was observed (Figure 5A). The results from Figure 5A suggest that the distal histidine plays a role in catalysis as well as its role in regulating HA affinity.

The final experiment with RHb:H73L was designed to test if the role of the distal histidine could be replaced in trans by addition of imidazole to RHb:H73L. The dissociation equilibrium constant for imidazole binding to ferrous RHb:H73L is 11 mM,[19] so imidazole concentrations ranging from 0 to 250 mM were added to the reaction mixtures, and HA

reduction rate constants were measured as a function of [HA] (Figure 5A). At each [HA], the data were fit to Equation 4. The observed value of $K_{D\text{-}HA}$ increased as expected because of competition from imidazole binding, and the koxidation value also increased. Surprisingly, the increase in $k_{oxidation}$ was linear with [HA] even at concentrations well beyond the values needed to saturate RHb:H73L ([HA] > 110 mM). These data indicate that the distal histidine plays a chemical role in HA reduction that can be partially accomplished by exogenous imidazole that is not proportional to imidazole saturation of the heme iron.

DISCUSSION

The results presented here suggest several reasons why phytoglobins catalyze HA reduction more efficiently than other hxHbs such as neuroglobin and cytoglobin, and pentacoordinate hemoglobins such as myoglobin and blood cell hemoglobin. The resulting model for RHb is that HA binding is the rate-limiting step and that once bound, it is rapidly converted to ammonium along with the oxidation of two molecules of RHb. These conclusions are supported by the following observations: 1) Reaction time courses at high [HA] sample the population of RHbP as a rapid reaction lost in the mixing dead time. 2) The reaction with the fraction of RHbHx is limited by dissociation of the coordinating distal histidine. 3) The affinity for HA is directly related to K_H (as described by Equation 3). These conclusions are important because they reveal a clear picture of the role of the distal histidine in HA reduction, provide a better estimate for the electron transfer rate of the reaction, and draw a structural analogy between other enzymes that helps to clarify the potential role of phytoglobins in plant anaerobic metabolism.

The role of the distal histidine in HA reduction. The distal histidine plays two roles in HA reduction by RHb; it competes with HA binding, and provides a low-spin heme ligand to facilitate electron transfer. At first thought it might seem that competition for binding would inhibit the reaction. But if the affinity for the distal histidine is not too large (K_H ~ 1), there are available populations of both RHb_P and RHb_{Hx}. If RHb_{Hx} is a superior electron donor compared to RHb_P and RHb:HA, then the net effect of competition by the distal histidine is to ensure the presence of rapidly reacting molecules (RHb_P), and electron donors (RHb_{Hx}), while at the same time preventing saturation of RHb by HA to form the inferior electron donor RHb:HA. The likelihood that RHbHx is the better electron donor is supported by the fact that the rate limit to HA reduction is $2*k_{-H}$ rather than k_{-H}, which is expected if all species contributed equally to electron transfer (Figure 2B).

The class 1 phytoglobins are the only hxHbs with K_H values near unity, and are thus the only ones that could support HA using this mechanism. K_H for neuroglobin and cytoglobin are both much larger and have populations of Hb_P near 0. Furthermore their k_{-H} values (~ 1 s^{-1}, depending on species origin and cysteine oxidation in Ngb[14]) are also lower than RHb, so the maximum observed values for HA reduction are expected to be lower even at very high [HA]. Thus, these hxHbs with tighter hexacoordination and slower kinetics of histidine dissociation will be poorer HA reductases because they lack the fastest phase of the reaction (the large K_H leaves no Hb_P), and the fraction of the reaction resulting from HA reacting with Hb_{Hx} is also slower due to the lower values of k_{-H}.

Pentacoordinate Hbs would face the opposite problem from that of tightly coordinating hxHbs. With no competition for the binding site, HA would saturate the the Hb (such as the case of RHb:H73L). If the HA-bound intermediate were a poor electron donor (as argued above for RHb), then the reaction rate would be limited by electron transfer. At lower HA concentrations the reaction rate might also be limited by slower electron transfer from the unbound Hb_P species [15]. A test of these ideas was not directly provided by the results with RHb:H73L though, because the roles of the distal histidine (or exogenous imidazole) in affecting HA binding, electron transfer, and chemical catalysis could not be deconvoluted. It is possible that the distal histidine is positioned to donate the proton needed for the conversion of HA to ammonium, and to facilitate the dissociation of ammonium once it is formed.

Intermolecular Electron transfer in RHb. Results from Figure 2B indicate that electron transfer occurs from RHb_{Hx} to RHb:HA. The electron transfer cross-reaction can be calculated from electron self-exchange rates for each species using Equation 5, where k_{ET} is the calculated electron transfer rate constants, k_{ESE} are the self-exchange rate constants, and K_{EQ} is the equilibrium constant ("driving force") for the reaction.[22]

$$k_{ET} = \sqrt[2]{k_{ESE,RHbHx} k_{ESE,RHb:HA} K_{EQ}} \qquad \text{Equation 5.}$$

The self-exchange rate constant for RHb_{Hx} ($k_{ESE,RHbHx}$) has been measured at 2,900 $M^{-1}s^{-1}$.[15] If we assume the same value for self-exchange with RHb:HA, we may use the observed rate of HA reduction to estimate the value of k_{ET} that would be need to support the reaction.

The results from Figure 2 demonstrate that HA reduction can be completed during the 3 ms dead time or our mixing apparatus. Assuming that this represents ten-times the half-life of the reaction, the reaction half-life can be set at 0.3 ms with the associated rate constant of 2,300 s^{-1}. If we calculate for a reaction using a total RHb concentration of 10 µM, then k^{ET} must be equal to 2.3 x108 $M^{-1}s^{-1}$, and K_{EQ} would be on the order of 10^9. Our previous estimate of 500 for KEQ was based on the minimum value needed to support the much lower absolute rates of HA reduction observed at sub-saturating [HA], without knowing the extreme rates that could be achieved by saturation of RHb_P. The value of 10^9 is a value much more in with electron transfer reactions measured in other systems.[23]

The relationship of HA reduction to physiologically important reactions. Our interest in HA reduction stems from a hypothesis that phytoglobins might play a role in plant anaerobic metabolism.[3,12] There is circumstantial evidence that phytoglobins and inorganic nitrogen aid in survival of hypoxia,[24-26] and that phytoglobins are genetically up-regulated in response to both,[16,25,27,28] yet there are no biochemical mechanisms known to explain these phenomena.

Many bacteria use nitrate and nitrite for respiration and/or as an aid for non-fermentative NADH oxidation to support anaerobic glycolysis [29]. In fact, it has been proposed that phytoglobins might use the “nitric oxide dioxygenase” (NOD) reaction to

oxidize NADH [25, 26]. The benefit of coupling nitrite and/or HA reduction to NADH oxidation rather than oxygen and nitric oxide (used in the NOD reaction), is that it would leave any oxygen present during hypoxic stress for use in oxygen respiration and ATP formation.

Plants lack a gene homologue for respiratory nitrite reductase such as the bacterial enzyme Nrf. Nrf uses a combination of bis-histidyl hexacoordinate heme groups and a pentacoordinate heme active site to deliver six electrons to nitrite to form ammonia [30]. The hexacoordinate heme sites are important for electron transfer, while the pentacoordinate site is necessary for nitrite binding. Nrf will also reduce nitric oxide and HA to ammonium. Another example of heme groups working together in support of inorganic nitrogen reduction is nitric oxide reductase, a respiratory enzyme found in denitrifying bacteria, which catalyzes the two electron reduction of nitric oxide to form nitrous oxide [31]. The mechanism used by RHb to reduce HA to ammonium shares features with these enzymes, but achieves the complete enzymatic structure through intermolecular interactions between RHb_P and RHb_{Hx}. Thus, while we are not sure whether or not phytoglobins really have a physiological role in anaerobic inorganic nitrogen reduction, they certainly catalyze these reactions and share chemical mechanisms with enzymes that support respiratory functions in other organisms.

REFRENCES

[1] Hendgen-Cotta, U. B., Kelm, M., and Rassaf, T. (2014) Myoglobin's novel role in nitrite-induced hypoxic vasodilation, Trends Cardiovasc. Med. 24, 69-74.

[2] Hendgen-Cotta, U. B., Kelm, M., and Rassaf, T. (2010) A highlight of myoglobin diversity: the nitrite reductase activity during myocardial ischemia-reperfusion, Nitric Oxide 22, 75-82.

[3] Sturms, R., DiSpirito, A. A., and Hargrove, M. S. (2011) Plant and cyanobacterial hemoglobins reduce nitrite to nitric oxide under anoxic conditions, Biochemistry 50, 3873-3878.

[4] Smagghe, B. J., Trent, J. T., III, and Hargrove, M. S. (2008) NO Dioxygenase Activity in Hemoglobins Is Ubiquitous In Vitro, but Limited by Reduction In Vivo, PLoS One 3, e2039.

[5] Gardner, P. R., Gardner, A. M., Martin, L. A., and Salzman, A. L. (1998) Nitric oxide dioxygenase: an enzymic function for flavohemoglobin, Proc. Natl. Acad. Sci. U. S. A. 95, 10378-10383.

[6] Gardner, P. R. (2012) Hemoglobin: a nitric-oxide dioxygenase, Scientifica 2012, 683729.

[7] Antonini, E. a. B., M. (1971) Hemoglobin and Myoglobin in their interaction with ligands Vol. 21, North-Holland, Amsterdam.

[8] Raychaudhuri, S., Skommer, J., Henty, K., Birch, N., and Brittain, T. (2010) Neuroglobin protects nerve cells from apoptosis by inhibiting the intrinsic pathway of cell death, Apoptosis 15, 401-411.

[9] Reeder, B. J., Svistunenko, D. A., and Wilson, M. T. (2011) Lipid binding to cytoglobin leads to a change in haem co-ordination: a role for cytoglobin in lipid signalling of oxidative stress, Biochem. J. 434, 483-492.

[10] Fago, A., Mathews, A. J., Moens, L., Dewilde, S., and Brittain, T. (2006) The reaction of neuroglobin with potential redox protein partners cytochrome b5 and cytochrome c, FEBS Lett. 580, 4884-4888.

[11] Liu, C., Wajih, N., Liu, X. H., Basu, S., Janes, J., Marvel, M., Keggi, C., Helms, C. C., Lee, A. N., Belanger, A. M., Diz, D. I., Laurienti, P. J., Caudell, D. L., Wang, J., Gladwin, M. T., and Kim-Shapiro, D. B. (2015) Mechanisms of Human Erythrocytic Bioactivation of Nitrite, J. Biol. Chem. 290, 1281-1294.

[12] Sturms, R., DiSpirito, A. A., Fulton, D. B., and Hargrove, M. S. (2011) Hydroxylamine reduction to ammonium by plant and cyanobacterial hemoglobins, Biochemistry 50, 10829-10835.

[13] Tiso, M., Tejero, J., Kenney, C., Frizzell, S., and Gladwin, M. T. (2012) Nitrite reductase activity of nonsymbiotic hemoglobins from Arabidopsis thaliana, Biochemistry 51, 5285-5292.

[14] Tiso, M., Tejero, J., Basu, S., Azarov, I., Wang, X., Simplaceanu, V., Frizzell, S., Jayaraman, T., Geary, L., Shapiro, C., Ho, C., Shiva, S., Kim-Shapiro, D. B., and Gladwin, M. T. (2011) Human neuroglobin functions as a redox-regulated nitrite reductase, J. Biol. Chem. 286, 18277-18289.

[15] Athwal, N. S., Alagurajan, J., Sturms, R., Fulton, D. B., Andreotti, A. H., and Hargrove, M. S. (2015) Electron self-exchange in hemoglobins revealed by deutero-hemin substitution, J. Inorg. Biochem. 150, 139-147.

[16] Smagghe, B. J., Hoy, J. A., Percifield, R., Kundu, S., Hargrove, M. S., Sarath, G., Hilbert, J. L., Watts, R. A., Dennis, E. S., Peacock, W. J., Dewilde, S., Moens, L., Blouin, G. C., Olson, J. S., and Appleby, C. A. (2009) Review: correlations between oxygen affinity and sequence classifications of plant hemoglobins, Biopolymers 91, 1083-1096.

[17] Kakar, S., Hoffman, F. G., Storz, J. F., Fabian, M., and Hargrove, M. S. (2010) Structure and reactivity of hexacoordinate hemoglobins, Biophys. Chem. 152, 1-14.

[18] Smagghe, B. J., Sarath, G., Ross, E., Hilbert, J. L., and Hargrove, M. S. (2006) Slow ligand binding kinetics dominate ferrous hexacoordinate hemoglobin reactivities and reveal differences between plants and other species, Biochemistry 45, 561-570.

[19] Halder, P., Trent, J. T., 3rd, and Hargrove, M. S. (2007) Influence of the protein matrix on intramolecular histidine ligation in ferric and ferrous hexacoordinate hemoglobins, Proteins 66, 172-182.

[20] Smagghe, B. J., Kundu, S., Hoy, J. A., Halder, P., Weiland, T. R., Savage, A., Venugopal, A., Goodman, M., Premer, S., and Hargrove, M. S. (2006) Role of phenylalanine B10 in plant nonsymbiotic hemoglobins, Biochemistry 45, 9735-9745.

[21] Trent, J. T., 3rd, Watts, R. A., and Hargrove, M. S. (2001) Human neuroglobin, a hexacoordinate hemoglobin that reversibly binds oxygen, J. Biol. Chem. 276, 30106-30110.

[22] Marcus, R. A. S., N. (1985) Electron transfers in chemistry and biology, Biochimica et Biophysica Acta(BBA) - Reviews on Bioenergetics 811, 265-322.

[23] Chou, M., Creutz, C., and Sutin, N. (1977) Rate constants and activation parameters for outer-sphere electron-transfer reactions and comparisons with the predictions of Marcus theory, J. Am. Chem. Soc. 99, 5615-5623.

[24] Dordas, C., Hasinoff, B. B., Igamberdiev, A. U., Manac'h, N., Rivoal, J., and Hill, R. D. (2003) Expression of a stress-induced hemoglobin affects NO levels produced by alfalfa root cultures under hypoxic stress, The Plant Journal 35, 763-770.

[25] Igamberdiev, A. U., and Hill, R. D. (2004) Nitrate, NO and haemoglobin in plant adaptation to hypoxia: an alternative to classic fermentation pathways, Journal of Experimental Botany 55, 2473-2482.

[26] Dordas, C., Hasinoff, B. B., Rivoal, J., and Hill, R. D. (2004) Class-1 hemoglobins, nitrate and NO levels in anoxic maize cell-suspension cultures, Planta 219, 66-72.

[27] Hunt, P., Klok, E., Trevaskis, B., Watts, R., Ellis, M., Peacock, W., and Dennis, E. (2002) Increased level of hemoglobin 1 enhances survival of hypoxic stress and promotes early growth in Arabidopsis thaliana, Proceedings of the National Academy of Sciences 99, 17197-17202.

[28] Ohwaki, Y., Kawagishi-Kobayashi, M., Wakasa, K., Fujihara, S., and Yoneyama, T. (2005) Induction of class-1 non-symbiotic hemoglobin genes by nitrate, nitrite and nitric oxide in cultured rice cells, Plant Cell Physiol. 46, 324-331.

[29] Cole, J. A., and Richardson, D. J. (2008) Respiration of Nitrate and Nitrite, EcoSal Plus 3.

[30] Clarke, T. A., Dennison, V., Seward, H. E., Burlat, B., Cole, J. A., Hemmings, A. M., and Richardson, D. J. (2004) Purification and spectropotentiometric characterization of Escherichia coli NrfB, a decaheme homodimer that transfers electrons to the decaheme periplasmic nitrite reductase complex, J. Biol. Chem. 279, 41333-41339.

[31] Shiro, Y. (2012) Structure and function of bacterial nitric oxide reductases: nitric oxide reductase, anaerobic enzymes, Biochim. Biophys. Acta 1817, 1907-1913.

FIGURES AND LEGENDS

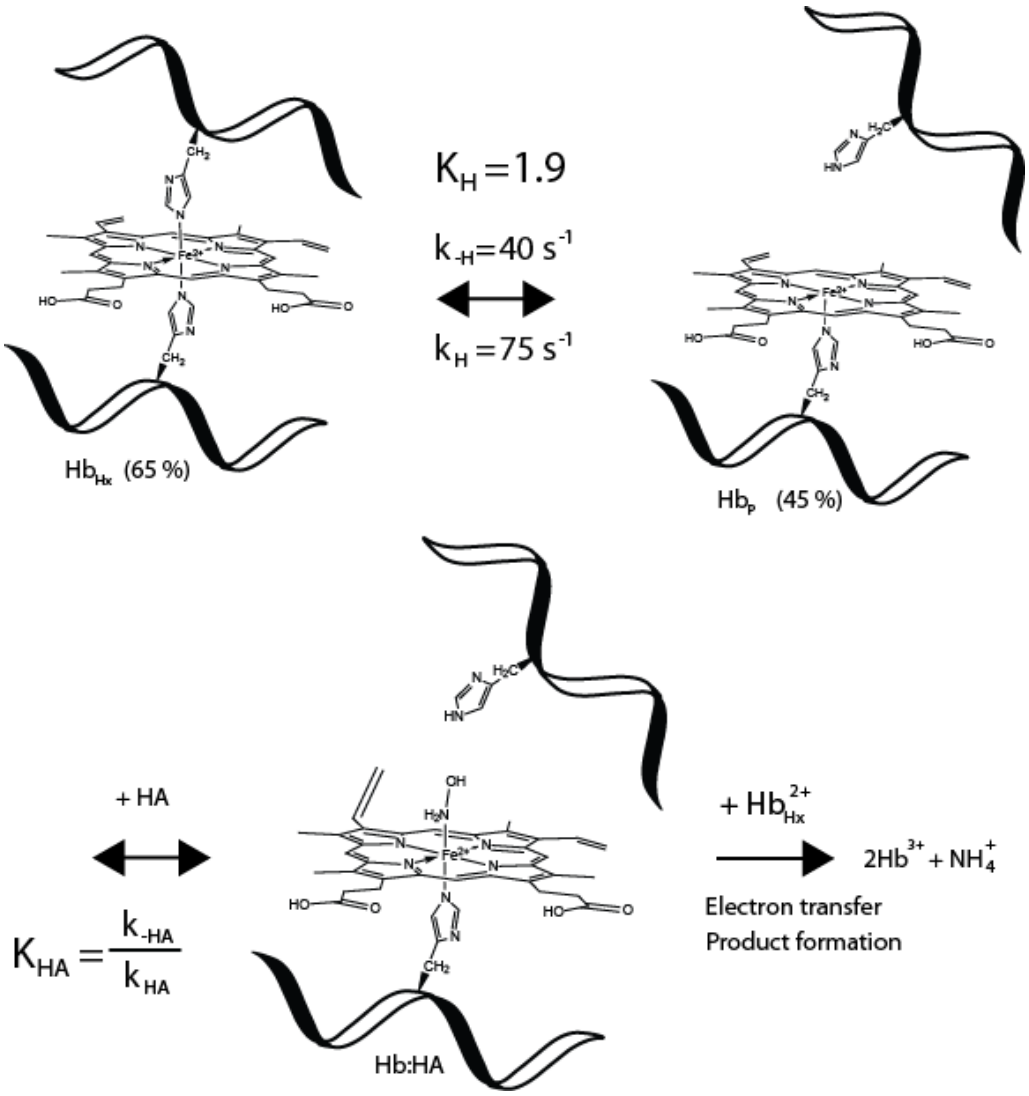

Figure 1. Hypothesized mechanism for HA reduction by hxHbs. An association equilibrium constant of 1.9 leads to a split population of $Hb^{2+}{}_{Hx}$ and $Hb^{2+}{}_{P}$ conformations. The $Hb^{2+}{}_{P}$ quickly binds to HA making a transition complex that eventually reacts with another $Hb^{2+}{}_{HX}$ resulting in the oxidation of Hb and ammonia formation.

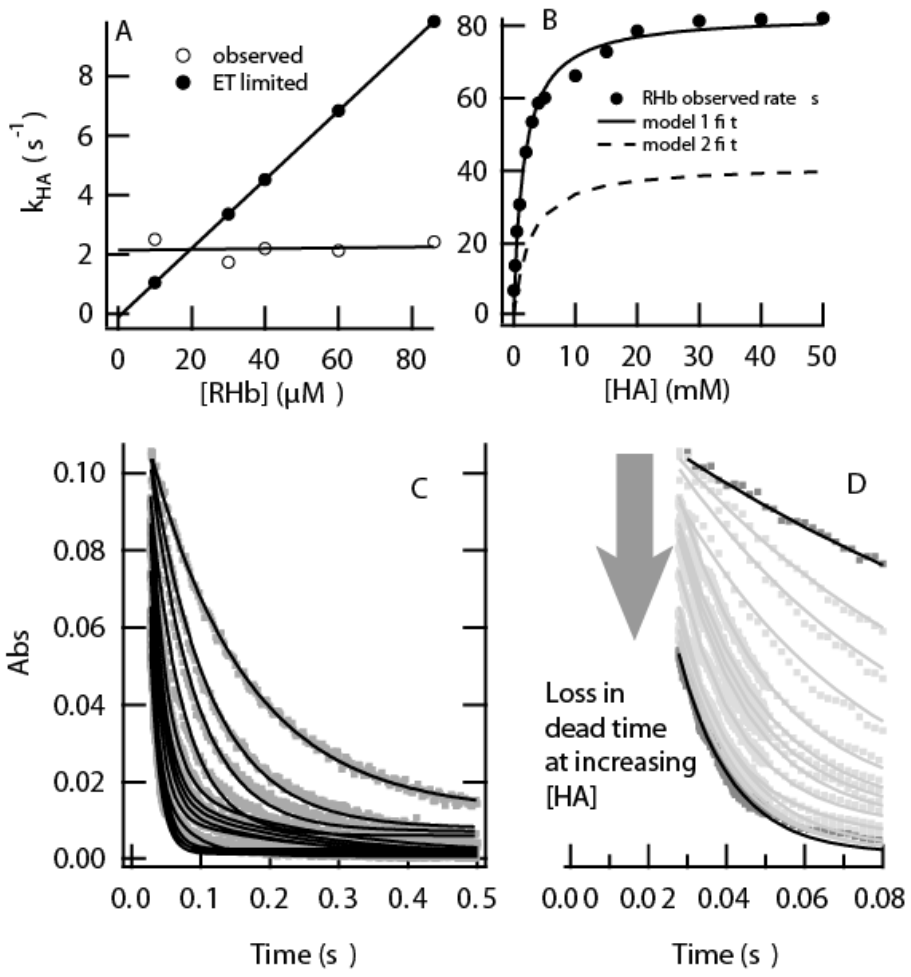

Figure 2. Kinetic analysis of the reaction mechanism. A) Open circles shows rate constants for HA reduction as a function of [RHb^{2+}] at fixed (50 μM) HA concentration. Filled circles represent the expected k_{Obs} calculated using equation 5, with assuming K_{EQ} value of 500 and k_{ESE} value for RHb and RHb_P:HA complex being equal. B) Filled circles represent the kObs for RHb, overlayed on it in solid line is the model 1 simulation and dotted line corresponds to the model 2 simulation for k_{Obs} dependence on HA. C) The observed absorbance decrease at 558nm for varied HA conc are plotted against time, with the solid lines representing the single exponential fits to the observed trends. D) Initial part of part C blown up to show the loss in starting absorbance units as [HA] is increased.

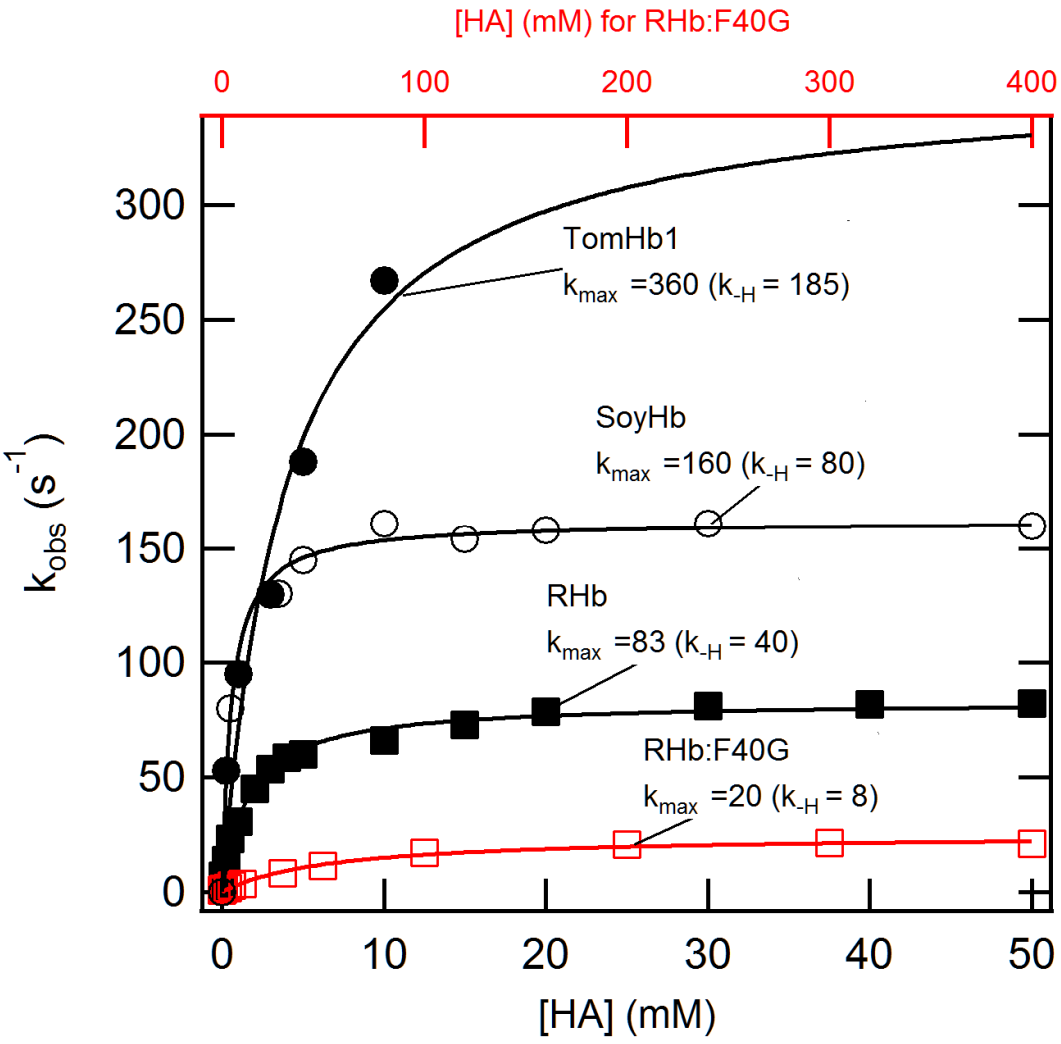

Figure 3. Model validation. Hypothesis that distal histidine off rate (k_{-H}) is the limiting factor and under the given conditions we should see a $k_{oxidation} = 2*k_{-H}$ was tested for different proteins having k_{-H} values (as labelled) both higher and lower than that of RHb.

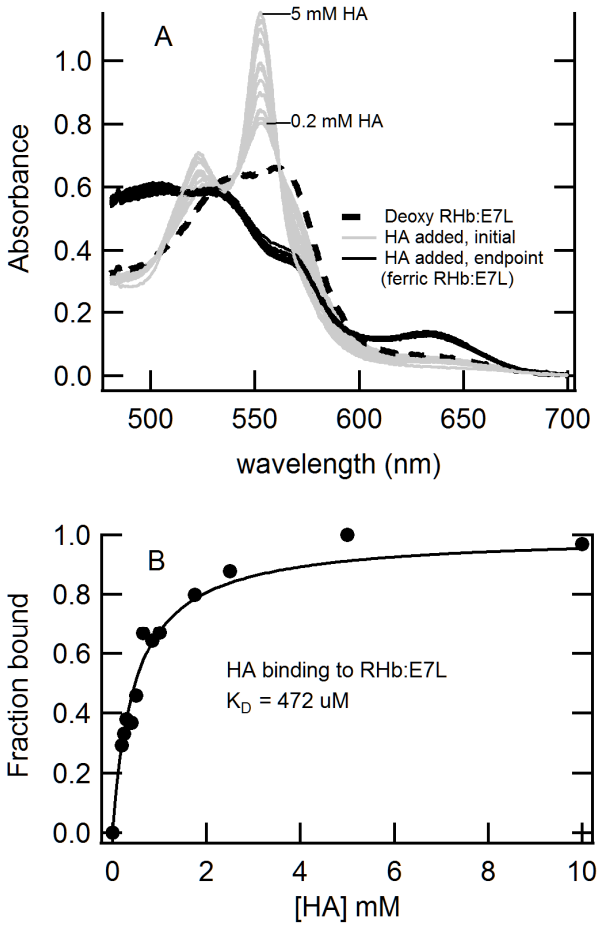

Figure 4. Role of distal histidine by mutation. RHb distal histidine was mutated to leucine (RHb:H73L) to observe the effect of distal histidine beyond competition with HA binding. A) Electronic spectrum in visible region for RHb^{2+}:H37L (RHb:E7L where represents the helix and 7 is the position of distal histidine on it) changes from a plateau (dotted line) looking feature to 'M'shape spectrum (gray lines) upon HA addition. The new spectrum represents the HA binding and it eventually turns into spectrum of RHb^{3+}:H73L (black lines). B) The RHb^{2+}:H37L M shape spectra absorbance maxima at 553nm for varied HA amount were used to calculate the fraction bound. This fraction bound was plotted against the HA concentration used and fitted to equation 1 to obtain the $K_{D\text{-}HA}$ for RHb:H73L.

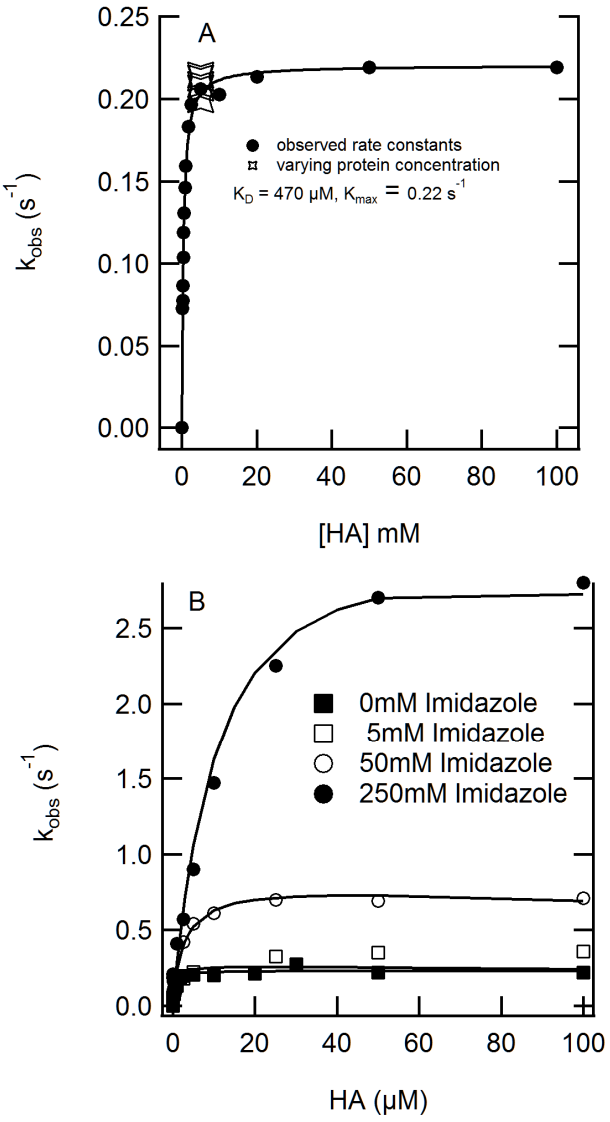

Figure 5. Role of distal histidine by exogenous substitution. A) RHb:H73L k_{Obs} for HA reduction are plotted against corresponding HA concentration (solid circles) and fitted to the equation 4 (overlayed line). The open start shape polygon represents the k_{Obs} upon varying RHb:H73L protein concentration form 10 – 75uM keeping HA concentration fixed at 5mM. B) Exogenous imidazole was added to the buffer and KObs dependencies against HA are shown, equation 4 fits are overlayed as represented by solid lines.

CHAPTER 4

GENERAL CONCLUSION

Reversible distal histidine-heme coordination in hemoglobins is believed to confer a physiologically relevant function. Numerous studies of hxHbs have pointed to varied roles like NO scavenging, pseudo-peroxidase activity, molecular signaling, and electron transfer. The detoxification of reactive species of nitrogen (NO) and oxygen (peroxides) seem to be characteristics of any hemoglobin. This general reactivity combined with low physiological concentrations of hxHbs argues against such roles in detoxification.

Our Lab has proposed an alternative physiological function for phytoglobins that have reversible endogenous hexacoordination of heme. We have proposed that instead of NOD, peroxidase, or oxygen transport activity, these Hbs might be acting as electron sinks by reducing nitrite to ammonia thereby replenishing NAD^+ for use in glycolysis. Our results have shown the class 1 plant nonsymbiotic Hbs are many orders faster at reducing nitrite and hydroxylamine (both known intermediates in nitrogen assimilation). The goal for this dissertation is to expand on this special biochemistry of nsHb1.

Chapter 2 describes a novel, robust spectroscopic method developed to figure out the electron self-exchange rates in these Hbs. The model nsHb1 (from rice) in our study was not amenable to traditional methods for determining electron self-exchange rates. The spectroscopic method developed gave us the ESE rate constant for rice nsHb1 and validated the low ESE rate for Mb, which was as unsettled question. The electron self-exchange rates,

as expected, were many orders higher for nsHb1 compared to Mb, and that corroborates with their higher hydroxylamine reduction rate.

In Chapter 3 we took the electron transfer knowledge and tested for its role in the two-electron hydroxylamine reduction. The results presented show that the electron transfer rate is not a limiting factor for hydroxylamine reduction. The role of the distal histidine was found to be rate determining, as its dissociation was found to be necessary for HA binding. The results also point out that nonsymbiotic class 1 phytoglobins have the unique feature of a mixed equilibrium population of hexacoordinate and pentacoordinate species, by virtue of their reversible endogenous histidine coordination. This mixed population has a role in that it allows for simultaneous hydroxylamine binding and faster electron transfer for reduction. This is missing in relatively homogenously populated traditional hemoglobins (like myoglobin and leghemoglobin, all pentacoordinate population) as well as in other hexacoordinate hemoglobins (like class 2 and 3 nonsymbiotic phytoglobins, with all hexacoordinate population). Potential roles of distal histidine in hydroxylamine stabilization and catalysis (proton donation) beside the ligand gating effect are also discussed upon.

The research highlights the specific but multifaceted role of the distal histidine in class 1 nonsymbiotic phytoglobins, but there are still questions that need to be answered. Attempts to artificially mix pentacoordinate (rice nsHb1 E7Lmutant) with hexacoordinate (rice nsHb1 F40G mutant) failed to retrieve any significant increase in hydroxylamine reduction (data not shown). Another attempt to mix rice nsHb1 F40G with soybean leghemoglobin also yielded no increase in hydroxylamine reduction (data not shown). Rice

nonsymbiotic hemoglobin used as model in our studies is dimeric and upon disrupting it by single amino acid mutation, we saw decline in hydroxylamine reduction activity (data not shown). These results point towards need to further investigate factors like role of dimerization and other amino acids in heme cavity that influence hydroxylamine reduction as that might bring us closer to understanding the physiological role of these proteins.

ACKNOWLEDGMENTS

I would like to thank my advisor, Dr. Mark Hargrove, for the support and guidance I have received. Above all I have learned from him, his enthusiasm and curiosity for research are the things I appreciate most, hoping some of that sticks with me too.

I would like to extend my gratitude to Dr. Alan DiSpirito, Dr. Alan Myers, Dr. Amy Andreotti, Dr. Laura Jarboe and Dr. John Robyt for the for their time, support and guidance throughout this endeavor. Dr. John Robyt had been an inspirational, and I acknowledge Dr. Amy Andreotti for the kind gesture of agreeing to be his replacement on my POS at this last stage of my research work, thank you. Dr. DiSpirito has been around and been my source to go to whenever I had problems or questions related to anaerobic reaction setup, and I appreciate that a lot. Dr. Jarboe and Dr. Myers have been quick to respond to my requests and their constructive participation in progression of this work is highly appreciated.

I would also like to acknowledge the faculty and staff, especially Connie Garnett, and Dr. Guru Rao at Roy J. Carver Department of Biochemistry, Biophysics and Molecular biology for making things easier for me. I extend my sincere gratitude for the endless support and valuable discussion that I had with my lab mates, past and present (Dr. Xiaoguang Wang, Jaganathan Alagurajan, Ashley Spooner, Denis Teimev, Dr. Smita Kakar, Dr. Ryan Sturms and Dr. Raji Joseph). I have been lucky to have friends like Dr. Abhijeet Kapoor, Dr. Chitvan Mittal and Dr. Santhosh Kumar Vammi, thank you all for making the stay in Ames memorable.

Nothing of this would have been possible without the endless support from my parents, Tarlok Singh and Jaspal kaur along with my sister Gursimran Kaur. They have been my inspiration for all that I have achieved and would continue to be for the coming achievements. I would like to thank my extended family in Kandial and Fremont for all the calls, support and encouragement, things got easier with you all on my side.